

**Polymer additives, contaminants and non-intentionally  
added substances in consumer products:  
Combined migration, permeation and toxicity analyses  
in skin**

Inaugural-Dissertation  
to obtain the academic degree  
Doctor rerum naturalium (Dr. rer. nat.)

submitted to the Department of Biology, Chemistry and Pharmacy  
of Freie Universität Berlin

by

Nastasia Bartsch

from Gräfelfing, Munich

2018

This thesis was carried out at the Federal Institute for Risk Assessment (BfR) in Berlin from May 2013 to February 2017 under the supervision of Prof. Dr. Dr. Andreas Luch.

1<sup>st</sup> Reviewer: Prof. Dr. Dr. Andreas Luch

2<sup>nd</sup> Reviewer: Prof. Dr. Daniel Klinger

Date of defense: 14 December 2018

## ERKLÄRUNG

---

Hiermit versichere ich, die vorliegende Dissertation mit dem Titel „Polymer additives, contaminants and non-intentionally added substances in consumer products: Combined migration, permeation and toxicity analyses in skin“ selbstständig und ohne Benutzung anderer als der zugelassenen Hilfsmittel angefertigt zu haben. Alle angeführten Zitate sind als solche kenntlich gemacht. Die vorliegende Arbeit wurde in keinem früheren Promotionsverfahren angenommen oder als ungenügend beurteilt.

Berlin, den 25. September 2018

Nastasia Bartsch

Die Dissertation wurde in englischer Sprache verfasst.

## Danksagung

Ich möchte meinen Dank auf diesem Wege an Herrn Prof. Dr. Dr. Luch richten, für die Möglichkeit, meine Doktorarbeit in der Abteilung Chemikalien- und Produktsicherheit am Bundesinstitut für Risikobewertung anzufertigen. Ich schätze sehr, dass Professor Luch stets meine interdisziplinäre Herangehensweise an das Thema gefördert hat, mir Raum gab, meine Ideen umzusetzen und mich darin bestärkte, meine Arbeit in einem breiten wissenschaftlichen Kontext zu betrachten.

Herrn Prof. Dr. Klinger gilt mein Dank für sein Interesse an meinem Projekt und für die Übernahme der Zweitgutachterschaft.

Frau Dr. Vieth, Herrn Dr. Hutzler und Herrn Dr. Kappenstein möchte ich für die konstruktiven und regen Diskussionsrunden während der Promotionszeit besonders danken. Ich bin sehr froh über ihre fachliche und persönliche Unterstützung beim Erstellen dieser Arbeit. Auch Frau Dr. Pfaff stand mir während dieser Zeit mit Rat und Expertise zur Seite, wofür ich sehr dankbar bin.

Meinen Projektpartnern danke ich für ihre Begeisterung für und das Vertrauen in mein Projekt. Durch die Kooperation mit Herrn Dr. Witzel und Dr. Kumpf war es mir möglich, die für diese Arbeit essentiellen Humanhautdaten zu generieren. Bei Herrn Dr. Lichtblau und Dr. Hörold möchte ich mich für die fachliche Unterstützung während des Polymerdesigns und für die Herstellung des Materials bedanken.

Eine schöne Promotionszeit hatte ich nicht zuletzt durch tolle Kollegen am BfR. Ein großes Dankeschön geht daher auch an Euch, für die gute Zusammenarbeit sowie für fachlich und menschlich bereichernde Gespräche. Mein besonderer Dank gilt dabei den Kollegen der Abteilung 7 und natürlich dem GZSZ Büro, für das gemeinsame Arbeiten unter Palmen. Herrn Dr. Bruhn danke ich sehr für die Zusammenarbeit bei der Entwicklung eines quantenchemischen Blickes auf meine Analyten. Barbara Gerding danke ich für ihre Unterstützung während meiner Anfangszeit im FDC Labor. Ihre zahlreichen Tipps im Umgang mit den Franz-Zellen trugen sehr zum Gelingen dieser Arbeit bei. Bei Karsten Schön möchte ich mich für seine Hilfe im analytischen Labor bedanken.

## DANKSAGUNG

---

Bei Lidia Schneider möchte ich mich besonders für ihren Eifer, ihr Verständnis für Experiment-optimierte Arbeitszeiten und die Unterstützung, speziell bei der Entwicklung des FDC-Assays für Additive, bedanken.

Die Zusammenarbeit mit Studenten und Gastwissenschaftlern während der Promotionszeit machte großen Spaß und brachte mein Projekt sehr voran. Daher gilt mein Dank Amelie Wilde, Mathilde Girard und Valerie van de Weijert für die erfolgreiche und schöne Zusammenarbeit.

Für die Momente abseits des Labors und Büros danke ich meinem Finnischkurs für eine tolle Zeit und die Fähigkeit, Dinge auch mal mit „Finnischer Logik“ anzugehen. Amelia möchte ich für ihr Mitfiebern während der letzten Jahre und für die vielen inspirierenden Gespräche danken.

Meiner Familie danke ich von Herzen für ihre Unterstützung und ihr Verständnis. Das Wissen um Euren Rückhalt gibt mir Schwung für große Schritte.

Ganz besonders danken möchte ich Dir, lieber Thorsten. Du hast von Anfang an die Idee Promotion mitgetragen, mich darin bestärkt und warst zu jeder Zeit grenzenlos für mich da.

## Table of contents

Zusammenfassung .....	1
Abstract.....	3
List of abbreviations .....	5
1 Introduction.....	9
2 Objectives.....	13
3 Dermal exposure of consumers to polymer additives, contaminants and NIAS .....	17
3.1 The Franz diffusion cell.....	17
3.2 Skin models .....	18
3.3 Transepidermal water loss - TEWL .....	18
3.4 Alternative migration testing and dermal exposure assessment .....	19
3.5 Visualization of skin penetration by PAHs and additives .....	20
4 Additives, contaminants and NIAS of toxicological relevance present in polymeric consumer products.....	22
4.1 Polycyclic aromatic hydrocarbons - PAHs .....	22
4.2 Mineral oil hydrocarbons - MOSH/ MOAH.....	32
4.2.1 Volatility dependent distribution of mineral oil components in human skin .....	33
4.3 Additives .....	36
4.4 Polymer composition – an analytical point of view .....	39
5 Degradation of polymeric material – What comes after stabilization?.....	42
5.1 Principles of polymer stabilization.....	42
6 Results .....	45
6.1 Target analysis of polycyclic aromatic hydrocarbons (PAHs) in consumer products and total content of polycyclic aromatic compounds (PACs) .....	45
6.2 Skin permeation of polycyclic aromatic hydrocarbons: A solvent-based <i>in vitro</i> approach to assess dermal exposures against benzo[a]pyrene and dibenzopyrenes .....	57
6.3 Chemical stabilization of polymers: Implications for dermal exposure to additives .....	81
6.4 Thermal stability of polymer additives: Comparison of decomposition models including oxidative pyrolysis .....	115

## TABLE OF CONTENTS

---

7	Discussion .....	147
7.1	PAHs and mineral oil components in consumer products .....	147
7.2	PAHs in skin contact.....	148
7.3	Characterization of stabilizers, plasticizers and degradation products in polymers and skin penetration .....	149
7.4	Prediction of additive degradation products.....	150
8	Conclusion & Outlook.....	152
9	References .....	155
10	List of publications.....	169
10.1	Articles .....	169
10.2	Conferences .....	169
	Annex I.....	171
	Annex II.....	174
	Annex III.....	181
	Annex IV .....	188

## Zusammenfassung

Während der alltäglichen Verwendung von verbrauchernahen Produkten aus polymerem Material denken die wenigsten Anwender an die damit verbundenen potentiellen gesundheitlichen Risiken durch entsprechende Inhaltsstoffe. Der Anwendungsbereich ist dabei ebenso vielseitig wie die Materialzusammensetzungen und umfasst beispielsweise Werkzeug, Lebensmittelkontaktmaterialien und Spielzeug. Umso wichtiger ist es, dass die für die Produkte eingesetzten Polymerformulierungen auf gesundheitlich unbedenklichen Ausgangsmaterialien beruhen und ihre Sicherheit während des gesamten Lebenszyklus unverändert bleibt. Dabei muss zwischen dem gezielten Einsatz von Polymeradditiven im Material (z.B. als Weichmacher oder Antioxidantien) und der Gruppe der nicht absichtlich zugesetzten Bestandteile (z.B. Kontaminanten, Abbau-/ Reaktionsprodukte) unterschieden werden.

In der hier vorliegenden Arbeit wurden polymere Verbraucherprodukte untersucht, welche für den Hautkontakt vorgesehen sind. Der damit verbundene dermale Expositionspfad kann neben der oralen und inhalativen Exposition einen Hauptweg der Eintragung von Fremdstoffen in den Organismus darstellen. Dies ist besonders kritisch zu bewerten, wenn es sich um toxikologisch relevante Fremdstoffe handelt, wie z.B. Polyzyklische Aromatische Kohlenwasserstoffe (PAK), Aminobenzol- oder Kresol- Derivate. Für die acht als wahrscheinlich krebserregend für den Menschen eingestuften PAK (CLP-Verordnung) (1) in Erzeugnissen gilt seit 2015 eine EU-weit einheitliche Restriktion in Spielzeugen und Verbraucherprodukten mit vorhersehbarem längerfristigem oder wiederholtem kurzzeitigem Hautkontakt (REACH-Verordnung) (2, 3). Der festgelegte Gehaltsgrenzwert dieser acht PAK erlaubt jedoch keine Rückschlüsse auf die tatsächliche dermale Exposition des Verbrauchers. Für eine gesundheitliche Risikocharakterisierung ist es daher zwingend notwendig, geeignete Methoden zur Ermittlung der dermalen Exposition zu entwickeln.

Im Rahmen dieser Arbeit wurden Expositions-Referenzwerte mit exzidiierter Humanhaut im Franz-Zell-Assay für herauslösbare Komponenten von Elastomeren und Gummi generiert. Für die Gruppe der PAK wurde zusätzlich, orientierend an den mittels Franz-Zell-Assay generierten Daten, ein alternatives Prüfverfahren für die Ermittlung der dermalen Exposition entwickelt, welches auf



der Migration von PAK in Simulanzlösung beruht. Daten zur Expositionsabschätzung, welche auf Migrationsdaten basieren, die mit diesem alternativen Prüfverfahren im Rahmen des nationalen Monitoringprogramms 2017 erhoben wurden, sowie eine darauf basierende Risikobewertung, wurden der EU-Kommission für die Überprüfung der Grenzwerte von PAK in Verbraucherprodukten und Spielzeug zur Verfügung gestellt.

Die im Rahmen dieser Arbeit durchgeführte Visualisierung der Hautpenetration nach Kontakt zu einem *N*-Phenyl-2-naphthylamin-haltigen Polyolefin bestätigte am Beispiel dieses Prokarzinogens, dass zahlreiche weitere Additive mit zum Teil toxikologischer Relevanz bei Hautkontakt migrieren, die Hautbarriere überwinden und so zu einem potentiellen gesundheitlichen Risiko führen können.

Eine detaillierte Charakterisierung polymeren Materials hinsichtlich der Zusammensetzung erfolgte durch den Einsatz instrumenteller Analytik. Die Entwicklung von Multi-Analyt-Methoden ermöglichte die Quantifizierung von 21 Additiven, 5 Abbauprodukten und 28 PAK. Die Polymere wurden zudem anhand ihres Zerfallsmusters mittels online-Kopplung von Pyrolyse an Gaschromatographie mit massenspektrometrischer Detektion identifiziert. Zu Klärung der Frage, ob durch Alterungsprozesse aus Additiven toxikologisch relevante Abbauprodukte entstehen können, wurden Additive in verschiedenen Alterungsmodellen getestet. Unter Modellbedingungen wurde gezeigt, dass Kresol-Derivate aus phenolischen Antioxidantien entstehen können, sowie Phthalate aus einem Phthalat-Ersatzweichmacher.

Die gewonnenen Daten können zur Verbesserung der Risikoidentifizierung und Priorisierung von Polymerbestandteilen für die Risikobewertung herangezogen werden.

## **Abstract**

Most people are not aware of the potential health risks associated with the ingredients of daily used polymeric consumer products. The application range is as diverse as the composition of the materials. Polymeric material is exemplarily used in tool handles, food contact materials and toys. It is thus even more important that the final product is harmless to health and ensures safe usage over the entire product life cycle. Analyzing the composition, intentionally added substances need to be distinguished from non-intentionally added substances. Unlike substances that were added for a defined purpose (e.g. plasticizers, antioxidants or processing aids), non-intentionally added substances are present as a result of material aging or inappropriate manufacturing processes (e.g. contaminants, decomposition or reaction products).

In this thesis, the focus was on polymeric consumer products that are designated for skin contact. Besides the oral and inhalative route, the dermal path of exposure may pose a major route for xenobiotics to enter the organism. This is of special concern in case of toxicological relevant xenobiotics like polycyclic aromatic hydrocarbons (PAHs), aminobenzene- or cresol-derivatives.

There is an EU-wide restriction on 8 PAHs that are classified as presumed to have carcinogenic potential to humans (1) in toys and consumer products effective since 2015 (REACH EG No. 1907/2006, EU No. 1272/2013) (2, 3). Articles shall not be placed on the market if any of their rubber or plastic components that come into direct as well as prolonged or short-term repetitive contact with the human skin contain more than 0.5 mg/kg or 1 mg/kg respectively. The limits set refer to the PAHs content in the material and do not mirror the actual dermal exposure of consumers. Therefore, it is crucial to study the real dermal PAH load in order to generate data for a reliable assessment of potential health risks.

In this thesis, dermal exposure to leachables of rubber and elastomers was investigated consequently using excised human skin in the Franz diffusion cell (FDC)-assay. Basing on this reference data, an alternative testing method was developed for dermal exposure assessment of PAHs. It uses a simulant suitable for the lipophilic PAHs and it realistically mirrors the combined permeation and migration of PAHs. Exposure data basing on this method was provided for the

European Commission in order to review the limit values of PAHs in consumer products and toys.

The skin permeation was visualized at the example of the procarcinogen *N*-phenyl-2-naphthylamine. Human skin was exposed *ex vivo* to a polyolefin entailing this antioxidant and a depth profile generated applying ATR-FTIR-microscopy. It was shown by this very graphic evaluation, that numerous polymer additives with in part toxicological relevance might migrate, overcome the skin barrier and ultimately lead to a potential health risk.

A detailed characterization of the polymeric material was conducted using broad analytics. The development of multi-analyte-methods allowed quantification of 21 additives, 5 degradation products and 28 PAHs. The polymers were identified applying pyrolysis coupled online to gas chromatography and mass-spectrometric detection. Furthermore, additives were tested in different aging protocols to identify potential degradation products of toxicological relevance. It was shown, that cresol-derivatives are formed as a consequence of degradation of phenolic antioxidants and phthalates are formed by degradation of a phthalate substitute plasticizer.

The results of this work can be useful to improve risk identification and to prioritize leachables of elastomers and rubber for risk assessment.

## List of abbreviations

The table below includes all abbreviations mentioned in the text, except for those used solely in the articles in chapter 6.

1-MN	1-methylnaphthalene
2-MN	2-methylnaphthalene
2-NA	2-Naphthylamine
5B	Pentylbenzene
5-Me-Chr	5-Methylchrysene
Ace	Acenaphthene
Acy	Acenaphthylene
AfPS	German Product Safety Commission; German: Ausschuss für Produktsicherheit
ALARA	as low as reasonably achievable (ALARA principle for genotoxic carcinogens)
Ant	Anthracene
ATR-FTIR	Attenuated total reflectance - Fourier transform infrared
B[a]A	Benzo[a]anthracene
B[a]P	Benzo[a]pyrene
B[b]F	Benzo[b]fluoranthene
B[c]F	Benzo[c]fluorene
B[e]P	Benzo[e]pyrene
B[g,h,i]Per	Benzo[g,h,i]perylene
B[j]F	Benzo[j]fluoranthene
B[k]F	Benzo[k]fluoranthene
C[c,d]P	Cyclopenta[c,d]pyrene
C11	n-undecane
C13	n-tridecane
Chr	Chrysene
CLH	Harmonised classification and labelling
CLP	Classification labelling and packaging
CM-SDB	Chloromethylated styrene-divinylbenzene copolymer
CMR	Carcinogenic, mutagenic, toxic for reproduction
CoRAP	Community rolling action plan
CyCy	Bicyclohexyl

## LIST OF ABBREVIATIONS

---

DB[a,e]P	Dibenzo[a,e]pyrene
DB[a,h]A	Dibenzo[a,h]anthracene
DB[a,h]P	Dibenzo[a,h]pyrene
DB[a,l]P	Dibenzo[a,l]pyrene
DB[a,l]P	Dibenzo[a,l]pyrene
DEHP	Diethylhexylphthalate/ Bis(2-ethylhexyl)phthalate
DMEM	Dulbecco's Modified Eagle Medium
DMSO	Dimethyl sulfoxide
DNA	Deoxyribonucleic acid
DOIP	Diocetyl isophthalate/ Bis(2-ethylhexyl)benzene-1,3-dicarboxylate
DOP	Diocetyl phthalate
ECHA	European Chemicals Agency
EDTA	Ethylenediaminetetraacetic acid
EH	Epoxide hydrolase
EU	European Union
CYP	Cytochrome P450-dependent
FDC	Franz diffusion cell
FID	Flame ionization detector
Flu	Fluorene
Fluo	Fluoranthene
GC	Gas chromatography
GJIC	Gap junction intercellular communication
HBSS	Hanks' Balanced Salt Solution
HAS	Hindered amine stabilizers
I[c,d]P	Indeno[1,2,3-c,d]pyrene
IARC	International Agency for Research on Cancer
Irganox 1081	2- <i>tert</i> -butyl-6-(3- <i>tert</i> -butyl-2-hydroxy-5-methylphenyl)sulfanyl-4-methylphenol
Istd	Internal standards
JRC	Joint Research Centre
LC	Liquid chromatography
LDPE	Low-density polyethylene

## LIST OF ABBREVIATIONS

---

LFGB	Food and feed act; German: Lebensmittel-, Bedarfsgegenstände- und Futtermittelgesetzbuch
LLE	Liquid- liquid extraction
LOQ	Limit of quantification
MMS	Methyl methanesulfonate
MOAH	Mineral oil aromatic hydrocarbons
MOSH	Mineral oil saturated hydrocarbons
MRM	Multiple reaction monitoring
MS	Mass spectrometry
Naph	Naphthalene
NBBS	<i>N</i> -butylbenzenesulfonamide
Neozon D	<i>N</i> -phenylnaphthalen-2-amine
NIAS	Non-intentionally added substances
NIST	National Institute of Standards and Technology
Nonox A	<i>N</i> -phenylnaphthalen-1-amine
OECD	Organisation for Economic Co-operation and Development
PACs	Polycyclic aromatic compounds
PAHs	Polycyclic aromatic hydrocarbons
PAK	Polyzyklische aromatische Kohlenwasserstoffe
PBT	Persistent, bioaccumulative, toxic
Per	Perylene
Phe	Phenanthrene
PVC	Polyvinyl chloride
Pyr	Pyrene
Pyr-GC-MS	Pyrolysis gas chromatography mass spectrometry
qNMR	Quantitative nuclear magnetic resonance spectroscopy
REACH	Registration, Evaluation, Authorisation and Restriction of Chemicals
RHE	Reconstructed human epidermis
<i>S.c.</i>	<i>Stratum corneum</i>
SSFL	Skin surface film liquids
TBB	1,3,5-tri- <i>tert</i> -butylbenzene
TEWL	Transepidermal water loss
Tinuvin P	2-(benzotriazol-2-yl)-4-methylphenol

## LIST OF ABBREVIATIONS

---

ToF	Time of flight
TOTM	Trioctyltrimellitate/ tris(2-ethylhexyl)benzene-1,2,4-tricarboxylate
U.S. EPA	United States Environmental Protection Agency
vPvB	Very persistent, very bioaccumulative
$\alpha$ -MSD	$\alpha$ -Methylstyrenedimer/ 2,4-diphenyl-4-methyl-1-pentene

# 1 Introduction

A large number of dermal contact surfaces of everyday life consist of polymeric materials. During the manufacturing process, additives are added for influencing physicochemical properties but also for preservation or coloring purposes. To meet functional requirements like longevity, haptic properties and factory costs, different polymers are used as the raw material of choice and modified by a variable number of additives in the majority of commodities. Besides intended additives with a defined function such as plasticizers, stabilizers, colorants and vulcanization accelerators, non-intended contaminants as well as decomposition products or so-called non-intentionally added substances (NIAS) can be ingredients of the material. There are several components among these that are potentially harmful to health. They are not covalently bound to the polymer and the material potentially undergoes mechanical stress, polymer weathering and aging. This affects both, the integrity of the polymer and the stability of additives. Considering that, potential toxic additives and their degradation products might migrate from the polymer. Therefore, dermal exposure of consumers via polymeric articles with skin contact is possible.

The human skin as a multilayered organ protects the body against dehydration and penetration of xenobiotics by a natural barrier, which is primarily formed by the *stratum corneum* (s.c.). It is the outermost layer of the epidermis and consists mainly of corneocytes, the terminally differentiated keratinocytes embedded in a lipid matrix in a “bricks and mortar manner” (4). Skin penetration must be distinguished from skin permeation in order to assess the bioavailability of a substance. As depicted in Figure 1, there are three pathways described as potential ways for xenobiotics to enter the viable epidermis (penetration: A) or to even pass it (permeation: B). A substance can overcome the s.c. i) intracellular, ii) intercellular or iii) follicular accordingly (5). The lipophilicity of chemicals is crucial for the permeability through the skin as well as the thickness of the s.c. and parameters like molecular weight and concentration of the substance (6).



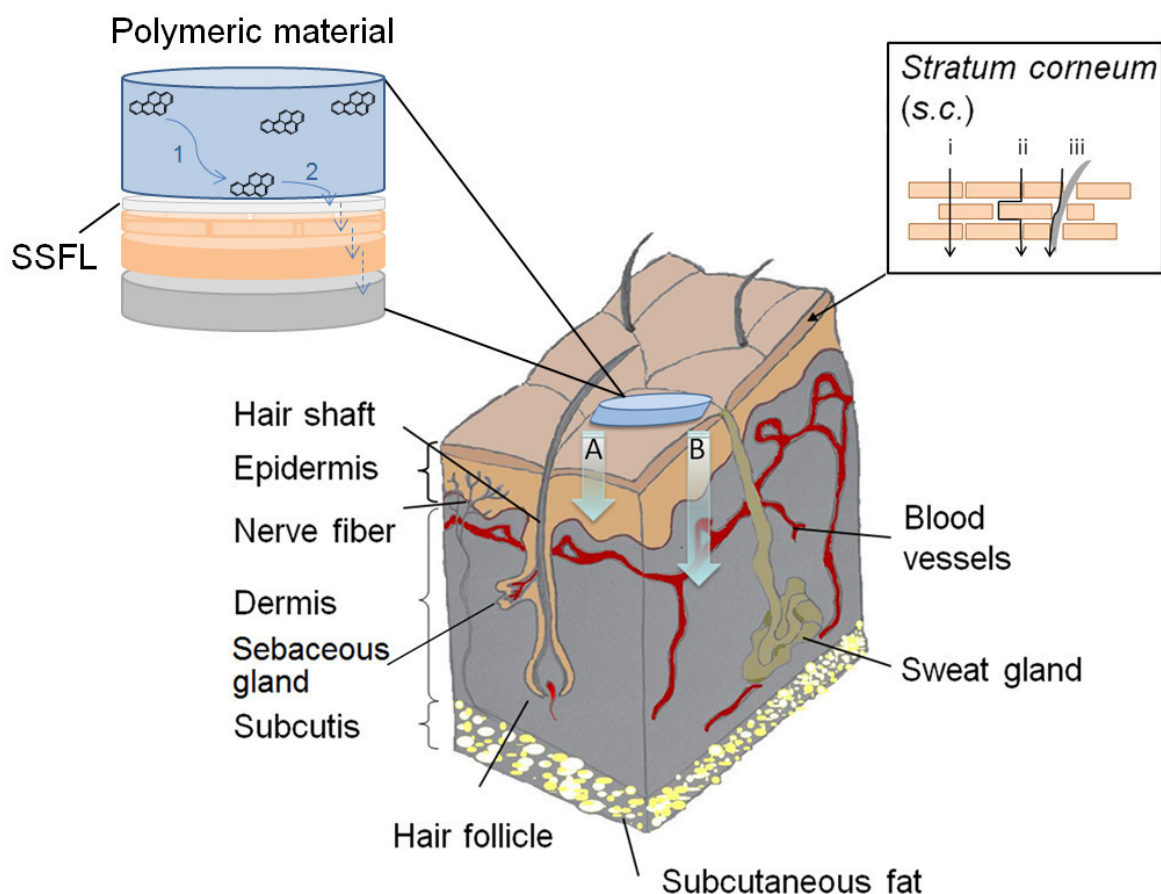


**Figure 1: Scheme of human skin.** Profile with penetration (A), permeation pathway (B) and close-up view of migration processes within polymeric material (top left) and s.c. (top right). SSFL: skin surface film liquids (modified (7)).

To study dermal distribution of chemicals, the Franz diffusion cell (FDC) is the most realistic *in vitro* tool. It can be operated with various test skins or skin models. When *in vivo* transdermal studies are ethically unacceptable because of the potential toxicity of the test substances, the FDC-assay with excised intact human skin is commonly used as reference for dermal exposure assessment (8). Once, the skin is mounted between the donor- and receptor-compartment, either formulations or solutions of analytes or whole discs of rubbers or elastomers can be applied onto the skin. The FDC-assay thereby allows investigation of human skin, which was directly exposed to consumer product specimens.

The dermal exposure to components of polymeric consumer products is a combined migration and permeation- or penetration-process. The basis for dermal exposure is the movement of compounds to the material surface (diffusion,

migration: step 1, Figure 1), release into the skin surface film liquids (SSFL) and subsequent uptake into the upper epidermal layers (desorption/ distribution/ sorption followed by skin penetration: step 2, Figure 1). The rate limiting step in this case is the diffusion process. It depends on the diffusion coefficient, the mobility of the compounds within the polymer or matrix, the size of the migrating compounds and the temperature. This relationship is described by Fick's 2<sup>nd</sup> law of diffusion, wherein the diffusivity D is expressed by the Arrhenius equation.

$$\frac{\partial c}{\partial t} = D \frac{\partial^2 c}{\partial x^2}$$

**Equation 1: Fick's 2<sup>nd</sup> law of diffusion.**

c: concentration, t: time, D: diffusion coefficient, x: distance.

$$D = D_0 \cdot e^{\frac{-E_A}{RT}}$$

**Equation 2: Arrhenius Equation – Mass diffusivity in solids D [cm<sup>2</sup> s<sup>-1</sup>].**

D<sub>0</sub>: pre-exponential factor, E<sub>A</sub>: activation energy [J], R: universal gas constant [8.314 J mol<sup>-1</sup> K<sup>-1</sup>], T: temperature [K].

The movement of ingredients within polymers is a key requirement in additivation of materials. It is exemplarily the basis for functional polymers like antistatic polymers. But with respect to dermal exposure the migration can result in a health risk for consumers to get exposed by skin contact to additives like plasticizers, stabilizers or processing aids. There is a lack of systematic knowledge yet about dermal exposure to numerous polymer additives like phenolic antioxidants, arylamines or to a comparatively new alternative trimellitic plasticizer. Therefore, suitable protocols were developed in this work to investigate a range of potentially harmful additives in the FDC-assay and to assess their dermal bioavailability from elastomers and polymers after skin contact.

Consumer products with high contents of PAHs were repeatedly identified by official control laboratories. PAHs are present as contaminants in rubbers and elastomers of commodities due to the application of mineral oil ingredients or carbon black to the raw material. Mineral oil ingredients often contain highly

alkylated polycyclic aromatic compounds (PACs) in their aromatic fraction. They are utilized as plasticizers or lubricants while carbon black contains PACs of no or low alkylation degree and is added to the polymer for coloring and abrasion resistance purposes. Among PAHs, several compounds have been identified as genotoxic carcinogens. A study on global atmospheric emission of PAHs in 2004 revealed consumer product usage (6.9%) after biofuel (56.7%) and wildfire (17.0%) as one of the major sources for discharge of the 16 PAHs listed as U.S. Environmental Protection Agency (U.S. EPA) priority pollutants (9). In terms of the associated health risk, 8 carcinogenic PAHs (Benzo[a]pyrene (B[a]P), Benzo[e]pyrene (B[e]P), Benzo[a]anthracene (B[a]A), Chrysene (Chr), Benzo[b]fluoranthene (B[b]F), Benzo[j]fluoranthene (B[j]F), Benzo[k]fluoranthene (B[k]F), Dibenzo[a,h]anthracene (DB[a,h]A) are classified as presumed to have carcinogenic potential to humans in the CLP Regulation (1) and restricted in consumer products with foreseeable skin contact and toys by Annex XVII of the REACH Regulation 1907/2006 (2) to 1.0 mg/kg and 0.5 mg/kg respectively in 2015 (3).

The dermal exposure assessment using data on migration of lipophilic PAHs from rubber or elastomers in commonly applied aqueous sweat simulant resulted in distinct underestimation as compared to the *ex vivo* human skin data. Therefore, there was a need to develop a suitable migration method that is adapted to the lipophilic properties of PAHs in skin contact. In this thesis, an appropriate ethanol-based method for skin exposure data has been developed and used to generate realistic migration data. In 2017, this alternative testing method was used in the national German monitoring program (10). Furthermore, the Joint Research Centre (JRC) of the Commission had the mandate to further investigate PAH migration with this method as the basis: migration studies of PAHs from rubber and plastic into SSFL using an emulsion of artificial sebum in aqueous sweat simulant were performed in addition to migration studies into ethanolic simulant (11). The relative migration rates of PAHs into artificial SSFL were in agreement with the rates generated applying ethanolic simulant to rubber and plastic containing PAHs as it was developed in this thesis.

## 2 Objectives

The presence of potentially harmful substances in consumer products does not intrinsically pose a risk. Factors like mobility of the substance within the material, ability to overcome the polymer-skin interface and ultimately the human skin barrier substantially have an impact on the associated health risk.

Therefore, the aim of this thesis was to characterize consumer products designated for skin contact in detail and to assess the potential dermal exposure of consumers to polymer ingredients. Key aspects were the identification of compounds and the method development for determination of transepidermal exposure and of the distribution of compounds within the skin and skin models.

### **FDC-assay and alternative migration testing on PAHs**

Up to now, aqueous sweat simulant is often utilized to assess dermal exposure to components present in consumer products like textiles or toys. In case of PAHs, specimens of PAH-containing commodities are placed into the simulant and stored under defined conditions for a certain time (12, 13). The resulting PAH-content in the aqueous simulant is determined afterwards and accounted as representative dermal PAH-load. But the comparability of aqueous sweat simulant to human skin is rather questionable at least for highly lipophilic components like PAHs. The potential accelerating effect of dermal lipids on skin penetration of lipophilic substances is not covered by this set-up, whereas lipids present on the skin surface get naturally into contact with the surface of consumer products during intended use. In this case, application of aqueous sweat simulant for migration studies results in a clear underestimation of dermal exposure. Because of this and of the carcinogenic properties of high molecular PAHs, one major aim of this work was to develop a more realistic exposure testing scenario. Therefore, a combined migration and skin penetration protocol was established using the FDC-assay with human skin. The FDC-assay provided reference values to establish a realistic alternative solvent-based migration testing method for PAHs with B[a]P as lead compound. The alternative simulant was ought to deliver similar results as compared to human skin, though it simplified the complexity of the multiphase skin system. Ethanol was used to adjust the lipophilicity of the aqueous simulant. Main practical aspects of this subproject that needed to be considered are listed below:

- Optimization of analytical evaluation utilizing tandem mass spectrometry coupled to gas chromatography (GC-MS/MS)
- Adaption of FDC-assay to PAHs and optimization of extraction and clean-up procedure for individual compartments (aqueous wash and receptor compartment, tape strips entailing s.c. layers and the remaining epidermis)
- Generation of reference data with human skin and consumer products in FDC-assay, comparison to other skin models used in FDC-assay
- Development of a suitable solvent-based migration simulant resulting in release of PAHs comparable to the human skin reference data

### **Characterization of polymers in consumer products**

The composition of polymers used in consumer products is very diverse concerning additivation and polymeric raw material. Recipes need to meet continuously new requirements and keep therefore changing (14). For this reason, an analytical multi-analyte-method was not only established for PAHs, but also for several important classes of polymer additives and for NIAS. Screening techniques were applied to polymeric materials of consumer products to identify frequently used additives in polymeric material. Also toxicological aspects were considered compiling the analyte lists. Furthermore, polymers were characterized using complementary analytical techniques. For instance, commodities were not only analyzed via targeted analysis for their content on PAHs utilizing GC-MS/MS, but also with regard to its total amounts of PACs by means of liquid chromatography coupled online to gas chromatography equipped with flame ionization detector (online-LC-GC-FID). Because of the extremely high number of PACs in consumer products made of rubber or elastomers, online-LC-GC-FID should be preparatively used to analyze the overall amount of mineral oil aromatic hydrocarbons (MOAH). To separate distinct PAH ring systems and to reveal their degree of alkylation, two dimensional gas chromatography was applied. The following main aspects of polymer characterization had to be considered in the practical part of this subproject:

- Ongoing addition of contaminants, additives and NIAS to the multi-analyte-methods

- Validation and optimization of GC-MS/MS multiple reaction monitoring (MRM) multi-analyte-methods
  - Selectivity: optimization of ion transitions and collision energy
  - Limit of detection (LOD); Limit of Quantification (LOQ)
  - Linearity and range
  - Accuracy: analyses of standard reference material
  - Recovery: yield of sample clean-up including diverse matrices
  - Precision: repeatability and intermediate precision
  - Reproducibility in case of PAHs method: interlaboratory trial
- Screening on frequently used polymer additives and contaminants in consumer products
- Identification of polymers using pyrolysis coupled to GC-MS (Pyr-GC-MS)

### **Dermal exposure assessment of polymer additives**

To expand the set of compounds in dermal exposure assessment by substances intentionally added to polymers, the FDC-assay was adapted to a range of polymer additives. In contrast to the structural homogenous class of PAHs the additives differed structurally and with respect to their field of application in polymers (Table 2, 3<sup>rd</sup> publication) (15). That posed certain additional analytical challenges:

- Application of equally effective extraction techniques for 10 structurally very different additives ranging from the neurotoxic plasticizer *N*-butylbenzenesulfonamide (NBBS: log  $P_{OW}$  2.0) to the phthalate substitute plasticizer trioctyltrimellitate (TOTM: log  $P_{OW}$  8.8)
- Development of a discrimination free sample clean-up procedure resulting in acceptable recoveries for all analyte-matrix combinations

### **Degradation pattern of polymer additives and aging**

Polymers including their additives are subject to aging processes. Because degradation products of once applied additives might completely differ in physico-chemical and toxicological properties, their occurrence in consumer products is of special concern. Up to now, little is known about aging products, its contribution to

consumer exposure and its toxicological relevance. Referring to this, additives included in this work were subject to aging protocols. The aim of this study was to generate degradation kinetics of additives under varying accelerated aging conditions and to compare the protocols with respect to resulting degradation products. In addition to the effect of accelerated aging on half-life times of the additives themselves, the stability of polymers with and without additivation should be investigated. Details on additive degradation analyses are listed below:

- Choice of suitable degradation protocols, analytes and matrices
- Optimization of extraction and evaluation techniques
- Compilation of data on degradation products including the implementation of a corresponding mass-spectrometric library containing mass spectra of additives and their degradation products recorded in the BfR laboratory
- Dermal exposure assessment of degradation products
- Application of quantum-chemical calculations on additives to reconsider experimental degradation findings

### 3 Dermal exposure of consumers to polymer additives, contaminants and NIAS

#### 3.1 The Franz diffusion cell

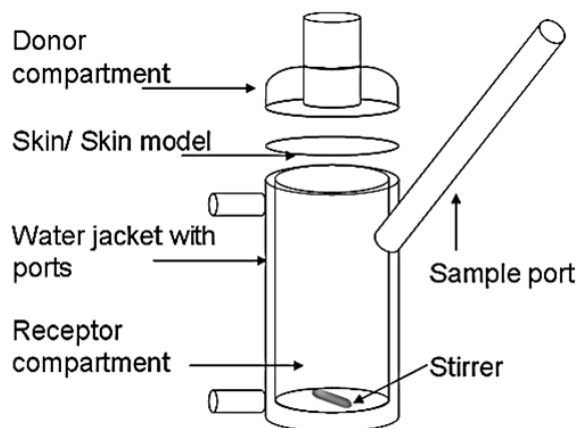


**Figure 2: Scheme of Franz diffusion cell set-up** (modified (16)).

Skin penetration is an important factor for assessment of dermal exposure. The *in vivo* testing of human skin penetration for CMR (carcinogenic, mutagenic, toxic for reproduction) or other toxic substances is ethically not acceptable. Therefore, an *in vitro/ ex vivo* method was adapted to CMR substances in polymeric material. According to the OECD guideline 428 “for the testing of chemicals – skin absorption: *in vitro* method” static FDCs were utilized for dermal exposure assessment (Figure 2). Utilization of excised human skin in FDCs is recommended as gold standard by which alternative testing protocols are compared. The data generated by applying the FDC-assay serve as reference values for the reliability of other testing methods. The receptor compartment was filled with saline solution to meet analytical and biochemical requirements. It was maintained at  $33 \pm 1^\circ\text{C}$  by a water jacket to simulate skin surface temperature. The application of test substances should be as realistic as possible (17). Therefore, a method to apply specimens of the original polymeric material of consumer products onto the skin was established. The distribution of PAHs and polymer additives into human skin and skin models was studied. This covered quantification of analytes in four compartments: 1) wash solution of donor compartment 2) tape strips with removed outermost s.c. layers 3) remaining epidermal layers 4) receptor solution. Tape stripping is a commonly used procedure to remove s.c. (18).



### 3.2 Skin models

Permeability of pig skin is close to that of human skin. Porcine epidermis is therefore known as a suitable skin model for human dermal exposure assessment (6). Due to the limited availability of animal skin or excised human skin and ethical reasons there is an increasing demand for alternative skin models. Reconstructed human epidermis (RHE) models are appropriate alternatives to porcine and human skin for *in vitro* testing (19). This could be shown for aqueous application of substances of diverse physico-chemical properties. Next to these keratinocytes based models, a completely synthetic multi-layered membrane on the basis of polyethersulfone and polyolefin was launched recently, Strat-M<sup>®</sup> membrane (MerckMillipore, Darmstadt, Germany). It was designed for usage in FDC. A good correlation of Strat-M<sup>®</sup> to human cadaver skin in permeability has been shown especially for chemicals with a molecular weight of less than 288 Da (20). Within this thesis, both reference skins, porcine and excised human skin, the RHE model EpiDerm 606X (MatTek, Ashland, MA) and the Strat-M<sup>®</sup> membrane were adapted to direct exposure to polymeric material of consumer products. The predictivity of each system was evaluated with respect to the permeability of the lipophilic PAH compound B[a]P (log P = 6.40) (21).

### 3.3 Transepidermal water loss - TEWL

For proving the integrity of excised skin used in the FDC-assay, a test for transepidermal water loss was conducted utilizing the AquaFlux device AF200 (Biox systems Ltd, London, UK). The principle of TEWL measurement bases on the flux of water diffusing from the viable epidermis through the s.c. towards the outer atmosphere *in vivo*. In case of the Franz cell set-up, it is the water diffusing from the receptor chamber through the skin specimen to the donor chamber. An increased TEWL is therefore indicative of damaged skin. To quantify this flux, the diffusing water is trapped as ice by a cold condenser coupled to the donor chamber. A humidity gradient appears and the water vapor flux density and TEWL can be detected by sensors (Figure 3).

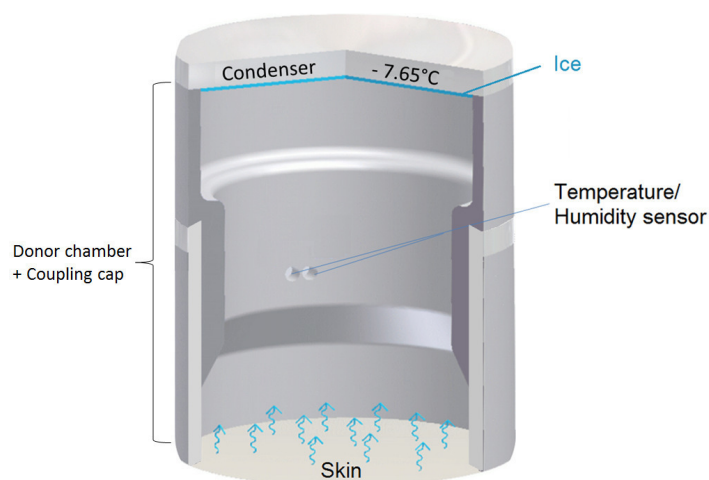


**Figure 3: Scheme of AF200 transepidermal water loss (TEWL) measurement** (adapted from Biox systems (22)).

### 3.4 Alternative migration testing and dermal exposure assessment

When dermal exposure assessment needs to be performed routinely, skin or skin models are used comparatively rare for cost and availability reasons. The complex FDC-assay is not practicable in these cases albeit this system generates the most realistic data. Up to now, migration procedure using aqueous sweat simulant is often required in several European standards like DIN EN ISO 105-E04 (13), DIN EN 1811 (23) or DIN EN 71-10 (24, 25). But correlations of those results with data generated in the FDC-assay using excised viable skin are almost missing.

Human sweat consists of 99.0–99.5% water and 0.5–1.0% solids (inorganic and organic in equal proportions). However, it does not represent the human SSFL much less the properties of the whole skin tissue (26). Averagely, the human SSFL are formed up to an amount of 50% by sebum. It is excreted by sebaceous glands. Main components are squalene, wax esters, triglycerides, free fatty acids, cholesterol esters, free cholesterol and vitamin E (26, 27). Thus, it is evident that artificial aqueous sweat solely is not sufficient to mimic dermal contacts of consumers to polymeric material. This is especially the case for lipophilic compounds for which the presence of lipids in the SSFL represents the driving force behind skin penetration. Hence this work revealed a significant underestimation of dermal B[a]P load after simulation of skin contact with

PAHs-containing consumer products when it was assessed utilizing artificial sweat compared to the results from excised human skin in FDC-assay.

Pursuant to Commission Regulation (EU) No 10/2011 there is a list of simulants to be used for testing migration of constituents of plastic materials and articles intended to come into contact with foodstuffs (28). It could be shown that water as prescribed simulant for milk is not sufficient to mimic its physico-chemical properties. However, the migration results for styrene out of polymeric matrix into milk with varying fat levels were directly correlatable to aqueous ethanol as simulant with varying levels of ethanol (29). Accordingly, addition of ethanol is suitable to adjust the degree of lipophilicity in aqueous simulant-based migration studies. This fact was adapted within the current work to the development of a new simulant, which is of virtual constitution and lipophilicity against high molecular PAHs similar to skin. The amount of B[a]P that migrated into the simulant under defined conditions is supposed to mirror the sum of permeated and penetrated B[a]P in the FDC-assay with human skin.

### **3.5 Visualization of skin penetration by PAHs and additives**

Most consumers are not aware of the dermal route of exposure to potentially harmful substances. Compared to oral exposure via food it is a more passive and unintentional way which contributes to the systemic exposure. Therefore, it is even more important to find a tool to clarify the relevance of the transdermal path. To illustrate the distribution of polymer additives and contaminants within the skin after contact, optical methods for non-destructive detection of fluorescent and non-fluorescent signals were applied. Exemplarily, pyrene - a PAH congener - is one of the most widely spread fluorophores used in cell biology in the form of probes (30). The auto-fluorescence of PAHs in general results from the delocalized electron systems. In case of pyrene, it can be used to label proteins for investigations on conformation changes (31).

In the present work, the auto-fluorescence of PAHs was used to analyze their percutaneous absorption. To investigate a depth profile of percutaneous PAH absorption, sections of the skin were performed perpendicular to the skin layers. The intensity of the fluorescent signal in inverted fluorescence microscopy was proportional to the amount of PAHs in the respective skin layers.

For non-fluorescent compounds migrating from polymers attenuated total reflectance - Fourier transform infrared (ATR-FTIR)-microscopy was applied as visualization tool to the skin sections alternatively. Distinct reference bands were assigned to the analytes of interest utilizing analytical standard substances. The skin sections were further divided in IR-spectrum grids using this technique. As a result heat maps were performed by displaying the intensity of the bands per grid point. These descriptive techniques impressively give an understanding of transdermal routes of exposure to potentially harmful polymer additives and also verify the analytical findings from FDC analyses.

## **4 Additives, contaminants and NIAS of toxicological relevance present in polymeric consumer products**

The majority of consumer products are made of a complex mixture of polymers and additives, which are intentionally added to modify the properties of polymers specifically. Beside additives also contaminants or NIAS are incorporated in polymers and might result into dermal exposure via skin contact. This chapter introduces substance classes of toxicological relevance and analytical techniques that can be used to reveal compositions of the tested material.

### **4.1 Polycyclic aromatic hydrocarbons - PAHs**

PAHs are unsubstituted and fused polycyclic aromatic hydrocarbons. In general, PAHs are formed through incomplete combustion of organic matter (32). They are ubiquitously present in the environment and there are several sources of exposure like tobacco smoke, grilled food or industrial processes (33-35). Some of them are genotoxic carcinogens (1, 36). Their presence in consumer products is conditioned by the usage of extender oil as plasticizer oil and of carbon black in polymeric formulations.

The 8 individual PAH compounds that are classified as presumed to have carcinogenic potential to humans category 1B are B[a]P, B[e]P, B[a]A, Chr, B[b]F, B[j]F, B[k]F and DB[a,h]A (1, 3). The main field of application of carbon black is in rubber for tires followed by non-tire applications as reinforcing agent (37). Furthermore, it is used as pigment, UV stabilizer and conductive additive in rubber, plastics, surface coatings and inks (37, 38). Because the dermal contact may contribute considerably to human exposure, the concentrations of these PAHs in consumer products made of polymers or rubber and with foreseeable direct prolonged or repeated short time skin contact are restricted to 1 mg/kg each, in toys the limit value is 0.5 mg/kg (2). Accordingly, in this thesis consumer products made of rubber or elastomers with black parts are particularly subject to exposure assessment of PAHs.

The furnace black manufacturing process is the most common way to produce carbon black, it needs heavy aromatic oils as feedstock (39). The oil is partially combusted in a closed reactor under defined reducing conditions including temperature (1400-1800°C) and residence time (0.03-10.00 s) (40). The exiting

carbon black consists mainly of pure elemental carbon agglomerates. It is collected in a filter and undergoes drying and any number of further processing steps to remove impurities (41). Further techniques like acetylene black, channel black or lampblack process receded due to environmental and yield issues (40). Depending on the feedstock used and the conducted processing steps, carbon black is available in various nuances of purity and particle size. Generally, the amount of PAHs in processed carbon black should be less than 1% (39).

The main focus is on long-term effects when it comes to the assessment of adverse health effects of PAHs. Depending on the route of exposure, the respective toxicity of the PAHs and the dose however, mixtures can cause eye or skin irritation, nausea and vomiting or inflammation (42). Long-term effects include various types of cancer, like lung, skin, bladder or gastrointestinal cancer. Interaction with deoxyribonucleic acid (DNA) and cardiopulmonary mortality are also reported as a consequence of chronic exposure to PAH (43).

Consumers are commonly exposed to a multitude of PAHs in products (44). There are basically three approaches to assess the risk associated: The surrogate approach, the relative potency approach or the concept of toxicity equivalency factors (TEFs) (45). While the surrogate approach considers the toxicity of B[a]P representative for the whole mixture, the carcinogenic potency of the individual PAHs can be differentiated by the concept of TEFs. By assigning a TEF of 1 to the lead compound B[a]P, the TEFs of all other PAHs express their individual relative carcinogenic potency to that of B[a]P (46). The TEFs were assigned to distinct PAHs according to several studies including *in vivo* carcinogenesis of rats and mice after PAH application and *in vitro* formation of PAH-DNA adducts (46). A compilation of TEFs and analytical information on the GC-MS/MS multi-analyte-method for PAHs is shown in Table 1. PAHs investigated in this work are either priority PAHs by U.S. EPA, by EFSA, by AfPS (German Product Safety Commission), classified by CLP Regulation as presumably carcinogenic for humans (carc. Cat. 1B) and restricted by Regulation (EC) No 1907/2006 (REACH) Annex XVII or are of interest because of their chemical structure (cf. Table 1). Also, a range of biological activity and physico-chemical properties was covered by the choice of PAH congeners. Previously reported studies showed a significantly higher carcinogenic potential of methylated PAH derivatives as compared to the unsubstituted parent compound or to the lead compound B[a]P.

For example 5-methylchrysene was found to be a stronger tumor initiator than the parent compound Chr and even B[a]P in mice and a potent carcinogen when tested on mice skin (47).

Because skin contact to PAHs can induce skin cancer, great emphasis was placed on the bioavailability of PAHs as a consequence of dermal contact to PAHs-containing consumer products in this thesis. The analytes were also applied without polymer matrix to human skin *ex vivo* in order to simplify this complex process of migration and penetration.

The distribution of individual PAHs within the skin layers was correlated to their molecular weight despite an initially migration step from the polymer to the skin surface. According to Fick's 2<sup>nd</sup> law of diffusion (cf. Equation 1) the mass diffusivity is proportional to the concentration gradient. As a consequence, the applied substances tend to migrate into the receptor solution which is free of PAHs in the beginning of the incubation period. As expected, the amount of PAHs in the receptor fluid is decreasing with increasing molecular size. Smaller PAHs consistently accumulated mainly in the receptor fluid. Nearly the entire initially applied amount of the smallest PAH naphthalene (Naph) was present in the receptor compartment after 24 hours indicating a high permeation rate through human epidermis (Figure 4). On the other hand, the five-ring PAHs (e.g. B[a]P) were mainly present in the s.c. and further epidermal layers but also permeated the epidermis to a lesser extent (10%). The six-ring dibenzopyrenes however did only occasionally enter the receptor fluid showing reservoir formation properties in the epidermis. In all cases a severe bioavailability needs to be considered.

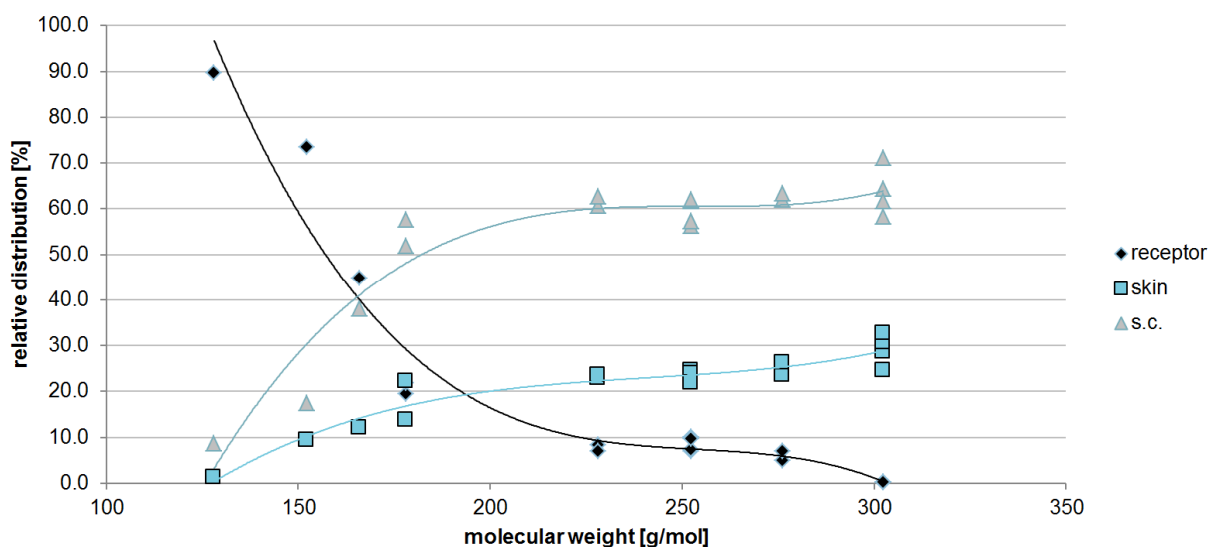


**Figure 4: Distribution of PAHs in human skin as a function of molecular weight.** A mixture of PAHs (cf. Table 1: Naph, Acy, Flu, Ant, Phe, B[a]A, Chr, B[b]F, B[a]P, B[e]P, I[c,d]P, B[g,h,i]Per, DB[a,l]P, DB[a,e]P DB[a,l]P, DB[a,h]P) solved in acetonitrile has been applied to human skin *ex vivo* in the FDC for 24 h with an amount of 50 ng per PAH each and skin, biological duplicates, (unpublished data).

The metabolism of B[a]P is well investigated. It has been the lead compound to study carcinogenic effects of PAHs for years after being isolated from coal tar in the early 1930s (48, 49). The metabolic activation of B[a]P by cytochrome P450-dependent (CYP) monooxygenases is responsible for its carcinogenicity, more precisely the diol-epoxide pathway (50). B[a]P is initially epoxidized by CYP1A1 to B[a]P-7,8-oxide which is further transformed by epoxide hydrolase (EH) to B[a]P-7,8-dihydrodiol (51, 52). Subsequently, this intermediate is oxidized in an additional CYP enzyme catalyzed process and the ultimate carcinogen B[a]P-(7R,8S)-diol-(9S,10R)-epoxide arises which may covalently bind to DNA with high stereoselectivity (53). Detoxification can take place via non-enzymatic hydrolysis (Figure 5). It was demonstrated that the metabolic capacity of excised human skin and keratinocytes based skin models is sufficient to activate B[a]P and cause genotoxic stress which may contribute to skin cancer (54).



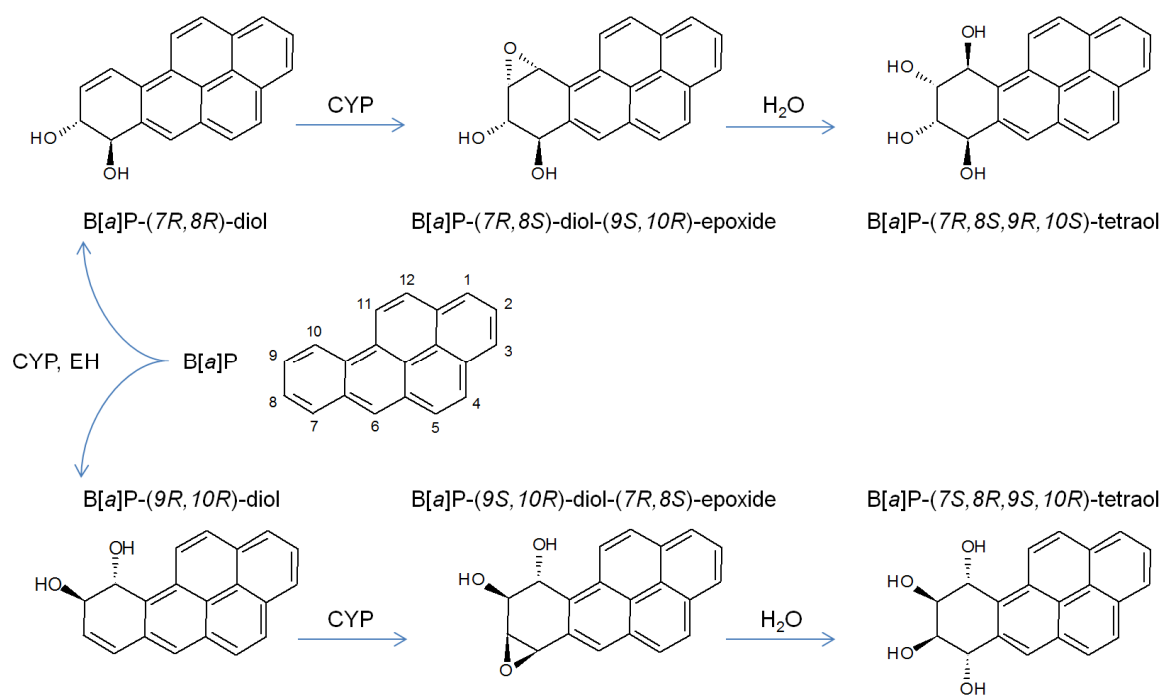


**Figure 5: Metabolic activation of B[a]P via diol-epoxide pathway to the ultimate carcinogen B[a]P-(7R,8S)-diol-(9S,10R)-epoxide.** CYP: cytochrome P450-dependent monooxygenases, EH: epoxide hydrolase, modified (50, 51).

Investigations on the relation between PAH structure and carcinogenic potential revealed significant differences among PAH representatives. The bay and fjord region turned out to play an outstanding role in carcinogenesis of PAHs (55). These structures are exemplarily present in B[a]P (bay) or DB[a,l]P (fjord) and lead to metabolically formation of highly electrophilic dilepoxides that can interact with DNA bases (56, 57) (Figures 5, 6). An increased contribution to non-genotoxic steps of tumor promotion of methylated PAHs with bay-like structures as compared to the non-methylated parent PAH was described (58, 59). 1-methylnaphthalene (bay-like), for example, inhibits the gap junction intercellular communication (GJIC) (60). The GJIC maintains the homeostatic control of neighboring cells. Inhibition can lead to clonal expansion of quiescent, initiated cells, constituting the tumor promotion phase (61).

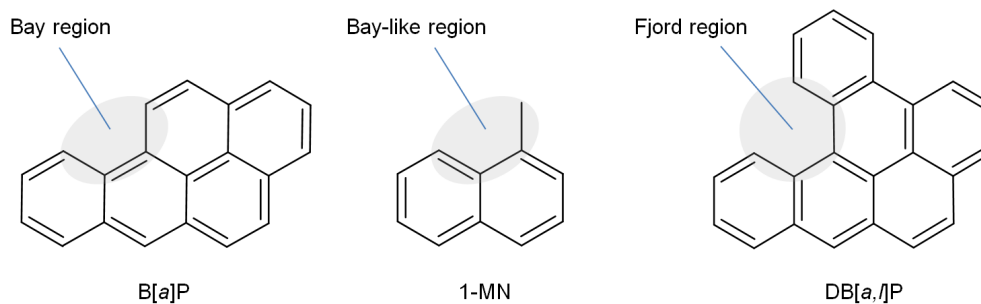
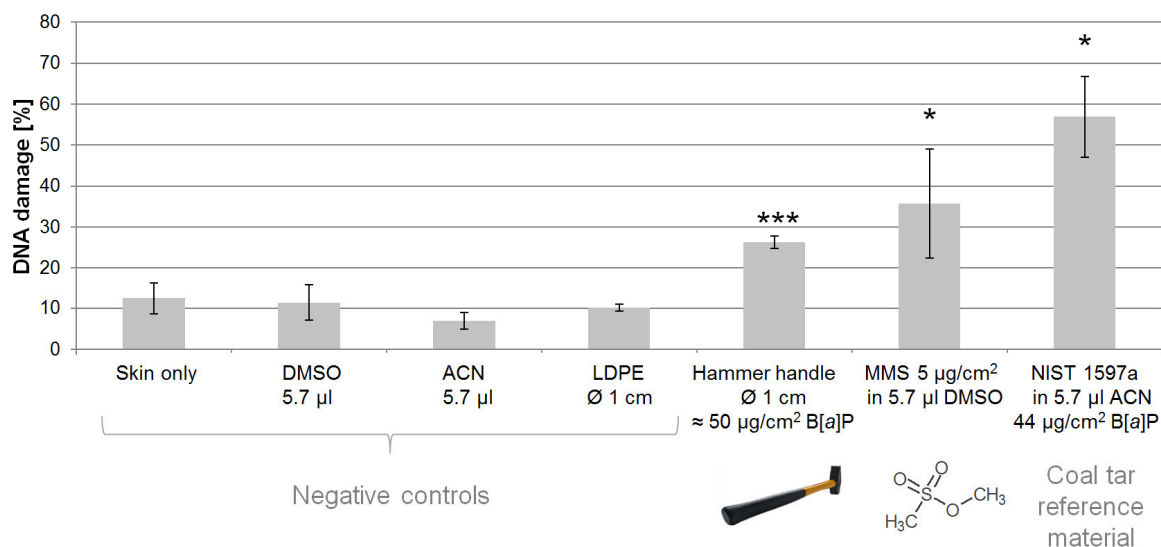


**Figure 6: Prominent chemical structures of PAHs involved in carcinogenesis.**

To understand the potential health risks associated with the transepidermal absorption of PAHs, it is important to follow up the skin integrity through several stages of exposure. The actual relevance of these studies was demonstrated by developing a comet-assay protocol (single-cell gel electrophoresis) for human skin *ex vivo*. The detailed procedure is described in Annex I. The influence of dermal exposure to consumer products entailing high PAH contents on DNA integrity in skin was investigated.

The comet-assay is a tool to detect DNA strand breaks in eukaryotic cells. It bases on the isolation of single cells in agarose with subsequent lysis using a detergent and salt to form nucleoids (62). The electrophoresis under alkaline conditions results in structures resembling comets in case of initial DNA damage. These are evaluated applying fluorescence microscopy. The fluorescence intensity and length of the comet tail relative to the comet head reflects the amount of DNA breaks (63).

The comet-assay has already been used on 3D reconstructed human epidermal skin models (64). In this thesis, it was applied to excised human skin immediately after abdominal plastic surgery to use a most realistic exposure model.

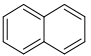
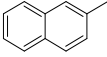
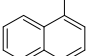
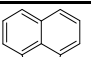
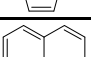
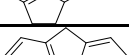
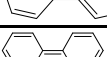
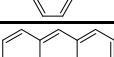
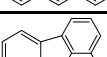
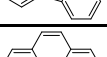
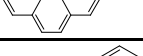
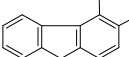
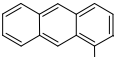


**Figure 7: DNA damage in human skin *ex vivo* after incubation in FDC with a consumer product assessed applying the comet-assay.** Combined evaluation of epidermis and dermis with biological duplicates; technical repetitions n=4; n=2 in case of coal tar reference material. Student's t-test was performed with  $\alpha=0.05$  (\*\* $p < 0.01$ ; \*  $p < 0.05$ ). Bars represent the standard error of the mean (unpublished data).

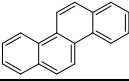
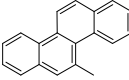
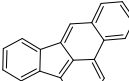
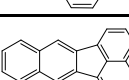
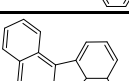
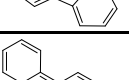
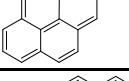
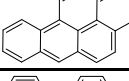
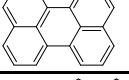
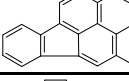
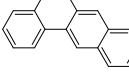
The results of the comet-assay clearly indicated significant higher genotoxicity *in situ* after dermal exposure to a consumer product that entails high amounts of PAHs (Figure 7) compared to an additive- and contaminant-free low-density polyethylene (LDPE) sample. The genotoxic effect observed needs to be considered a combined event of all genotoxic leachables of the handle, some of which might still be unknown.

## Leachables of toxicological relevance present in polymeric consumer products

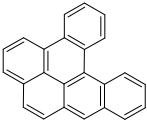
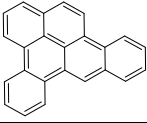
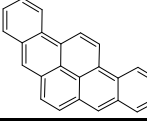
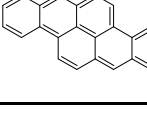
**Table 1: Information on PAHs and validation parameters of the respective GC-MS/MS MRM multi-analyte-method.**

No.	Compound	Abbreviation	CAS	TEF	Structure	Nominal mass [Da]	LOD [ng/ml]	Precurs or Ion	Product Ion Quanti	Product Ion Quali	Rf [min]
1	Naphthalene <sup>a, d</sup>	Naph	91-20-3	0- 0.001		128	6.41	128	102	127; 77	6.77
2	2-Methylnaphthalene	2-MN	91-57-6	-		142	2.58	142	142	141; 115	7.90
3	1-Methylnaphthalene	1-MN	90-12-0	-		142	2.57	142	142	141; 115	8.21
4	Acenaphthylene <sup>a, d</sup>	Acy	208-96-8	0.001		152	1.10	152	151	150; 126	10.15
5	Acenaphthene <sup>a, d</sup>	Ace	83-32-9	0.001		154	1.94	154	153	152; 127	10.40
6	Fluorene <sup>a, d</sup>	Flu	86-73-7	0.0005- 0.001		166	0.72	166	165	140	11.44
7	Phenanthrene <sup>a, d</sup>	Phe	85-01-8	0- <0.01		178	0.96	178	177	176; 152	13.75
8	Anthracene <sup>a, d</sup>	Ant	120-12-7	0- 0.01		178	1.18	178	177	176; 152	13.82
9	Fluoranthene <sup>a, d</sup>	Fluo	206-44-0	0.001- 0.08		202	0.61	202	201	200; 152	16.86
10	Pyrene <sup>a, d</sup>	Pyr	129-00-0	0- 0.001		202	2.19	202	201	200; 152	17.90
11	Benzo[c]fluorene <sup>b</sup>	B[c]F	205-12-9	20		126	1.81	216	216	215; 213; 189	19.39
12	Benz[a]anthracene <sup>a, b, c, d</sup>	B[a]A	56-55-3	0.005- 0.2		228	0.88	228	228	226; 202	24.46
13	Cyclopenta[c,d]pyrene <sup>b</sup>	C[c,d]P	27208-37-3	0.012- 0.4		226	1.92	226	226	225; 224; 225; 200	25.00

Leachables of toxicological relevance present in polymeric consumer products

14	Chrysene <sup>a, b, c, d</sup>	Chr	218-01-9	0.01- 0.17		228	1.40	228	228	226; 202	25.10
15	5-Methylchrysene <sup>b</sup>	5-Me-Chr	3697-24-3	7		242	0.93	242	242	241; 239; 226	28.85
16	Benzo[b]fluoranthene <sup>a, b, c, d</sup>	B[b]F	205-99-2	0.1- 0.8		252	0.43	252	252	250; 251; 250; 226; 248	35.06
17	Benzo[k]fluoranthene <sup>a, b, c, d</sup>	B[k]F	207-08-9	0.03- 0.1		252	0.40	252	252	250; 251; 250; 226; 248	35.30
18	Benzo[j]fluoranthene <sup>b, c, d</sup>	B[j]F	205-82-3	0.045- 0.52		252	1.05	252	252	250; 251; 250; 226; 248	35.56
19	Benzo[e]pyrene <sup>c, d</sup>	B[e]P	192-97-2	-		252	1.46	252	252	250; 251; 250; 226; 248	38.16
20	Benzo[a]pyrene <sup>a, b, c, d</sup>	B[a]P	50-32-8	1		252	3.48	252	252	250; 251; 250; 226; 248	38.57
21	Perylene	Per	198-55-0	-		252	4.77	252	252	250; 251; 250; 226; 248	39.54
22	Indeno[1,2,3-c,d]pyrene <sup>a, b, d</sup>	I[c,d]P	193-39-5	0.067- 0.1		276	1.93	276	276	274; 250	45.80
23	Dibenz[a,h]anthracene <sup>a, b, c</sup>	DB[a,h]A	53-70-3	0.1- 10		278	2.73	278	278	276; 274; 252	45.90
24	Benzo[g,h,i]perylene <sup>a, b, d</sup>	B[g,h,i]Per	191-24-2	0.009- 0.03		276	4.25	276	276	274; 250	47.87

Leachables of toxicological relevance present in polymeric consumer products

25	Dibenzo[a, <i>l</i> ]pyrene <sup>b</sup>	DB[a, <i>l</i> ]P	191-30-0	1- 100		302	16.22	302	302	301; 300	56.96
26	Dibenzo[a, <i>e</i> ]pyrene <sup>b</sup>	DB[a, <i>e</i> ]P	192-65-4	0.2- 1		302	15.26	302	302	300	59.46
27	Dibenzo[a, <i>l</i> ]pyrene <sup>b</sup>	DB[a, <i>l</i> ]P	189-55-9	0.1- 12		302	10.60	302	302	300	60.77
28	Dibenzo[a, <i>h</i> ]pyrene <sup>b, d</sup>	DB[a, <i>h</i> ]P	192-51-8	0.9- 11		302	15.67	302	302	300	61.50
<b>Internal standards (Istd)</b>											
1	Naphthalene-d <sub>8</sub>	Naph-d <sub>8</sub>	1146-65-2			136		136	134	108	6.73
2	Acenaphthylene-d <sub>8</sub>	Acenaph-d <sub>8</sub>	93951-97-4			160		160	160	158; 156	10.11
3	Phenanthrene-d <sub>10</sub>	Phe-d <sub>10</sub>	1517-22-2			188		188	184	160	13.69
4	Fluoranthene-d <sub>10</sub>	Fluo-d <sub>10</sub>	93951-69-0			212		212	210	208; 160	16.79
5	Pyrene-d <sub>10</sub>	Pyr-d <sub>10</sub>	1718-52-1			212		212	210	208; 160	17.82
6	Chrysene-d <sub>12</sub>	Chr-d <sub>12</sub>	1719-03-5			240		240	238	236; 212	24.86
7	Benzo[a]pyrene-d <sub>12</sub>	B[a]P-d <sub>12</sub>	63466-71-7			264		264	260	232	38.35
8	Benzo[ <i>g,h,i</i> ]perylene-d <sub>12</sub>	B[ <i>g,h,i</i> ]Per-d <sub>12</sub>	93951-66-7			288		288	288	286	47.67
9	Dibenzo[a, <i>l</i> ]pyrene-d <sub>14</sub>	DB[a, <i>l</i> ]P-d <sub>14</sub>	158776-07-9			316		316	314	312	60.48

List of priority PAHs: a) 16 U.S. EPA priority PAHs, b) 16 EFSA priority PAH, c) 8 CLP Regulation carc. Cat. 1B d) 18 AfPS priority PAHs

## 4.2 Mineral oil hydrocarbons - MOSH/ MOAH

Mineral oil is used as raw material in many applications such as printing oil, plasticizer oil in consumer products, technical lubricants or in cosmetics. It is principally refined and divided into fractions of different volatility by distillation of crude oil (65). Further physico-chemical processing steps like extractions are applied after distillation to isolate particular petroleum fractions as for example light and heavy naphtha. From a chemical perspective, mineral oil was processed by different steps from crude oil and consists of aliphatic compounds like paraffins (open chain alkanes) and naphthenes (hydrocarbons with at least one saturated ring) and aromatic compounds (66). Mineral oil saturated hydrocarbons (MOSH) and mineral oil aromatic hydrocarbons (MOAH) are typical constituents. Different from unsubstituted PAHs, the MOAH are predominantly highly alkylated polycyclic aromatic hydrocarbons (67). The final concentration of aromatic hydrocarbons in the product depends on the grade of the oil refining. The content of this portion in mineral oil vary and the particular composition is attributable to the respective feedstock used. Technical hydrocarbons usually entail a higher amount of MOAH up to 35 % while this fraction is minimized in so-called food grade white oils and waxes by further hydrogenation steps (68).

Mineral oil hydrocarbons can be organized according to their carbon-number and maximum volatility region. An exposure to alkanes with a carbon-number of  $>C_{35}$  is negligible with respect to missing absorption (68). A feeding study with Fischer 344 rats revealed MOSH of  $C_{16} - C_{35}$  accumulating mainly in liver, adipose tissue and spleen (69). Oral administration of MOSH is of low acute toxicity in general. The accumulation in liver, however, caused formation of microgranulomas in rats associated with inflammatory responses (70). But its relevance for humans is unclear and still under discussion. In a study with 37 subjects, the distribution of mineral oil hydrocarbons in various human tissues was investigated. While MOAH did not accumulate, the MOSH varied in composition and amount between subjects and organs and highest amounts were found in mesenteric lymph nodes (71).

Exposure to MOAH fraction is undesirable because it might contain carcinogenic aromatic compounds such as PAHs. Skin painting studies on rat skin demonstrate that mineral oils may induce skin cancer (72). But the carcinogenic potential of

mineral oil is closely linked with the purity, the composition and the amount of MOAH present in the final product (73). There is also evidence of mineral oils used in printing inks being endocrine disruptors and exposure might contribute to the estrogenic burden in humans (74).

Recently, mineral oil components have been identified in human milk (75), tissues and organs (71). Thus, the need for research on routes of exposure was emphasized. The transfer of mineral oil components into food from packaging material was reported as a potential source for oral exposure (76). Especially food packaging made of recycled board is of concern because printing ink from newspapers as part of the recycling process is still present in the final product (77, 78). Cosmetic products containing mineral oils, waxes or white oils might be an additional source of dermal exposure (79). But highly purified pharmaceutical grade products are used in cosmetics, so the risk of skin cancer is unlikely. In consumer products of polymeric material mineral oil is commonly used as plasticizer (80). A detailed profile of MOSH and MOAH was determined of several consumer products designated for skin contacts within this thesis (7) and identified as potential source of transepidermal exposure.

#### **4.2.1 Volatility dependent distribution of mineral oil components in human skin**

Mineral oils are used as plasticizer oils in consumer products of polymeric material and may result in dermal exposure. Usually, the purity of oils as well as their volatility, viscosity and range of carbon number are unknown. But these parameters may influence the biodistribution in and the kinetics on human skin and could be relevant for dermal exposure.

To characterize these effects corresponding studies on biodistribution of mineral oil fractions in skin have been performed using the FDC-assay (unpublished data). The FDC protocol for dermal exposure assessment of liquid or paste-like mineral oil formulations is described in Annex I of this thesis.

Two mineral oil products were chosen to cover different volatility regions reflecting different ranges of carbon-numbers with respect to real exposure scenarios and to adapt the FDC to diverse mineral oil components: oil used in printing ink (Gravex 913, (81)) and petrolatum (vaseline) (Figure 8). Both products were analyzed applying online-LC-GC-FID to determine the hydrocarbon composition.



While Gravex 913 is composed of hydrocarbons in the range of C<sub>13</sub> - C<sub>27</sub>, vaseline entails higher molecular hydrocarbons in the range of C<sub>20</sub> - C<sub>50</sub>. Also the amount of aromatic hydrocarbons within the formulation differs: Gravex is composed of approx. 25% aromatic hydrocarbons and vaseline entails only 2% of this aromatic fraction (Figure 8). The recovery of hydrocarbons was >96% in both cases as related to the weighed portion. The remaining part might entail additives in case of Gravex 913 or might result from discrimination of higher molecular hydrocarbons during sample clean-up or online-LC-GC-FID-analysis in case of vaseline. The MOAH content in vaseline might be present due to usage of slack wax or base oil in the formulation instead of pharmaceutical grade raw material only.

Accordingly, the more volatile hydrocarbons of Gravex 913 (both, aromatic and saturated) showed significantly higher accumulation in the epidermal layers as compared to the low volatility fractions of vaseline. After 24 h of incubation, more than 70% of the total amount of applied Gravex 913 hydrocarbons entered the epidermis. However, less than 10% of the respective fractions of vaseline overcame the human skin barrier under equal conditions. No hydrocarbons were detectable in the receptor solution in all cases. The detailed results for MOSH and MOAH are illustrated in Figures 9 and 10. As a result, skin permeation of mineral oils clearly depends on volatility, viscosity and carbon numbers respectively. Mineral oils with lower carbon numbers amount to higher transepidermal exposure. The results are in excellent accordance with the size dependent distribution of PAHs reported in this work in chapter 4.1 (Figure 4).

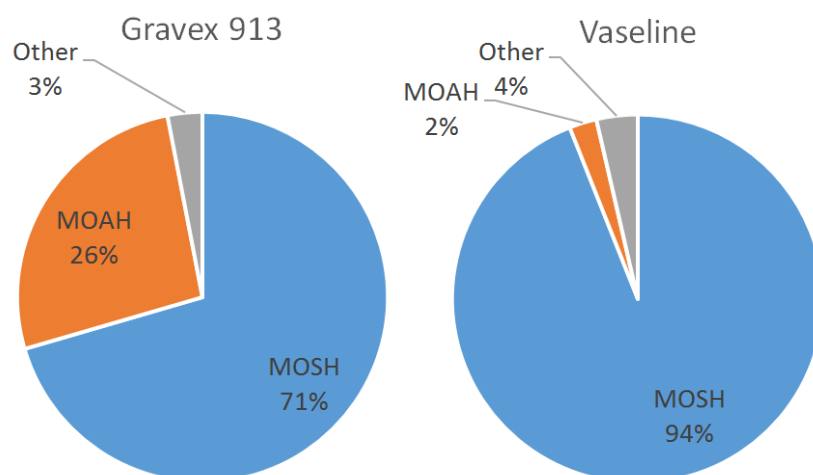


**Figure 8: Composition of two mineral oil basing formulations.** Printing ink oil (Gravex 913) and a vaseline sample were characterized with respect to their hydrocarbon composition and analytical recovery using online-LC-GC-FID (7).

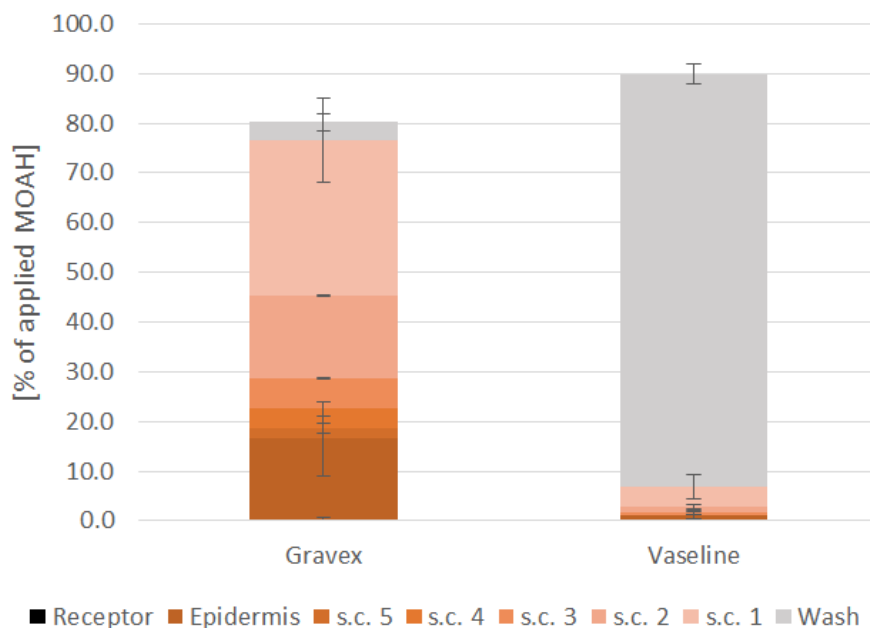


**Figure 9: Recovery and MOAH distribution within human epidermis after contact to mineral oil based products in FDC.** Excised human skin was incubated for 24 h with either Gravex 913 (printing oil) or vaseline in FDC. Recovery refers to the originally applied portion of MOAH. Gravex: n=2, vaseline: n=3. Bars represent the standard error of the mean.

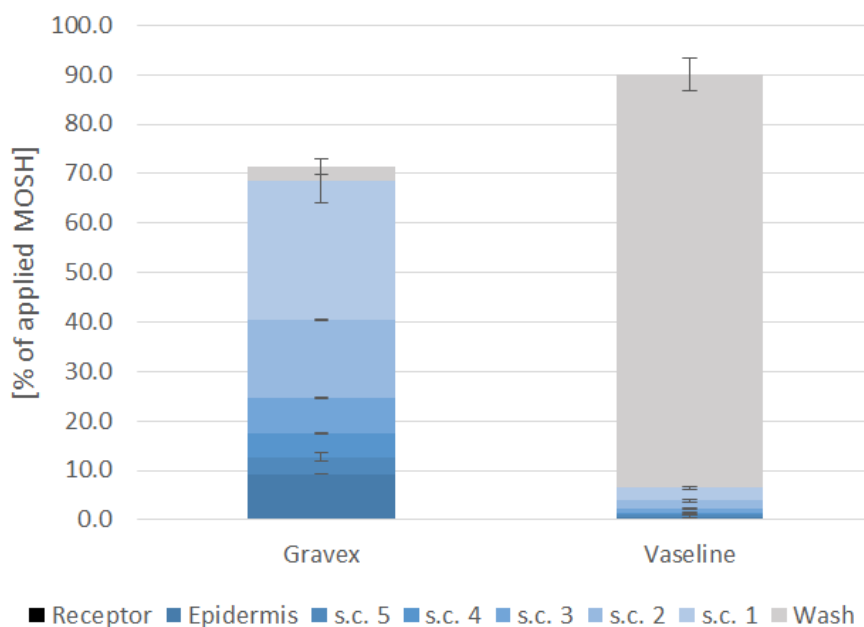


**Figure 10: Recovery and MOSH distribution within human epidermis after contact to mineral oil based products in FDC.** Excised human skin was incubated for 24 h with either Gravex 913 (printing oil) or vaseline in FDC. Recovery refers to the originally applied portion of MOSH. Gravex: n=2, vaseline: n=3. Bars represent the standard error of the mean.

### 4.3 Additives

Polymer additives are intentionally used to influence the haptic occurrence, technical properties and production costs of the final product. For stabilization and longevity of a product, phenolic and arylamine based stabilizers are commonly used, while phthalates and phthalate substitutes are used as plasticizers. Because of their toxicological properties the question needs to be addressed whether dermal exposure may occur. This issue has been investigated in this thesis for representative additives of the additive classes described in this chapter.

#### Phenolic stabilizers

Sterically hindered phenols are commonly used as stabilizers or antioxidants respectively in polymers and rubber. These can be classified according to the amount and regions of *tert*-butyl groups in 2, 4 or 6-position (82). The phenolic moieties are responsible for the actual stabilization process by acting as radical scavengers (Figure 11). Most stabilizers have an additional so called secondary structure which determines the physical behavior of the additive in the polymer matrix (83) (cf. Figure 11, R<sub>1</sub> or R<sub>2</sub>).

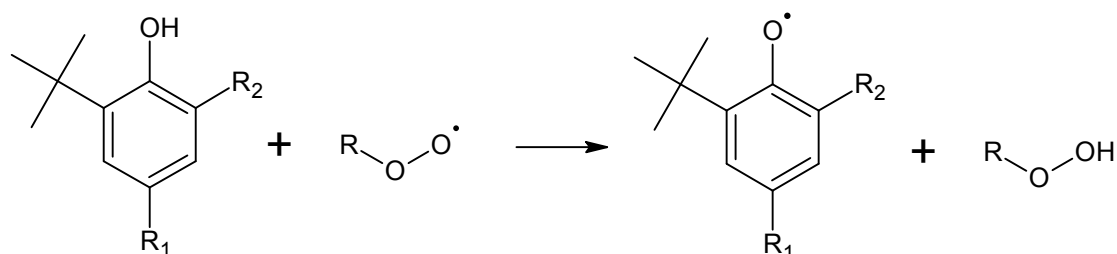


**Figure 11: Initial reaction of the stabilization process of phenolic antioxidants.** R<sub>1</sub>, R<sub>2</sub>: secondary structure residues of the antioxidant; R: residue specific to the respective polymer.

From a toxicological point of view, the usage of phenolic antioxidants in consumer products is still under debate. Dermal exposure to phenol derivatives such as 4-*tert*-butylphenol can lead to vitiligo and the substance was also proven to cause oxidative stress in melanocytes in this context (84). The interference of antioxidants used in rubber biomaterial with tumor promotion was investigated and increased tumor incidence for some phenolic additives determined (85).

There are some regulations concerning the usage of phenolic stabilizers in food contact materials and further commodities. The amount of phenolic antioxidants

present in consumer products made of rubber is regulated in the BfR recommendation XXI. on commodities based on natural and synthetic rubber (86). Depending on the intended use of the product, mainly duration of food contact, different compositions of phenolic antioxidants are recommended with a combined maximum content of 1%. There is a special category of commodities according to § 2 of the German food and feed act (German: *Lebensmittel-, Bedarfsgegenstände- und Futtermittelgesetzbuch* (LFGB)). This category entails commodities intended for use as eating utensils or that may be expected to be placed in the mouth (e.g. toys). In case of teething rings, pacifiers or baby bottle nipples only two antioxidants are recommended to be used for pre-stabilization purposes: 2,6-di-*tert*-butyl-4-methylphenol for synthetic rubber (max. 1%) and 2-*tert*-butyl-6-[(3-*tert*-butyl-2-hydroxy-5-methylphenyl)methyl]-4-methylphenol (Antioxidant 2246) for natural rubber matrix (max. 0.4%) (86). The latter was investigated in this thesis because of this precarious field of application to reveal potential risks associated with aging of this additive.

The toxicological classification of several additives investigated in this thesis is still in progress. The U.S. EPA characterized the hazard associated with bridged alkylphenols some years ago and attributed moderate persistence and low bioaccumulation properties (87).

The evaluation of the sulfur-bridged phenol 2-*tert*-butyl-4-(5-*tert*-butyl-4-hydroxy-2-methylphenyl)sulfanyl-5-methylphenol (Santonox), however, needed to be regarded separately because of its different physico-chemical and toxicological properties compared to carbon-bridged phenols. It is currently on the Community rolling action plan (CoRAP) list of the European Chemicals Agency (ECHA) as suspected CMR, PBT (persistent, bioaccumulative, toxic)/ vPvB (very persistent, very bioaccumulative) substance, potential endocrine disruptor and sensitizer (88). The CoRAP is part of the REACH Regulation and indicates substances for evaluation by the Member States. A substance is subject to evaluation within three years after being listed. This process aims to clarify the initial concern of a potential risk to human health or the environment (89). Additionally, Santonox will be evaluated in the next years because of its wide dispersive use. It was demonstrated in this thesis that dermal contact to Santonox entailing polymers leads to reservoir formation of this additive in the s.c. (15).

### **Secondary arylamines used as stabilizers**

The polymer protective functionality of the secondary arylamines bases on a radical chain stopping mode of action by donating a hydrogen (90). *N*-phenylnaphthalen-2-amine (Neozon D) is a commonly used antioxidant. Its toxicity is attributed to the potential metabolic activation to the carcinogen 2-naphthylamine (2-NA). Previously reported studies on Neozon D in humans and mammalian species revealed that 2-NA is excreted into urine to a slight extent after exposure to Neozon D and metabolically dephenylation of the substance of origin (91, 92). The exposure to 2-NA is of concern because it is classified to be a known carcinogen to humans (Cat. 1A) according to the European CLP Regulation (1) and the International Agency for Research on Cancer (IARC) (93). An increased risk of bladder cancer has been observed in workers exposed to Neozon D and 2-NA working in the rubber and dye industry, where 2-NA has been formerly used to synthesize azo dyes (94). Neozon D has also been identified as a major sediment contaminant and its environmental toxicity has been studied. There is evidence for Neozon D affecting the photosynthesis in algae by acting as an intracellular reactive compound leading to irreversible cumulative damage (95).

The structural similarity between *N*-phenylnaphthalen-1-amine (Nonox A) and the procarcinogen Neozon D demands further risk evaluation. Currently, Nonox A is under discussion by the ECHA as a suspected PBT/ vPvB substance and the data are currently under review (96). It will therefore be decided in the next years if further risk management measures are required. In this work, both arylamines were found to enter the viable human epidermis *ex vivo* and the dermal route of exposure emphasized.

### **Phthalates and other plasticizers**

The group of phthalates is commonly used as plasticizers in polyvinyl chloride (PVC). Phthalates and other plasticizers can be added to the material with a final concentration in the high percentage range. They are used in consumer products like children's toys, food packaging and medical devices (97).

Phthalates are of research and regulative interest because of the associated toxicity. Developmental toxicity and the rat phthalate syndrome were identified as end points of major concern (98). It was demonstrated that exposure to phthalates with three to eight carbon atoms in the main side chain during gestation leads to

androgen deficiency in the male offspring, e.g. exposure to diethylhexylphthalate (DEHP) (99). The effects on the reproduction system are the most critical ones. Consequently, DEHP and further phthalates are classified presumed human reproductive toxicant (Cat. 1B) by the CLP Regulation (1). DEHP is listed in the Annex XIV of the REACH Regulation as substance of high concern and therefore subject to authorization. Furthermore, in Annex XVII of the REACH Regulation the use of 3 classified phthalates (DEHP, DBP, BBP) in toys and child care articles is restricted to a limit value of 0.1% by weight of the plasticized material (2).

Therefore, the demand for phthalate substitutes as plasticizers steadily increased over the last years. TOTM is a commonly used DEHP substitute. It shows weaker hepatotoxicity than DEHP (100), low skin sensitization properties in a patch test (101) but estrogenic activity in estrogen receptor alpha and beta (102). It was found that the interactions between TOTM and polymer are temperature related either basing on TOTM aggregates or free TOTM (103).

Not all of the possible plasticizer-matrix combinations provide equal flexibility. Exemplarily, the plasticization effects of dioctyl phthalate (DOP) in PVC decrease with increasing LDPE incorporations (104). To meet this matrix interactions, two different types of plasticizers are available: external and internal plasticizers (105). While TOTM and DEHP are external plasticizers embedded in the polymer by non-covalent interactions of polar groups, NBBS is a plasticizer mainly used in the polymerization process of polyamide (PA), polyacetals and polycarbonates (106) and is a representative of internal plasticizers. It is a water-soluble neurotoxic polymer additive and often reported as an environmental contaminant (107-109).

#### **4.4 Polymer composition – an analytical point of view**

The selection of representative additives, contaminants, NIAS and degradation products of toxicological relevance investigating dermal exposure, was based on their occurrence in polymeric consumer products and consequently on their analytical detection. Different analytical methods have been developed, optimized and adapted to various analyte-matrix combinations.

The motivation to choose the respective analytical techniques was to meet requirements of the analytes and to cover different substance classes of toxicological relevance. As target approach GC-MS/MS-technique was used to identify and quantify polymer additives, contaminants and degradation products as

a basis with high selectivity and sensitivity. Pseudo-transitions of the precursors in the developed multiple reaction monitoring (MRM) method for PAHs enabled matrix signal minimization with enhanced sensitivity (110, 111).

The non-targeted approach using GCxGC-ToF-MS is commonly applied to identify petroleum metabolites in environmental samples from fuel release sites (112). Furthermore, it is used in oil spill forensics to determine fingerprint chromatograms in order to make the oil traceable to its origin (113). In this work, the two dimensional gas chromatography was used on extracts of polymeric material from consumer products to efficiently separate components in a complex mixture. Further, it was used to characterize single species of a group of structurally related substances. While the aromatic hydrocarbon components were quantified as total MOAH using online-LC-GC-FID, the degree of alkylation of particular PAHs has been characterized applying GCxGC-ToF-MS. Because PAH derivatives evidently have different biological modes of action, it is important to classify the exposure to PAHs from consumer products accordingly. Therefore, the degree of PAH alkylation was determined in addition to the PAH amount in complex mixtures like coal tar extracts and black polymers in this work.

Online-LC-GC-FID became a versatilely applicable tool for the quantitative analysis of mineral oil. Furthermore, the normal phase LC is preparatively used to generate mineral oil fractions separated into MOSH and MOAH in this set-up in the field of edible oils, cosmetics and packaging material. One major advantage is that the whole LC-fraction can be transferred to the GC resulting in high sensitivity (114). The FID is suitable because it provides a linear response for a wide concentration range of organic compounds. An alternative method to investigate mineral oil hydrocarbons and PAHs is the quantitative nuclear magnetic resonance spectroscopy (qNMR). The NMR analysis of MOSH and MOAH bases on the different spectral regions of the signal of aromatic protons and protons of saturated compounds (115). Therefore, there is no need for fractionation prior to analyses in case of pure mineral oil samples without interfering matrix.

Pyrolyzates of the polymeric material were used in this thesis to determine the material composition. Online-Pyr-GC-MS is mainly used for identification purposes in material science. Unique substances, or substance clusters, need to be

identified in the decomposition pattern and attributed to certain areas of the raw material for positive identification (116).

The online-Pyr-GC-MS does not require extensive sample preparation. The thermal impact can directly be applied to the material of interest or chemical standard substances. This aspect allows investigations on matrix effects. Furthermore, this technique was used in this work to accelerate aging of material and additives and directly transfer resulting degradation products online to the GC-MS-system for separation and detection.

ATR-FTIR spectroscopy is a technique commonly applied to polymers to reveal compositions, to determine the state of conservation and to monitor degradation processes (117). In this thesis, it was not only used to follow up the depletion of polymer additives within the material but also to visualize the skin penetration process by additives during contact to polymers. The coupling to microscopy using a germanium crystal allows non-invasive analysis of the sample and imaging. An advantage is that multiple analytical techniques can be applied to the same sample. That makes FTIR-microscopy applicable even to analyses of old master paintings (118). The special correlation of IR signal to certain structures of a sample is also very important for tissue analysis. The distribution of intrinsic factors (119) as well as of xenobiotics (15) can be traced in particular tissue structures.



## 5 Degradation of polymeric material – What comes after stabilization?

In general, degradation products might be of concern in consumer products because of their diversity and unknown chemical structure. The amount and composition of degradation products that are formed during a product life cycle essentially depend on the thermal and mechanical load. Data on degradation products in polymers are rare. To cover this with respect to worst case scenarios and screening, accelerated aging needs to be employed in material research.

The polymeric material loses its integrity during aging and effects like brittleness or color changing (e.g. yellowing) occur. Aging of polymeric material thus facilitates the release of once embedded or absorbed components, especially lipophilic ones (120).

The aging of material is mainly triggered by the impact of oxygen, light or heat on the polymer (cf. Figure 12). The resulting homolytic cleavage causes radical formation leading to a radical cascade reaction. For example, the thermal decomposition of poly(dimethylsiloxane) (PDMS) causes formation of  $\text{CH}_3$  radicals by homolytic cleavage of the Si- $\text{CH}_3$  bond and subsequent formation of methane by hydrogen abstraction (121).

The progress of this cascade can be slowed down by addition of stabilizers to the material. Some of these show a higher affinity to interact with the radicals compared to the polymer itself, form less reactive intermediates and thereby stop further radical formation. The resulting reaction products are considered NIAS.

### 5.1 Principles of polymer stabilization

There are mainly three types of stabilizers used in polymers:

- a) Primary antioxidants – e.g. sterically hindered phenols, secondary aromatic amines
- b) Secondary antioxidants – e.g. sulfur-based hydroperoxide decomposers
- c) Multifunctional stabilizers – combined primary and secondary antioxidative functionalities.



( $R_2N-O\cdot$ ). It is formed and regenerated continuously while hydroperoxide is decomposed into the respective alcohol.

Another group of stabilizers is of particular importance for the weatherability of polymers. Benzotriazole based stabilizers are added to the material in order to increase its UV resistance. Different to previously described antioxidants, 2-(benzotriazol-2-yl)-4-methylphenol (Tinuvin P) stops radical formation prior to initialization of the radical cascade by quenching excited species and absorbing UV light (126).

## 6 Results

### 6.1 Target analysis of polycyclic aromatic hydrocarbons (PAHs) in consumer products and total content of polycyclic aromatic compounds (PACs)

Nastasia Bartsch, Christoph Hutzler, Bärbel Vieth, Andreas Luch, *Polycyclic Aromatic Compounds*, 2016, 37: 114-121.

Issue 2-3: The 25<sup>th</sup> International Symposium on Polycyclic Aromatic Compounds (ISPAC 25)

Published online: 13 Jun 2016

DOI: 10.1080/10406638.2016.1189440

Link: <https://doi.org/10.1080/10406638.2016.1189440>

Involvement of the author within this publication: Project planning: 65%, project execution: 90%, data analysis: 80%, writing of the manuscript: 80%

**Abstract**

The fabrication of consumer products is tightly linked to the usage of polymeric materials. The application of mineral oil products as plasticizers or lubricants in this manufacture is very common and so is the addition of carbon black for coloring and abrasion resistance purposes. Whereas mineral oils often contain highly alkylated aromatic species, alkylation of polycyclic aromatic compounds (PACs) is rather low or even absent in the case of carbon black. Since they are broadly applied in various products, consumers might get exposed to PACs, for instance, via dermal contacts. Here, we characterized several commodities not only via the common way of targeted analysis for their contents on PAHs, but also with regard to its total amounts of unsubstituted and substituted aromatic hydrocarbons.

The methods applied to analyze consumer products were as follows: (i) online coupling of liquid chromatography to gas chromatography with flame ionization detection (LC-GC-FID) for quantification of total PAH and MOSH (mineral oil saturated hydrocarbon) contents; (ii) coupling of tandem mass spectrometry to gas chromatography (GC-MS/MS) to quantify occasionally occurring PAHs with high specificity; and (iii) 2D gas chromatography coupled to mass spectrometry (GCxGC-ToF-MS) to characterize the complex mixtures concerning analytes' ring systems and degrees of alkylation. We found PAH contents in the range of parts per million (ppm) in consumer products while overall amounts of aromatics were in the percent range.

**Keywords:** Consumer products; online-LC-GC; PAHs; total PAC content.

## Introduction

Mineral oils obtained from distillates of crude oil containing highly alkylated polycyclic aromatic compounds (PACs) are often used as plasticizers or lubricants in the manufacture of polymers. Since crude oil is a product of anaerobic decomposition of organic matter, it consists of hydrocarbons of various sizes and substitutions. Among PACs, several extremely potent carcinogens could be identified in crude samples<sup>1</sup>. As it could be shown that parts of mineral oil constituents are present in human tissues<sup>2</sup>, the source of exposure for mineral oil saturated hydrocarbons (MOSHs) and corresponding mineral oil aromatic hydrocarbons (MOAHs) is of particular interest. Similarly, carbon black that contains PACs of no or low alkylation degree might have also been added for the purpose of coloring and abrasion resistance. Hence, consumers might be exposed to PACs through a range of different PAC-containing products, for instance via dermal contacts (Figure 1).

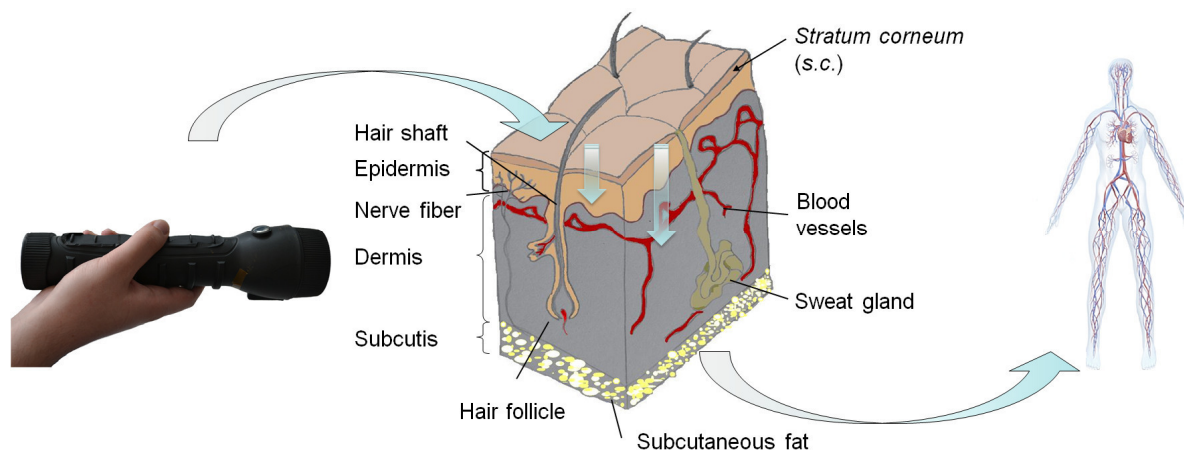


**Figure 1.** Schematic migration and penetration of PACs: from consumer products to body burden.

Consumer products that will cause skin contacts to polymers during predictable usage have been evaluated with respect to PAC profiles of the polymer. Especially, black polymers have been tested due to their potential carbon black content. We characterized several commodities applying a commonly performed targeted analysis for their contents on PAHs. We also looked into the total amounts of unsubstituted and substituted aromatics as well as saturated hydrocarbons. The results of targeted and untargeted analyses of PACs were compared with respect to the total amount of MOAHs in relation to the amount of the eight “EU PAHs” addressed in the European REACH regulation and rated as carcinogens (CMR 1B).

## Materials and methods

### *PAH analysis using GC-EI-MS/MS*

The sample material was shredded into small pieces of about 2 x 2 x 1 mm using a scalpel. Subsequently, the extraction was performed at 60°C in toluene for 2.5 h using an ultrasonic bath according to the ZEK 01.4-08 method<sup>3</sup>. Aliquots were evaporated close to dryness and resolved in acetonitrile for analysis. PAH analyses were conducted by means of GC-MS/MS (GC7890-MS7000A; Agilent, Waldbronn) using an Rxi-17SilMS column (30 m/0.25 mm ID/0.25 µm df; Restek, Bad Homburg), as well as a pre-column (5 m x 0.25 mm ID.; Phenomenex, Aschaffenburg, Germany). Helium was used as carrier gas (purity ≥99.999%, Linde, Pullach, Germany). The instrument was utilized with a MultiPurpose Sampler MPS (Gerstel, Mülheim, Ruhr, Germany). Injection temperature program using a cooled injection system (PTV-type CIS; Gerstel) applying an injection volume of 1 µl was 45°C, followed by a ramp of 12°C/s to 340°C. The following GC temperature program was used: 70°C for 0.5 min, structured ramp: 25°C/min to 110°C for 0.5 min, 12°C/min to 250°C, 1°C/min to 270°C, 10°C/min to 280°C, 4°C/min to 320°C, then 4°C/min to 340°C. Tandem MS analysis was carried out in multiple reaction monitoring (MRM) mode. To ensure specificity, a pseudo fragmentation reaction was monitored in addition to at least two other fragmentations for each analyte. The MRM parameters for the eight PAHs that have been prioritized by the European Union were as follows: for analysis of chrysene (Chry) and benz[*a*]anthracene (B[*a*]A),  $m/z=228$  has been selected as precursor and pseudo-transition ion at a collision energy (CE, collision gas: nitrogen 5.0, purity ≥ 99.999%, Linde, Pullach, Germany) of 18 V and two further transitions to  $m/z=226$  (26 V) and to  $m/z=202$  (20 V). For benzo[*a*]pyrene (B[*a*]P), benzo[*e*]pyrene (B[*e*]P) and benzo[*b/k/j*]fluoranthenes (B[*b/k/j*]F),  $m/z=252$  has been selected as precursor and pseudo-transition ion at CE of 35 V, as well as further transitions to  $m/z=251$  (35 V), 250 (42 V), 226 (35 V) and  $m/z=250$  to 248 (40 V), respectively. For analysis of dibenz[*a,h*]anthracene (DB[*a,h*]A) one pseudo-transition ion of  $m/z=278$  (35 V) has been evaluated, and ion transitions of  $m/z=278$  to 276 (40 V) as well as  $m/z=278$  to 274 (40 V) and to  $m/z=252$  (30 V) were selected as further product ions. To ensure a linear range of quantification, calibration stocks of standard solutions in acetonitrile were used in concentrations of 15 – 1000 ng/ml or 30 – 2000 ng/ml. Data were acquired with Enhanced MassHunter B.06.00 software (Agilent) and Maestro 1.4. software (Gerstel) with a dell workstation.

## **Mineral oil hydrocarbon analysis using LC-GC-FID and GCxGC-ToF-MS**

Polymeric material of consumer products was prepared similar as described in the section above (PAH analysis) but submerged in hexane. Extraction was performed at room temperature for 24 h. Subsequently, aliquots were either analyzed via LC-GC-FID (Phoenix 9000, K8880561; Brechbühler; Schlieren, CH and Thermo Scientific; Waltham, MA), or by means of GCxGC-ToF-MS (G3440A-7890A; Agilent) in scan mode.<sup>4,5</sup> Online-LC-GC-FID parameters<sup>6</sup> were applied with the LC column LiChrospher Si 60 (250 mm/2 mm ID/5 µm; Grace, Columbia, MD, USA), GC column ZB-1HT Inferno (15 m/0.25 mm ID/0.10 µm df; Phenomenex) and base temperature of FID of 385°C. A sample volume of 50 µl was injected, for MOSHs transfer at 1.7 min for 3.2 min and backflush at 6 min for 15 min was applied and for MOAHs at 4 min for 5.5 min with backflush at 6 min for 15 min. Data were acquired using ExaChrom (version 4.6; Brechbühler) and Phoenix software (LC-GC 9000; Brechbühler).

Using GCxGC-ToF-MS with column DB 17 (15 m/0.25 mm ID/0.25 µm df; Agilent) in first dimension with an uncoated pre-column (10 m/0.53 mm ID.; Phenomenex) and column ZB-5 (1.6 m/0.18 mm ID/0.18 µm df; Phenomenex) in second dimension, analyses were carried out by collecting total ion chromatograms in the scan mode and the mass range of 35 – 500 amu using a sample volume of 1 µl. Helium was supplied at a constant flow rate of 1.0 ml/min (purity ≥99.999%, Linde). The temperature of the split/splitless injection system, which was operated in splitless mode, was set to 300°C. Temperature program for first oven with initial temperature of 70°C applied for 1 min was a ramp of 7°C/min to 330°C for 8 min, while secondary oven ran with initial temperature of 80°C for 1 min and a ramp of 7°C/min to 340°C for 8 min. Modulator ran with a temperature ramp of 7°C/min, an initial temperature of 90°C for 1 min to 350°C for 8 min and a modulation time of 7.5 s. Data were acquired using ChromaTOF software (version 4.2x; LECO, St. Joseph, MI, USA).

## ***Identification of polymer materials using Pyr-GC-MS***

To characterize the tested materials given in Table 1 in more detail, pyrolysis followed by gas chromatographic separation and mass spectrometry was conducted (thermal desorption unit (TDU) and Pyrolyzer Module as well as MPS, Gerstel, Mülheim, Ruhr and 7890A-5975C GC/MSD system; Agilent). Polymers were cut to size and placed into pyrolysis tubes. The Pyr-GC-MS parameters were as follows: For chromatographic separation an



HP-5MS GC column (30 m x 0.25 mm i.d., 0.25  $\mu\text{m}$  df; Agilent, Delaware, New Castle, USA) and helium as carrier gas (purity  $\geq 99.999\%$ , Linde, Pullach, Germany) were used. The injection system was formed by a TDU mounted with a Pyrolyzer Module for TDU onto a CIS (all items from Gerstel). Pyrolysis parameters: lead time 0.10 min, follow-up time 1.00 min, initial time 0.33 min, initial temperature 700°C, and pyro in last hold. TDU parameters: initial temperature 50°C, followed by 720°C/min up to 320°C and a final hold for 1.4 min. CIS parameters: initial temperature of 120°C followed by an increase of 12°C/min up to 320°C and a final hold for 3.0 min. Chromatographic separation was performed using the following GC oven program: 50°C for 6 min, 10°C/min to 320°C, hold for 3 min. MS analyses were carried out by collecting total ion chromatograms in the scan mode and the mass range of 30 – 500 amu. Resulting pyrograms upon pyrolysis at 700°C were evaluated with respect to characteristic degradation patterns.<sup>7</sup> Pyrolysis data were acquired with MSD ChemStation software E.02.02. (Agilent Technologies) and converted from ChemStation data files using MassHunter MSD translator and further processed with MassHunter Workstation Software.

## Results

Table 1 summarizes results of characterization of consumer products investigated with regard to polymer type as well as PAH and PAC contents. The PAC contents were further separated into the amounts of the lead compound, that is benzo[*a*]pyrene (B[*a*]P), the sum of the eight EU PAHs, as well as into the total amount of MOAHs. Additionally, the MOAH corresponding fraction of MOSHs has been determined.

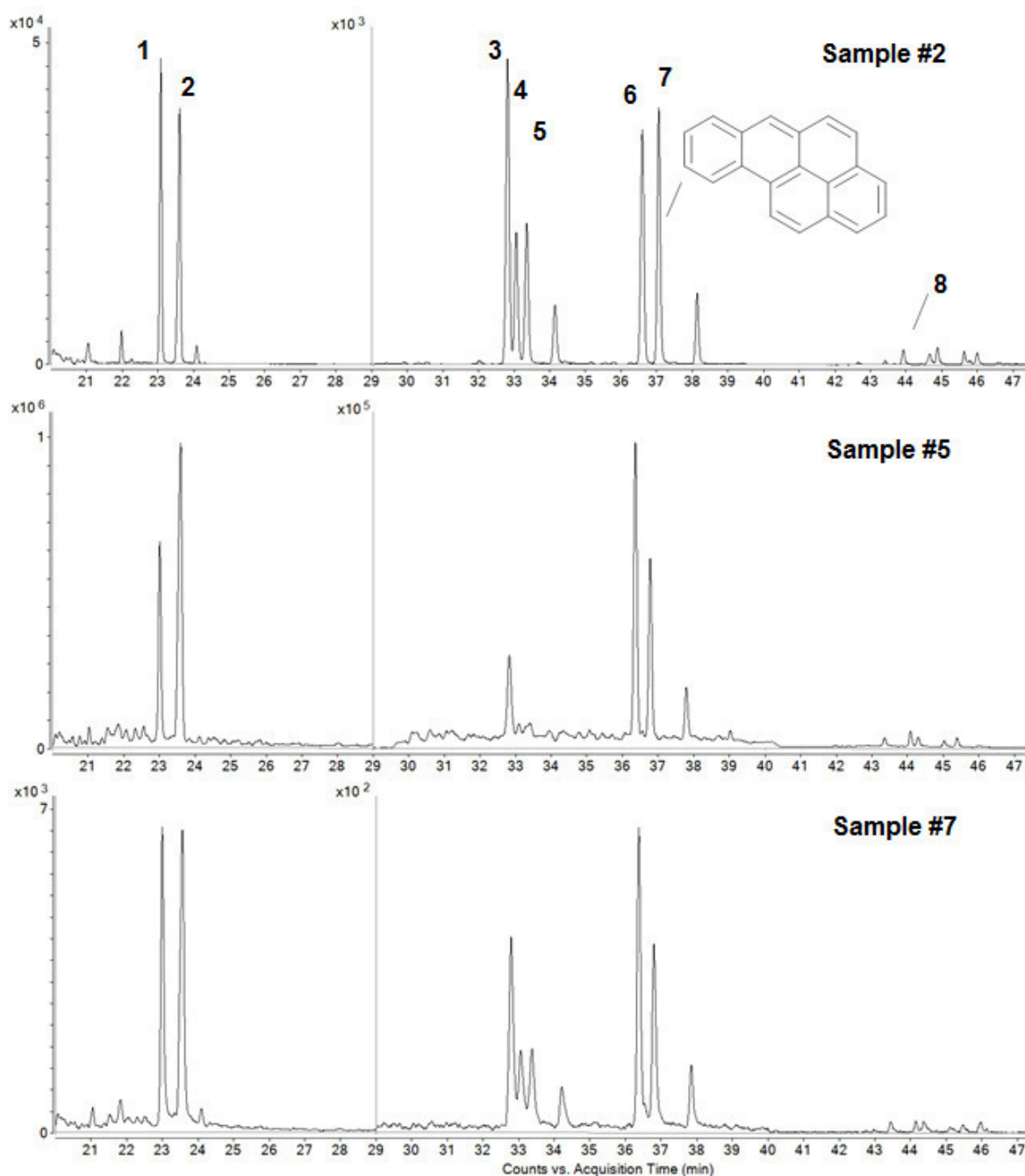


**Figure 2.** PAH target analysis of selected commodities. Representative GC-MS/MS extracted ion chromatograms (EIC; pseudotransitions of  $m/z=228, 252, 278$ ) of sample extracts in toluene with highlighted EU PAHs: benz[*a*]anthracene (1), chrysene (2), benzo[*b*]fluoranthene (3), benzo[*k*]fluoranthene (4), benzo[*j*]fluoranthene (5), benzo[*e*]pyrene (6), benzo[*a*]pyrene (7), dibenz[*a,h*]anthracene (8).

PAHs and total content of PACs in consumer products

**Table 1.** PAC / PAH profiles of commodities. Volatility ranges of mineral oil aromatic hydrocarbons (MOAHs) significantly differing from that of the corresponding mineral oil saturated hydrocarbons (MOSHs) are highlighted in gray, indicating enrichment of aromatic compounds in the polymer.

Characterization of samples			PAH content [mg/kg]		Mineral oil content [%]		Maximum C volatility LC-GC		Ratio
No.	Consumer product	Material entailed	Σ EU PAHs	B[a]P	MOSH	MOAH	MOSH	MOAH	MOAH / EU PAHs
1	Hammer handle	PN: polynorbornene, CSM: chlorosulfonated polyethylene	n.d.	57	0.9	2.1	C <sub>22</sub>	C <sub>12</sub> C <sub>14</sub> -C <sub>22</sub>	n.d.
2	Hammer handle	CSM: chlorosulfonated polyethylene	2212	166	0.9	1.1	C <sub>22</sub>	C <sub>12</sub> C <sub>14</sub> -C <sub>22</sub>	5
3	Hammer handle	CM-SDB: chloromethylated styrene-divinylbenzene copolymer	2685	266	0.7	0.4	C <sub>14</sub> C <sub>22</sub>	C <sub>14</sub>	2
4	Wheel of children's handcart	IIR: isobutylene-isoprene rubber	553	82	5.9	1.0	C <sub>20</sub> C <sub>30</sub>	C <sub>20</sub> C <sub>30</sub>	18
5	Flashlight	PVA: poly(vinyl acetate)	1110	96	1.8	3.3	C <sub>22</sub>	C <sub>9</sub> -C <sub>12</sub> , C <sub>12</sub> -C <sub>19</sub> C <sub>22</sub>	30
6	Ladle handle	EPDM: ethylene-propylene-diene rubber	28	4	>23	0.3	C <sub>13</sub> C <sub>38</sub>	C <sub>13</sub> C <sub>38</sub>	107
7	Tapeline	PVC: poly(vinyl chloride)	39	5	1.3	0.2	C <sub>12</sub> C <sub>22</sub> C <sub>28</sub>	C <sub>12</sub> C <sub>22</sub> C <sub>28</sub>	77

### ***PAH analysis***

For the investigation of consumer products, we used a targeted approach for 28 different PAHs and focused on the eight EU PAHs.

In all commodities investigated, the eight EU PAHs were quantified. The amount of the lead compound B[a]P ranged from about 60 up to 270 mg/kg polymer and the sum of all eight compounds together reached a total of more than 2.6 g/kg in case of sample #3 (cf. Figure 2, Table 1).

### ***MOSH & MOAH – mineral oil fractions examined***

Total contents of saturated as well as aromatic hydrocarbons in consumer products were quantified using liquid chromatography online coupled to gas chromatography with flame ionization detection (online-LC-GC-FID).

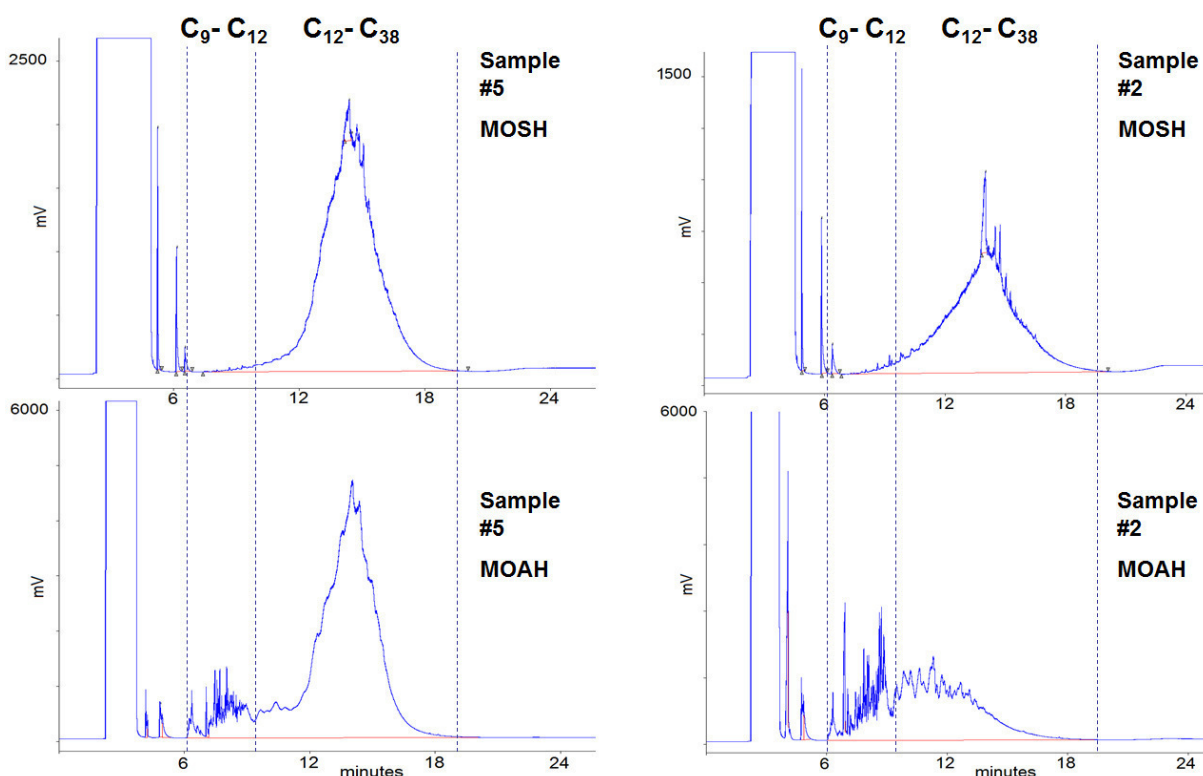


**Figure 3.** Online-LC-GC-FID chromatogram of consumer product extracts. Left: Extract of sample #5; Right: Extract of sample #2 with MOSH and MOAH chromatograms each.

Online-LC-GC-FID analyses have been evaluated not only according to the quantification of mineral oil compounds, but also with respect to the origins of MOSH and MOAH fractions. Chromatograms in **Figure 3** point to mineral oil components of different origins in the consumer products assessed: Different volatility maxima of MOSH and

corresponding MOAH fractions were detectable (cf. Table 1). **Table 1** highlights MOAH volatility maxima in gray, which are not present in the MOSH fraction of the respective consumer product.

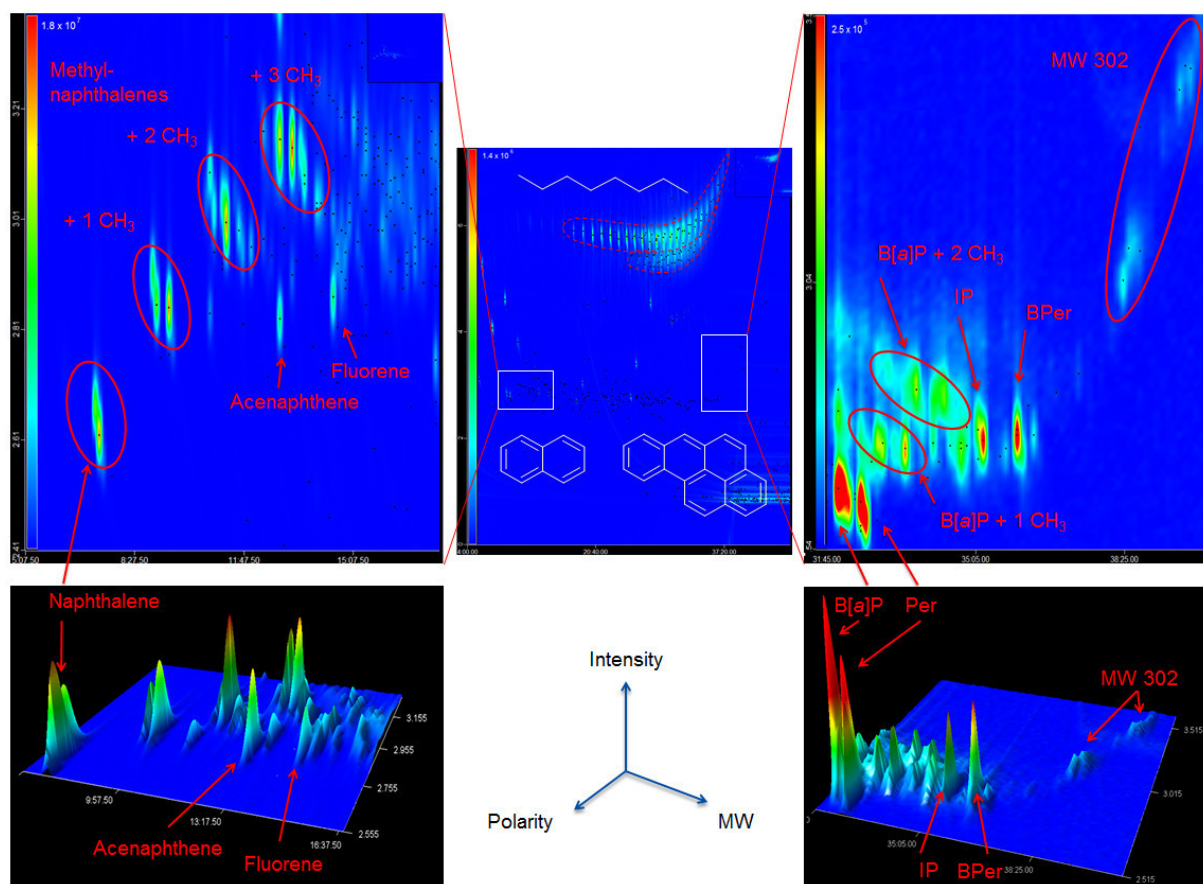


**Figure 4.** Two-dimensional gas chromatography. Heat maps and 3D chromatograms of the extract of sample #2. Center: total ion chromatogram (TIC); Left: extracted ion chromatogram (EIC) for naphthalene and derivatives; Right: EIC of benzo[*a*]pyrene (B[*a*]P) and dibenzopyrenes with molecular weight (MW) of 302. Per: perylene; BPer: benzo[*g,h,i*]perylene; IP: indeno[1,2,3-*cd*]pyrene; + *x* CH<sub>3</sub>: degree of methylation.

Moreover, MOAH chromatograms revealed a fine structure of peaks especially in early volatility regions (C<sub>9</sub>-C<sub>12</sub>), each of which representing individual PAHs. Changes in this characteristic cluster provide hints for different origins of PAHs<sup>8,9</sup>. Whereas, in sample #5 smaller PAHs dominate the pattern, sample #2 entails more of higher molecular PAHs in the volatility range of C<sub>12</sub>-C<sub>38</sub>.

### ***Untargeted analysis of consumer products with GCxGC-ToF-MS***

To characterize the complex mixtures concerning analytes' ring systems and degrees of alkylation, 2D gas chromatography coupled to mass spectrometry (GCxGC-ToF-MS) was applied.

In the total ion chromatogram (TIC) of the hexane extract of hammer handle #2, a broad area of saturated hydrocarbon peaks becomes apparent on top of the heat map (Figure 4). Directly below, the related iso-alkylated compounds are highlighted. Right at the bottom, MOAHs and their alkylated derivatives are located after 2D separation. By means of high resolution GCxGC-ToF-MS, single compounds in the MOAH region become detectable, from small ring systems and its alkylated derivatives (e.g. naphthalenes) to pentacyclic B[a]P and hexacyclic systems, such as benzo[*g,h,i*]perylene or dibenzopyrenes, even in a non-targeted approach.

### **Conclusion**

In this study, PAH and PAC composition profiles of consumer products are presented for various polymeric materials. Our results point to complex mixtures of mineral oil compounds used in the manufacture of the products investigated. As part of the mineral oil mixtures, we detected penta- and hexacyclic PAHs that have been shown to be carcinogenic in rodents. Since the pentacyclic lead compound B[a]P has been proved to cause genotoxic stress in human skin *ex vivo*<sup>10</sup>, its occurrence in consumer products designated for skin contacts is one of the main concerns in this study. The results for B[a]P all exceed the limit value of 1 mg/kg material set for products, such as sport equipment and household utensils, tools, clothes or wristbands<sup>11</sup>.

With respect to the total aromatic fraction, however, it proved insufficient to focus on targeted analysis only (cf. Table 2). We found a high variability in the relation between MOAH and PAH contents, with the amounts of MOAHs being up to 100-fold higher than the amounts of EU PAHs (sample #6). Additionally, in three consumer products of distinct polymeric composition, various sources of aromatic compounds were detectable (sample #1, 2, 5) via online-LC-GC-FID when comparing the maxima of the volatility ranges of MOAH with those of the corresponding MOSH fraction. This finding suggests that MOAH-enriched oil extracts are present next to carbon black as an additional source of MOAHs. These were likely added during manufacturing of the polymer for texturizing purposes.

## Funding

This work was funded by Intramural Research Funding, project no. SFP1322-514.

## References

1. Hutzler, C., A. Luch, and J.G. Filser. "Analysis of carcinogenic polycyclic aromatic hydrocarbons in complex environmental mixtures by LC-APPI-MS/MS." *Anal. Chim. Acta.* 702 (2011): 218-224.
2. Barp, L., C. Kornauth, T. Würger, M. Rudas, M. Biedermann, A. Reiner, N. Concin, and K. Grob. "Mineral oil in human tissues, Part I: Concentrations and molecular mass distributions." *Food Chem Toxicol.* 72 (2014): 312–321.
3. ZLS (Zentralstelle der Länder für Sicherheitstechnik). "Testing and validation of polycyclic aromatic hydrocarbons (PAH) in the course of GS-mark certification, ZEK 01.4-08." (2011). Available from: [http://www.zls-muenchen.de/de/left/aktuell/pdf/zek\\_01\\_4\\_08\\_pak\\_verbindlich\\_engl\\_30112011.pdf](http://www.zls-muenchen.de/de/left/aktuell/pdf/zek_01_4_08_pak_verbindlich_engl_30112011.pdf), effective 02/2014.
4. Biedermann, M., L. Barp, C. Kornauth, T. Würger, M. Rudas, A. Reiner, N. Concin, and K. Grob. "Mineral oil in human tissues, Part II: Characterization of the accumulated hydrocarbons by comprehensive two-dimensional gas chromatography." *Sci Total Environ.* 506–507 (2015): 644–655.
5. Mondello, L., M. Zoccali, G. Purcaro, F.A. Franchina, D. Sciarrone, S. Moret, L. Conte, and P.Q. Tranchida. "Determination of saturated-hydrocarbon contamination in baby foods by using on-line liquid–gas chromatography and off-line liquid chromatography-comprehensive gas chromatography combined with mass spectrometry." *J Chromatogr A.* 1259 (2012): 221–226.
6. Biedermann, M., and K. Grob. "On-line coupled high performance liquid chromatography–gas chromatography for the analysis of contamination by mineral oil. Part 1: Method of analysis." *J Chromatogr A.* 1255 (2012): 56-75.
7. Tsuge, S., H. Ohtani, and C. Watanabe. 2010. *Pyrolysis-GC/MS data book of synthetic polymers - pyrograms, thermograms and MS of pyrolyzates.* (Oxford: Elsevier, 2010).
8. Yebra-Pimentel, I., R. Fernández-González, E. Martínez Carballo, and J. Simal-Gándara. "Searching ingredients polluted by polycyclic aromatic hydrocarbons in feeds due to atmospheric or pyrolytic sources." *Food Chem.* 135 (2012): 2043-2051.
9. Pontevedra-Pombal, X., L. Rey-Salgueiro, M.S. García-Falcón, E. Martínez-Carballo, J. Simal-Gándara, and A. Martínez-Cortizas. "Pre-industrial accumulation of anthropogenic polycyclic aromatic hydrocarbons found in a blanket bog of the Iberian Peninsula." *Environ Res.* 116 (2012): 36-43.
10. Brinkmann, J., K. Stolpmann, S. Trappe, T. Otter, D. Genkinger, U. Bock, M. Liebsch, F. Henkler, C. Hutzler, and A. Luch. "Metabolically competent human skin models: Activation and genotoxicity of benzo[a]pyrene." *Toxicol. Sci.* 131 (2013): 351-359.
11. The European Parliament and the Council on the Registration, Evaluation, Authorisation and Restriction of Chemicals (REACH). Commission regulation (EU) No 1272/2013 amending annex XVII to regulation (EC) No 1907/2006. (2013).

## **6.2 Skin permeation of polycyclic aromatic hydrocarbons: A solvent-based *in vitro* approach to assess dermal exposures against benzo[a]pyrene and dibenzopyrenes**

Nastasia Bartsch, Jochen Heidler, Bärbel Vieth, Christoph Hutzler, Andreas Luch, *Journal of Occupational and Environmental Hygiene*, 2016, 13: 969-979.

Published online: 05 Jul 2016

DOI: 10.1080/15459624.2016.1200724

Link: <https://doi.org/10.1080/15459624.2016.1200724>

Involvement of the author within this publication: Project planning: 65%, project execution: 90%, data analysis: 95%, writing of the manuscript: 80%



## **ABSTRACT**

Consumer products with high contents of polycyclic aromatic hydrocarbons (PAHs) were repeatedly identified by market surveillance authorities. Since several of the individual compounds have been identified as genotoxic carcinogens, there might be health risks associated with the usage of these items. It therefore becomes reasonable to argue to reduce PAH contents in consumer products to a level as low as possible. This study presents data on the migration of PAHs from consumer products into aqueous sweat simulant or aqueous ethanol and on its combined migration and penetration into human skin. Product specimens were either submerged in simulant, or placed directly on test skins in Franz cell chambers to simulate dermal contacts. Migration of hexacyclic dibenzopyrenes became detectable by using ethanolic simulant, but not in aqueous sweat simulant. Similarly, migration of the pentacyclic model carcinogen benzo[*a*]pyrene (B[*a*]P) into aqueous sweat simulant was significantly lower when compared with human skin or skin models. The results point to a gross underestimation (about two orders of magnitude) when using aqueous sweat simulant instead of human skin for assessing PAH migration. On the other side, the usage of 20% ethanol as simulant revealed good agreement to the actual exposure of human skin against B[*a*]P migrating out of contaminated products. Our results underline that aqueous sweat simulant is not suitable to study dermal migration of highly lipophilic compounds.

## **KEYWORDS**

dibenzopyrenes, benzo[*a*]pyrene, dermal exposure, skin models, Franz cell, migration

## INTRODUCTION

Due to their versatility polymers are the raw material of choice when it comes to the fabrication of commodities (1). There are several reasons why such commodities may contain polycyclic aromatic hydrocarbons (PAHs) to different extents. For instance, carbon black that contains PAH impurities is added during fabrication to increase abrasion resistance of the material and to vary its color (2). An additional source of PAHs in consumer products is the application of mineral oils, commonly used as plasticizers. These oils are derived from vacuum distillation of petroleum which mainly consists of a complex mixture of hydrocarbons including PAHs. Since PAHs may in part withstand refining processes they might still be present in plasticizer-containing polymers used to produce certain products (3, 4). Galea et al. found in human volunteers that dermal contacts to petroleum products occur in various ways (5). This finding emphasizes the need for assessing the level of exposure against carcinogenic PAHs by characterizing their migration behavior and release from the products, as well as their subsequent penetration through the skin. In general, PAHs consist of fused aromatic rings and are formed during incomplete combustion of organic matter (6, 7). Eight PAHs are classified as carcinogens category 1 B according to the CLP-Regulation (EU VO 1272/2008) (8). The genotoxicity of benzo[*a*]pyrene (B[*a*]P) has already been proven in skin models by applying the comet assay (9), as has its migration into polyethylene foil and pig skin (10). Epidemiology identified occupational exposures against complex PAH-containing mixtures such as coal tar or coal tar pitches (consisting of up to 50% of PAHs with 1-2% B[*a*]P) as being carcinogenic in humans (11). One common way to classify PAHs refers to their carcinogenic potency in relation to the marker compound B[*a*]P as reference (12, 13) (**Figure 1**). This scaling refers to the so-called toxicity equivalence factors (TEFs) based on results from the mouse skin bioassay, and the TEF of B[*a*]P is set to be 1. Among dibenzopyrenes some are rated with 10-fold stronger carcinogenicity when compared to B[*a*]P (e.g., dibenzo[*a,l*]pyrene, DB[*a,l*]P; dibenzo[*a,i*]pyrene, DB[*a,i*]P; and dibenzo[*a,h*]pyrene, DB[*a,h*]P), while dibenzo[*a,e*]pyrene (DB[*a,e*]P) is judged being equal to B[*a*]P (**Figure 1**) (14). Even though the higher molecular weight PAHs are usually present in consumer products only at much lower levels compared to B[*a*]P, in light of their 10-fold higher TEFs the dermal exposure to dibenzopyrenes is of great relevance for human health.

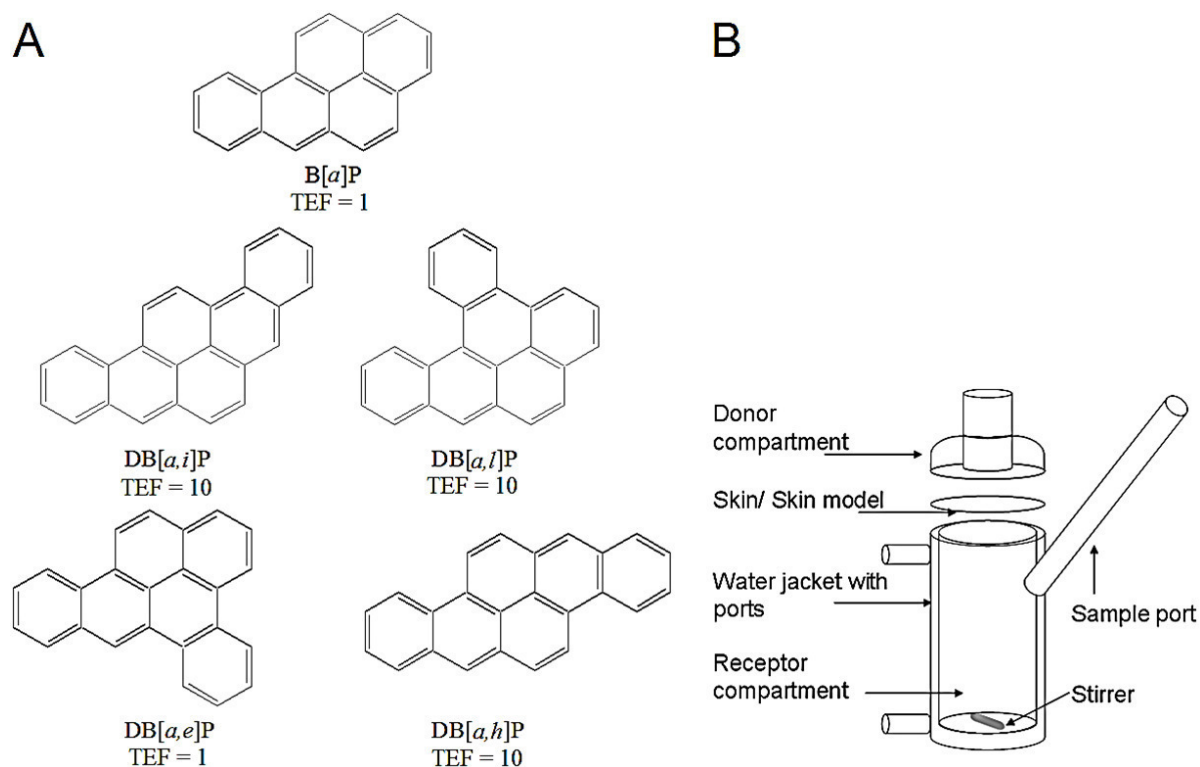


**FIGURE 1.** Chemical structures of B[a]P and of four different dibenzopyrene isomers with its respective toxicology equivalence factor (TEF) (A). Scheme of the Franz cell chamber setup to measure skin penetration *in vitro* or *ex vivo* (B).

For dermal exposure studies with commodities such as, e.g., toys, usually aqueous sweat simulant is used in standard migration tests (15). Especially for highly lipophilic compounds like PAHs this procedure seems highly questionable. We therefore compared different methods to assess the route of dermal exposure and the extent of uptake of B[a]P and dibenzopyrenes into the human body. Besides solvent-derived approaches with different simulants, the Franz cell chamber assay was performed using the classic static diffusion test model (Figure 1) (16). This model has been proven as important test method when it comes to the characterization of transdermal drug administration (17). We not only used this system to evaluate the distribution of standard chemicals in different Franz cell compartments, but also to simulate skin contacts with PAH-containing consumer products. Ultimately, we determined the amounts of PAHs that migrated from the product to the skin and that subsequently passed the epidermal barrier to enter subepidermal layers or systemic circulation.

## MATERIALS AND METHODS

### Chemicals

The following PAHs were investigated: the PAH surrogate cocktail (containing acenaphthylene-d<sub>8</sub>, benzo[*g,h,i*]perylene-d<sub>12</sub>, B[*a*]P-d<sub>12</sub>, fluoranthene-d<sub>10</sub>, naphthalene-d<sub>8</sub>, phenanthrene-d<sub>10</sub>, pyrene-d<sub>10</sub>), DB[*a,i*]P-d<sub>14</sub> and chrysene-d<sub>12</sub> were all obtained from Cambridge Isotope Laboratories (CIL Inc., Tewksbury, MA, USA). Deuterated PAHs were mixed to obtain an internal standard stock solution of 7 µg/ml. PAH-Mix 45 and PAH-Mix 15 were purchased from Dr. Ehrenstorfer GmbH (Augsburg, Germany), similar as 7*H*-benzo[*c*]fluorene, and 1- or 2-methylnaphthalene and then were combined to obtain positive control stock and calibration solutions of 15 – 2000 ng/ml in acetonitrile. As positive control for analysis of phthalates, a mixture of 15 plasticizers was used in a concentration range of 250 – 1000 ng/ml (EPA Method 8061A Phthalate Esters Mixture, Restek, Bellefonte, PA, USA) in hexane. Solvents for GC or LC analyses and for sample preparation (dichloromethane, acetone, acetonitrile, ethyl acetate, methanol, ethanol and hexane) were purchased from Sigma-Aldrich (St. Louis, MO, USA) or Merck KGaA (Darmstadt, Germany). All water consuming preparation steps have been conducted using Milli-Q water (Merck KGaA) with the resistance of >5 MΩ•cm at 25°C. For validation of Franz cell assay, amounts of B[*a*]P were applied onto human skin at levels of 0.01 – 1 µg per total penetration area of 1.76 cm<sup>2</sup>. B[*a*]P was solved in water enriched with 2% IGEPAL<sup>®</sup> CA-630 (Sigma-Aldrich) to increase its solubility.

### Migration testing using a solvent-based approach

To test the ability of various simulants for mimicking human skin properties with regard to chemical's migration behavior, the amount of B[*a*]P migrating from a PAH-containing sample into aqueous sweat or ethanolic simulant was analyzed, and compared to the amount of B[*a*]P permeating human test skin in the Franz cell chamber. Positive controls using standard solutions of PAHs have been evaluated to ensure the accuracy of the system. Negative controls using simulant only were performed in parallel to exclude PAH contamination of the set up.

The actual migration experiments were performed using aqueous acidic and basic sweat simulants (prepared according to DIN ISO 105-E04 (18); pH 5.5 and pH 8) as well as ethanolic simulant. Rectangle specimens were taken from all PAH-containing products. A detailed documentation of the surface that was brought into contact with the simulant was conducted prior to migration. This was done using a caliper taking eight measured points

and calculating the total surface including cut surfaces. Migration experiments then were performed by submerging the defined specimens in either 10 ml ethanolic simulant or 25 ml sweat simulant. Samples of similar dimension as used for skin penetration were shaken in a water bath at 22°C or 37°C circling horizontally for 24 h. Referring to a standardized test method (DIN ISO 105-E04) (18) with sweat simulant, the solvent-based approach has been tested at 37°C as well, not to mirror body temperature but to generate data of B[a]P load in the same order as found for human skin penetration. Additionally, migration of PAHs at 22°C has been monitored to characterize the influence of the temperature. Regularly about 2 cm<sup>2</sup> of the test item was used, for the analysis of dibenzopyrenes even up to 8 cm<sup>2</sup>. This was supposed to be comparable to a maximum permeation area of 1.76 cm<sup>2</sup> with a diameter of 15 mm as it is limited in the Franz cell chamber assay. After incubation the ethanolic migration solutions were diluted with Milli-Q water (Merck KGaA) to yield a content of 4% ethanol. After adding 10 µl of the internal standard PAH mixture the test solutions were concentrated, purified and separated from the aqueous matrix by means of solid phase extraction (SPE) (cartridges: Bond Elut C18, Agilent, Waldbronn, Germany; SPE station: Phenomenex, Aschaffenburg, Germany; vacuum pump: VP 86, VWR, Darmstadt, Germany). Before usage SPE cartridges have been conditioned with methanol and three times with 4% ethanol (applying a volume of 10 ml each). The diluted samples were then loaded onto the cartridges. After 1 h under full vacuum, the elution was performed using 10 ml dichloromethane. The samples were vaporized under nitrogen close to dryness to be resolved in acetonitrile and subsequently analyzed via EI-GC-MS/MS.

### **Skin permeation experiments**

The proposal to conduct permeation studies with real human skin samples was reviewed and approved by an independent ethics committee. Experiments were performed by investigating single compartments of the Franz cell set-up individually (**Figure 1B**). The respective washing solutions contained all analytes that were unable to pass the skin barrier but migrated out of the test specimen or, in the case of positive controls, remained on the surface of the skin model. Porcine and human skin were separated after diffusion testing via tape stripping into the *stratum corneum* and the remaining epidermal layers, while other skin models were analyzed in total. The overall contents in the epidermal layers provided the numbers of the total penetration of the respective compound. On the other side, the receptor chamber fluid contained all analytes that were able to permeate the test

skin specimen and that are thus likely to reach systemic circulation under *in vivo* conditions.

### **Skin and skin model preparation**

*In vitro* percutaneous absorption experiments were performed with human and porcine epidermis, the keratinocytes model EpiDerm 606X (MatTek, Ashland, MA, USA), and the synthetic membrane Strat-M (MerckMillipore, Darmstadt, Germany) that mimics human epidermis. The pig skin originated from the flanks of a male animal and was obtained from VION food GmbH (Perleberg, Germany). It has been delivered on ice unscalded in its natural condition, sheared and cut into pieces of approximately 10 x 20 cm. Human skin was obtained from plastic surgery (Charité, Berlin, Germany and Universität Saarland, Saarbrücken, Germany) and originated from female abdomen. Skin was stored at  $-20^{\circ}\text{C}$  until use. The utilized reconstructed human epidermis (RHE) model EpiDerm 606X (MatTek) was prepared according to the instructions of the manufacturer. The synthetic membrane Strat-M was single welded and ready to use.

### **Experimental set up: permeation testing**

For permeation experiments static Franz cells (PermeGear, Hellertown, PA, USA) were used with 15 mm diameter (permeation area of  $1.76\text{ cm}^2$ ) and a receptor volume of 12 ml (**Figure 1B**). The skin model samples were prepared in advance by cutting off the epidermal layers of semi-thawed porcine skin with a thickness of  $300\text{ }\mu\text{m}$  using a dermatome (Aesculap AG, Tuttlingen, Germany). The RHE model was removed from its agars. Subsequently, sections of 22 mm diameter were punched out of the skin or skin model and then its integrity visually verified. The Strat-M membrane was used as delivered. All epidermis models were mounted between the receptor and donor compartment in the Franz cell system with the upper side (*stratum corneum*) facing the donor chamber. It has been ensured that no air bubbles could interfere with the contacts between the lower epidermal layer or membrane facing the receptor chamber and the receptor solution. As receptor medium a constantly magnetically stirred sodium chloride solution (0.9%) was used and maintained by a water jacket at  $33 \pm 1^{\circ}\text{C}$  for analysis of the keratinocytes model, the Strat-M and porcine as well as human epidermis. Prior to clean up of all compartments, the surface tension of the skin model and again its integrity have been visually controlled. If the convex surface collapsed or the skin became damaged over time, this particular set up was discarded for further evaluation.

The test solutions or samples were placed onto the skin and the donor chamber thoroughly covered with parafilm (American National Can, Greenwich, CT, USA). The volume applied for PAH control analysis consisted of 10  $\mu$ l of a PAH mix stock solution in acetonitrile with a total concentration of 1  $\mu$ g/ml. To exclude PAH contamination of the tested skins and skin models as well as utilized solvents, in each single experiment negative controls were performed in parallel. For that purpose, a similar volume of 10  $\mu$ l acetonitrile without PAHs was applied to the skin. Specimens of consumer goods were punched out to yield a sample with a diameter of 10 mm made of elastomeric material. This sample was then placed into the donor compartment thereby ensuring its direct contact to the skin. The epidermal test models were moistened with 10  $\mu$ l sodium chloride solution (0.9%) in advance. The duration of permeation experiments was 24 h.

Finally, specimens have been removed and test skins from all experiments were washed three times with 1 ml sodium chloride (0.9%). Each washing step was performed by soaking up the saline solution using a pipette and ejecting it onto the skin again about ten times. Deuterium labeled internal standards were added into all compartment solutions prior to further preparation. The washing solution was transferred into flasks with ground glass joints and filled up with sodium chloride solution to 5 ml. The receptor medium was transferred into test tubes with ground glass joints and its exact volume documented. To isolate the *stratum corneum*, if applicable, tape stripping was performed five times per skin specimen and the collected tape strips containing the separated layers were suspended in 10 ml acetonitrile, while the test skins were taken up with 3 ml ethyl acetate each and extracted for 30 min using an ultrasonic bath at room temperature. To ensure removal of the PAH containing *stratum corneum*, cryosections of unstripped as well as two to five times stripped epidermis were evaluated via fluorescence microscopy. The *stratum corneum*-containing solution was transferred into test tubes with ground glass joints and the PAHs isolated in a liquid-liquid extraction step with 5 ml hexane. The epidermis extract was transferred to a test tube and the remaining skin washed with 1 ml ethyl acetate twice. To concentrate the receptor and wash solutions, SPE was subsequently accomplished in a similar way as done after migration experiments (cf. above; Bond Elut C18, Agilent, Waldbronn, Germany). However, here conditioning was performed using 3 ml of solvent each step, first methanol followed by three times Milli-Q water. Samples were finally eluted with 3 ml dichloromethane. All compartment solutions prepared (i.e., wash solution in 3 ml dichloromethane subsequent to SPE, *stratum corneum* in 5 ml hexane, epidermis extract in 5 ml ethyl acetate, receptor compartment content in 3 ml

dichloromethane subsequent to SPE) were evaporated close to dryness under nitrogen using a concentration workstation (Turbovap, Biotage, Uppsala, Sweden). Finally the samples were dissolved in 130  $\mu$ l acetonitrile.

### **Validation of the Franz cell assay**

The Franz cell system was validated by applying solutions of B[a]P in water containing 2% of IGEPAL (applied amounts of 1, 0.1 and 0.01  $\mu$ g, respectively) onto human skin specimens. Total recoveries of 99 – 124% confirmed the extraction efficiency and the validity of the method used (**Supplementary Figure A**).

### **Analysis of PAHs**

The PAH contents of the samples were determined as follows: The samples were extracted according to the ZEK 01.4-08 method (19), followed by analytical quantification using LC-APPI-MS/MS (20) or GC-EI-MS/MS respectively. The analytical system for GC-EI-MS/MS operation was formed by a GC7890A-MS7000A set up (Agilent, Santa Clara, CA, USA) with parameters as follows: For chromatographic separation an Rxi-17SilMS GC column (30 m x 0.25 mm i.d., 0.25  $\mu$ m df; Restek, Bad Homburg, Germany) and helium as carrier gas (purity  $\geq$  99.999%, Linde, Pullach, Germany) were used as well as a pre-column (5 m x 0.25 mm i.d.; Phenomenex). The instrument was utilized with a MultiPurpose Sampler MPS (Gerstel, Mülheim, Ruhr, Germany). Injection temperature program using a cooled injection system (PTV-type CIS; Gerstel) and an injection volume of 1  $\mu$ l was 45°C, followed by a ramp of 12°C/s to 340°C. The following GC temperature program was used: 70°C for 0.5 min, structured ramp: 25°C/min to 110°C for 0.5 min, 12°C/min to 250°C, 1°C/min to 270°C, 10°C/min to 280°C, 4°C/min to 320°C, then 4°C/min to 340°C. Tandem MS analysis was carried out in multiple reaction monitoring (MRM) mode. To ensure specificity, a pseudo fragmentation reaction was monitored in addition to at least two other fragmentations for each analyte. For B[a]P, B[e]P, benzofluoranthenes and perylene, m/z=252 has been selected as precursor and pseudo-transition ion at a collision energy (CE, collision gas: nitrogen 5.0, purity  $\geq$  99.999%, Linde, Pullach, Germany) of 35 V, as well as further transitions to m/z=251 (35 V), 250 (42 V), 226 (35 V) and m/z=250 to 248 (40 V), respectively. For analysis of dibenzopyrenes one pseudo-transition ion of m/z=302 (30 V) has been evaluated, and ion transitions of m/z=302 to 301 (30 V) as well as m/z=302 to 300 (25 V) were selected as further product ions. To ensure a linear range of quantification, calibration stocks of



standard solutions in acetonitrile were used in concentrations of 15 – 1000 ng/ml or 30 – 2000 ng/ml.

### **Fluorescence microscopy**

After Franz cell assay with either standard solution of analytes or commodity specimens, the epidermis was fixed in Tissue Tek O.C.T. (Sakura, Alphen aan den Rijn, AV, The Netherlands) and sliced into sections of 10  $\mu\text{m}$  with an HM 550 OP cryotome (Thermo Fisher Scientific, Waltham, MA, USA). Evaluation of sections was conducted with an Axio Observer A1 fluorescence microscope (Zeiss, Thornwood, NY, USA) applying a fluorescence filter of 350 nm absorption (abs) / 450 nm emission (em).

### **Analysis of polymer materials**

To characterize the polymeric material of the commodity goods to be tested, attenuated total reflectance—Fourier transformed infrared (ATR–FTIR) spectra were collected using a Nicolet 6700 spectrometer (Thermo Electron Corporation, Madison, WI, USA). The material has been cut to obtain appropriate sizes and passivated in an atmospheric environment for at least 24 h prior to IR analysis.

### **Pyrolysis gas chromatography mass spectrometry (Pyr-GC-MS)**

To characterize the composition of commodities in more detailed, Pyr-GC-MS was performed using a 7890A-5975C GC/MSD System (Agilent, Santa Clara, CA, USA). The samples were cut to size and placed into pyrolysis tubes. The Pyr-GC-MS parameters were as follows. For chromatographic separation an HP-5MS GC column (30 m x 0.25 mm i.d., 0.25  $\mu\text{m}$  df; Agilent, Delaware, New Castle) and helium as carrier gas (purity  $\geq$  99.999%, Linde, Pullach, Germany) were used. The injection system was formed by a thermal desorption unit (TDU) mounted with a Pyrolyzer Module for TDU onto a CIS and an MPS (all items from Gerstel). Pyrolysis parameters: lead time 0.10 min, follow-up time 1.00 min, initial time 0.33 min, initial temperature 700°C, and pyro in last hold. TDU parameters: initial temperature 50°C, followed by 720°C/min up to 320°C and a final hold for 1.4 min. CIS parameters: initial temperature of 120°C followed by an increase of 12°C/min up to 320°C and a final hold for 3.0 min. Chromatographic separation was performed using the following GC oven program: 50°C for 6 min, 10°C/min to 320°C, hold for 3 min. MS analyses were carried out by collecting total ion chromatograms in the scan mode and the mass range of 30 – 500 amu.

### **Analysis of polymer composition**

Extracts of the polymer materials were further characterized with regard to its additive contents by means of an MRM multi-method applying GC-EI-MS/MS. The material was cut to size, passivated in an atmospheric environment for at least 24 h and submerged in acetone at room temperature during 2 h of ultrasonic treatment. To identify plasticizers, a phthalate standard mix (EPA Method 8061A Phthalate Esters Mixture) was analyzed together with extracts of the commodity goods with an injection volume of 1  $\mu$ l each. The analytical system for GC-EI-MS/MS operation was identical to that used for PAH analysis. The parameters of the GC oven program were as follows: 70°C for 1.5 min, then 25°C/min to 250°C for 5 min, 3°C/min to 280°C for 1 min and finally 25°C/min to 300°C for 9 min. The initial temperature of the CIS was 45°C followed by a structured ramp of 12°C/s to 280°C for 20 min and 12°C/s to 340°C for 5 min. In the case of diisobutyl phthalate (DIBP) ion transitions used were  $m/z=223$  to  $m/z=149$ , and  $m/z=149$  to  $m/z=121$ ,  $m/z=93$  and  $m/z=65$ , respectively. Transitions monitored for dibutyl phthalate (DBP) were  $m/z=167$  to  $m/z=149$ , and  $m/z=149$  to  $m/z=121$ ,  $m/z=93$  and  $m/z=65$ , respectively. For diethylhexylphthalate (DEHP) the ion transition from  $m/z=279$  to  $m/z=149$  was used.

### **Data acquisition and analysis**

GC-MS/MS data were acquired using the Enhanced MassHunter B.06.00 software (Agilent) and Maestro 1.4. software (Gerstel) with a dell workstation. Generated data for PAHs and phthalates have been processed using MassHunter Workstation software (Qualitative Analysis version B.06.00 and Quantitative Analysis version B.05.00, Agilent). For PAHs linear regression calibration in concentrations of 15 - 1000 ng/ml or 30 - 2000 ng/ml was performed. Selected qualifier and quantifier ions were extracted and automatically integrated accompanied by manual control. Two tailed Student's t-tests has been performed using Microsoft Excel 2010 with  $\alpha=0.05$ .

Pyrolysis data were acquired with MSD ChemStation software E.02.02. (Agilent Technologies) and converted from ChemStation data files using MassHunter MSD translator and further processed with MassHunter Workstation Software and by applying a deconvolution algorithm. Settings for deconvolution were as follows: To filter compounds, only peaks with at least 5,000 counts of absolute area were taken into consideration and mass criteria of 500 counts of absolute height. Peak window criteria of left delta  $m/z$  0.3 and right delta  $m/z$  0.7 had been applied.

The resulting total compound chromatograms (TCC) were evaluated by comparing extracted spectra with reference data from the NIST database library (NIST MS search 2.0, National Institute of Standards and Technology, Gaithersburg, MD). Identification of compounds was restricted by a similarity score of 80%.

Microscopy was carried out using AxioVision Rel.4.8. software (Zeiss) and FTIR data were evaluated with Omnic 8.3 software (Thermo Fisher Scientific).

## **RESULTS AND DISCUSSION**

To assess the levels of dermal exposure of consumers, the following different analytical approaches focusing on B[a]P as lead compound among PAHs were applied: (i) standardized migration testing with aqueous or ethanolic simulants, and (ii) penetration studies using human or porcine skin as well as skin models in the Franz cell chamber system. Results from both models were compared to corresponding reference data obtained by using real human skin *ex vivo*.

### **Characterization of the products investigated**

Consumer products that will cause skin contacts to polymers during predictable usage have been evaluated concerning PAH contents of the polymer. As carbon black is, in addition to aromatic extender oils, an important source for PAH contamination, especially black polymers have been tested. Furthermore, carbon black is often added to elastomers in consumer products that are subject to mechanical load to increase abrasion resistance. Extender oil is commonly utilized simultaneously with carbon black in elastomers to modify its properties. For further penetration and migration studies, four commodities made of different polymers and elastomers and different additives were chosen encompassing moderate to high B[a]P contents (**Table 1**).

Because the polymer itself as well as the additives may affect PAH migration the materials have been characterized analytically. ATR–FTIR was performed to characterize the materials in a first step. The obtained spectra revealed significant differences between the hammer handles and the wheel of children’s handcart (**Supplementary Figure B**; compare samples #1-3 with #4).

**TABLE 1. PAH contents of selected commodity goods and results of material evaluation using Pyr-GC-MS.**

Sample #	1		2		3		4	
Product	Handle of hammer		Handle of hammer		Handle of hammer		Wheel of childrens handcart	
PAH	content [mg/kg]							
B[a]P	57		166		266		82	
DB[a,l]P	1.5		3.0		2.6		2.0	
DB[a,e]P	6.0		20.0		9.5		5.8	
DB[a,i]P	1.3		6.5		3.0		2.1	
DB[a,h]P	1.8		4.4		3.1		3.0	
Presumed material	PN	CSM	CSM	CM-SDB	CM-SDB	IIR	IIR	

*Notes:* PN: polynorbornene, CSM: chlorosulfonated polyethylene, CM-SDB: chloromethylated styrene-divinylbenzene copolymer, IIR: isobutylene-isoprene rubber.

In a second step, pyrolysis produced data that mainly confirmed the FTIR findings at first glance. However, additional matching using a commercial library of mass spectra subsequently revealed more complex differences with regard to polymer composition (**Table 1, Supplementary Figure C**). The pyrogram patterns obtained offer the opportunity to further characterize the original polymers that were used for the production of the respective commodities. The most noticeable peak in pyrograms of samples #1-3 originates from the plasticizer diethylhexylphthalate (DEHP, also named bis(2-ethylhexyl)phthalate), but also dibutylphthalate (DBP) and di-isobutylphthalate (DiBP) have been identified in all samples. The occurrence of these different phthalates in the pyrograms associated with samples #2-4 could be confirmed by complementary GC-MS/MS analysis (**Supplementary Figure D**). In contrast to samples #1-3, phthalate levels were much lower in sample #4 (wheel of handcart). This finding is in accordance with the FTIR analyses that revealed matching differences in the spectra obtained, e.g., carbonyl ( $1750\text{ cm}^{-1}$ ) and ester bond vibrations ( $1250\text{ cm}^{-1}$ ), both of which represent prominent functional groups in phthalates (**Supplementary Figure B**).

Since 2,4-dimethyl-1,3-pentadiene has been formed during pyrolysis of sample #4 it could be concluded that this particular material partially consists of isobutylene-isoprene rubber (IIR) (21). Unlike samples #1-3 benzenediamines could also be identified in sample #4, indicating that the material underwent vulcanization. According to the Pyr-GC-MS

fingerprint analyses, chlorosulfonated polyethylene (CSM) is present in samples #1 and #2. That finding is of great interest as this polymer is known to show good miscibility with other polymers and resulting blends can be reinforced with carbon black as filler agent (22). The addition of carbon black to the polymer might therefore be a source of PAH contamination in this case (23). The content of B[a]P quantified via GC-MS/MS varied between 60 and 270 mg/kg in the test commodities and thus was rather high. Conversely, the total amount of the four dibenzopyrenes investigated reached only values between 10 and 34 mg/kg. All data are summarized in **Table 1**.

### **Consumer products in Franz cell chamber assay and visualization of PAH penetration into human skin**

In exposure research the dermal pathway is quite unique due to the various skin layers and the corresponding barrier function properties (24). In the present study the barrier function of natural human skin has been tested with certain PAH-containing consumer products. To this end, we looked into skin penetration and spatial distribution of the lipophilic marker compound B[a]P. However, real exposure conditions cannot completely be simulated by applying dissolved chemicals onto test skins in the Franz cell chamber assay. Since there is a lack of methodological standardization, the kind of application of test substances needs to be critically checked because the (solvent) vehicle may greatly affect penetration (25). In the case of PAHs this has been demonstrated for B[a]P by Wester and colleagues (26). The authors pointed to significant differences in percutaneous absorption of B[a]P when applied as contaminant in soil compared to B[a]P dissolved in acetone (26). The soil was prepared containing  $^{14}\text{C}$ -labelled B[a]P to an amount of 10 ppm, while the acetone solution had a concentration of about 100  $\mu\text{g}/\text{ml}$ . In the latter case, about 120  $\text{ng}/\text{cm}^2$  of initially applied 500  $\text{ng}/\text{cm}^2$   $^{14}\text{C}$ -labelled B[a]P penetrated into the skin of a corpse during 24 h of incubation. By contrast, only 5.6  $\text{ng}/\text{cm}^2$  of the chemical was found in the skin when being a contaminant of soil, applied with a total contamination of 400  $\text{ng}/\text{cm}^2$  in the first place (26).

By using real commodity goods brought into direct contacts with human skin, a penetration model has been established in the frame of our work that closely mirrors everyday exposure scenarios. The items used were contaminated with B[a]P in the range of 57 to 266 mg/kg material (**Table 1**).

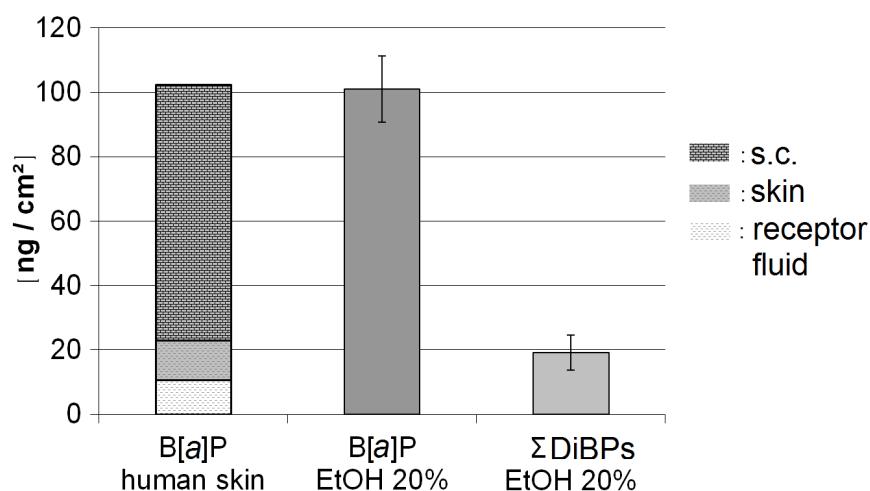


**FIGURE 2.** Comparison of the combined migration and penetration of B[a]P into human skin with the migration of B[a]P or the sum of dibenzopyrene isomers (DiBPs) into 20% ethanolic simulant. Left column: Combined migration and penetration of B[a]P from of sample #2 into human skin, n=1. Different compartments of the Franz cell set-up are indicated (s.c., *stratum corneum*; skin, receptor fluid). Middle and right columns: Quantification of the migration of B[a]P and the four dibenzopyrenes (DB[a,l]P, DB[a,e]P, DB[a,i]P, DB[a,h]P) into 20% ethanol at 37°C (individual TEFs were considered; see text for further explanation). Experimental set up has been performed in triplicates for migration studies and bars show the standard error of the mean.

The results of the Franz cell chamber assay using human skin *ex vivo* show that a total of 102 ng/cm<sup>2</sup> B[a]P penetrated the skin when brought into contact and incubated with the material of a conventional hammer handle (sample #2, **Figure 2** left bar). About 80% of this amount remained in the upper epidermal *stratum corneum* layer even after an incubation period of 24 h (in case of sample #2: 80 ng/cm<sup>2</sup> of 102 ng/cm<sup>2</sup>, **Figure 2**: left bar, dark grey segment). The other 20% of the penetrated amount of B[a]P were nearly equally distributed in the remaining epidermal layers and the receptor fluid (in case of sample #2: 22 ng/cm<sup>2</sup> of the total of 102 ng/cm<sup>2</sup>, **Figure 2**: left bar, light grey and white segments). According to this result it has thus been shown that lipophilic PAHs, such as B[a]P, migrate further into deeper (living) skin layers or can even reach systemic circulation. In the Franz cell system, the fraction reaching the receptor fluid of the chamber is to be considered as the amount that will become systemically available in the case of real human skin exposure (27).

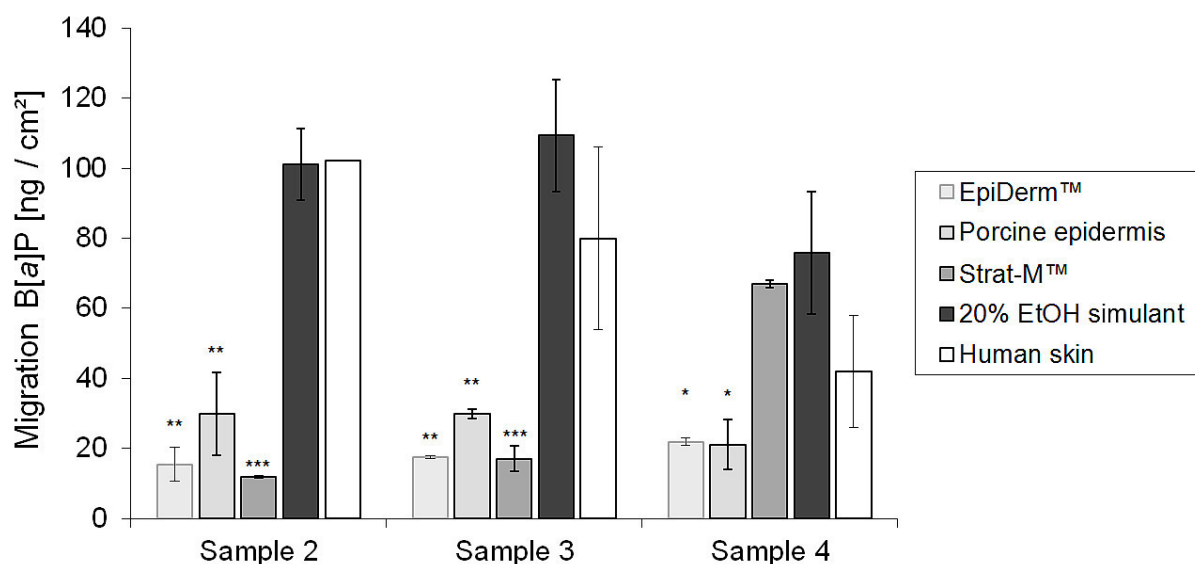


**FIGURE 3.** Migration of B[a]P into 20% ethanolic simulant solution and its comparison with other skin models that have been applied in the Franz cell assay. B[a]P was released from the three different product samples #2, 3 and 4 (cf. Table I). The tests were performed at 37°C for ethanolic simulant and at 33.5°C for all other models (incubation period: 24 h). Bars show the standard error of the mean. n=1 for sample 2 with human skin, n=2 for porcine epidermis and EpiDerm skin model, n=3 for others. Asterisks indicate significant differences concerning B[a]P load compared to the 20% ethanolic simulant system (\*\*\* p < 0.001; \*\* p < 0.01; \* p < 0.05).

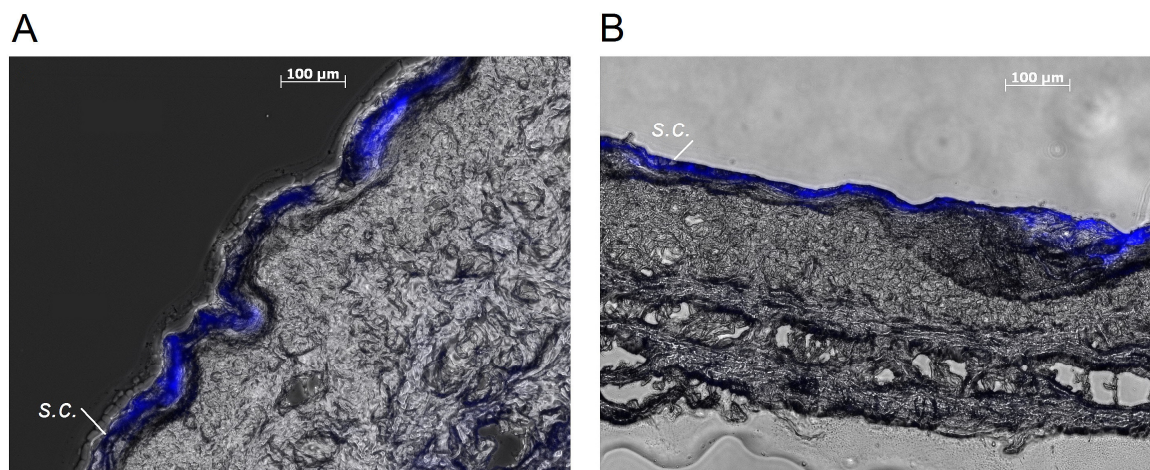


**FIGURE 4.** Cryosections of human skin (10 µm) after contact with a PAH containing consumer product. Evaluation by fluorescence microscopy at 350 nm (abs) / 450 nm (em). Fluorescence signal depicted in blue. Human skin specimen exposed to 1 µg B[a]P/cm<sup>2</sup> in acetonitrile for 24 h at room temperature as positive control (**A**). Section of human skin after contact with sample #3 (hammer handle) for 24 h at room temperature (**B**). *s.c.*, *stratum corneum*.

Similarly, using porcine skin or the skin models EpiDerm and Strat-M the penetration of B[a]P could be confirmed (**Figure 3**). Yet in comparison to the results obtained with human skin, B[a]P migration was significantly lower in the case of porcine skin or the EpiDerm model. Additionally, the PAH accumulation in human epidermis could be confirmed by visualization via its fluorescence signal (**Figure 4**) taking advantage of the conjugated aromatic ring system of PAHs (**Figure 1A**). B[a]P dissolved in acetonitrile was applied as positive control (**Figure 4A**). Direct contacts between sample #3 (266 mg/kg B[a]P) and human skin *ex vivo* resulted in an accumulation of PAHs in the upper epidermal layer (**Figure 4B**), but not in subepidermal layers.

#### **A solvent-based approach to predict skin penetration of B[a]P and to analyze PAHs of high toxicological relevance**

Aqueous sweat simulants are often used to assess dermal exposure to certain compounds found in products intended for skin contact (15, 18). Hamm and coworkers studied the potential release of PAHs from cured rubber materials containing carbon black as reinforcing agent into drinking water, artificial sweat, saliva and rainwater for 7 days at 30°C (23). They concluded that once incorporated into a rubber matrix, PAHs are hardly available to aqueous media and that these results should be considered in the assessment of PAH exposure resulting from rubber articles. In the present study we clearly demonstrated



that aqueous sweat simulant reveals unsuitable for the testing of B[a]P migration out of rubber materials. In comparison to the data obtained with the Franz cell chamber using human skin – which is always considered as reference method representing the real exposure most precisely – an underestimation of at least two orders of magnitude was observed (**Figure 5**, samples #1 and #2: light grey bars compared to white bars).

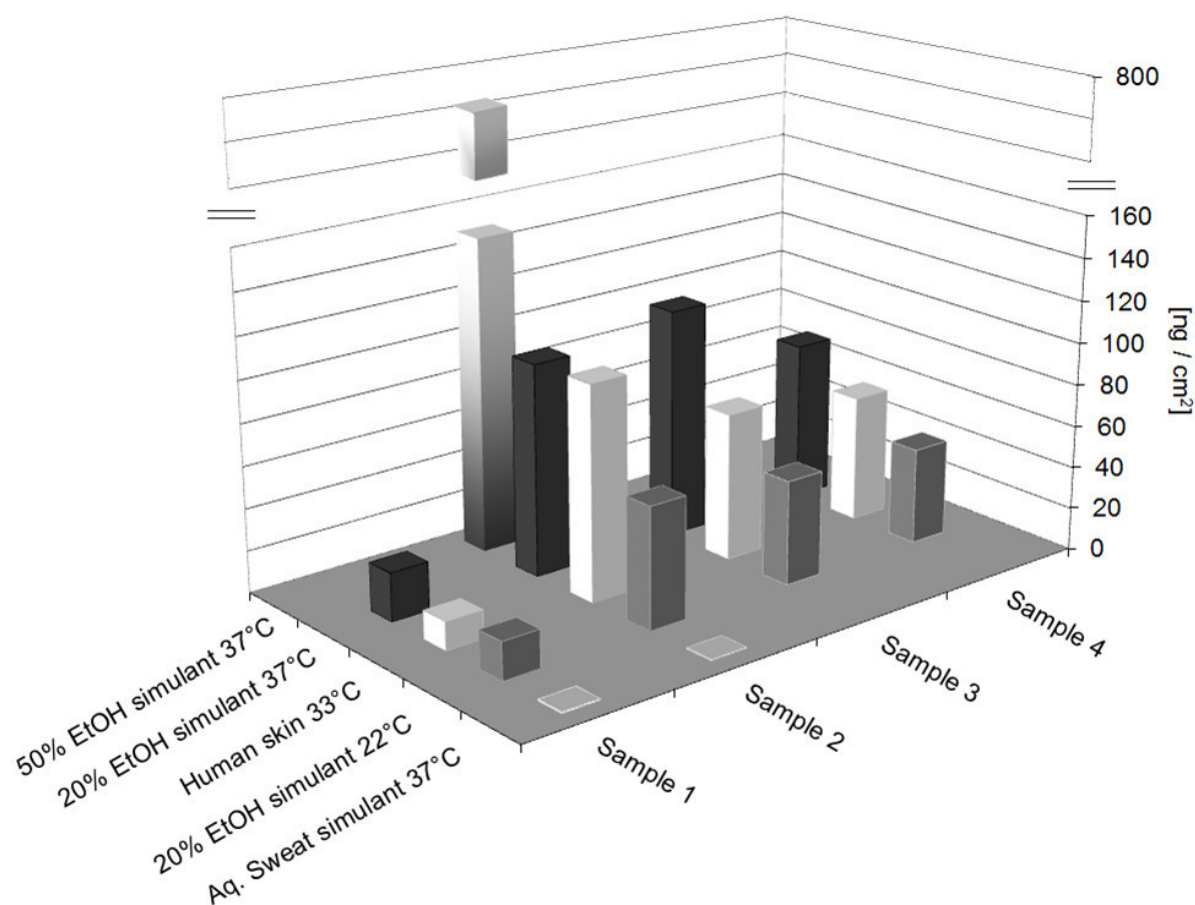


**FIGURE 5.** Migration of B[a]P out of four different product samples (cf. Table 1) into liquid simulation systems in comparison to its permeation through human skin (white bars). The average values of three independent analyses for each simulant are depicted (incubation time: 24 h, incubation temperature: 22°C or 37°C).

Since data from the literature have suggested that 95% ethanol would be an alternative fat simulant (28, 29), pre-tests with high concentrations of ethanol have been conducted. Our results however show that 95% ethanol leads to an overestimation of the migrating amounts of B[a]P due to solvent-induced maceration of the material and subsequent extraction of the analytes. To find a simulant which mimics more appropriately the influence of proteins, fat and water as it can be found in skin, migration studies have been performed using 50% ethanolic simulant, which is statutorily set as simulant to mirror milk

matrix (30). Migration analysis using 50% ethanolic simulant still resulted in an overestimation of the B[a]P release of about one order of magnitude when compared to the human skin reference (**Figure 5**; bicolored bar of sample #2 compared to white bar). By further refining the simulation system it could be shown that 20% of ethanol at 37°C nicely mirrors the real human skin exposure that results from direct contacts to anyone of the four commodities tested (**Fig. 5** black bars compared to white bars). Compared to a standardized synthetic membrane designed for diffusion cell testing (Strat-M), 20% ethanol again revealed much better in terms of reflecting the real level of B[a]P migration and penetration into real human skin (**Figure 3**, see samples #2 and #3). In the case of sample #4 both systems, the Strat-M membrane and 20% ethanol were performing equally well. Altogether 20% ethanol at 37°C was demonstrated suitable to represent real human skin in PAH migration testing of commodities consisting of different materials.

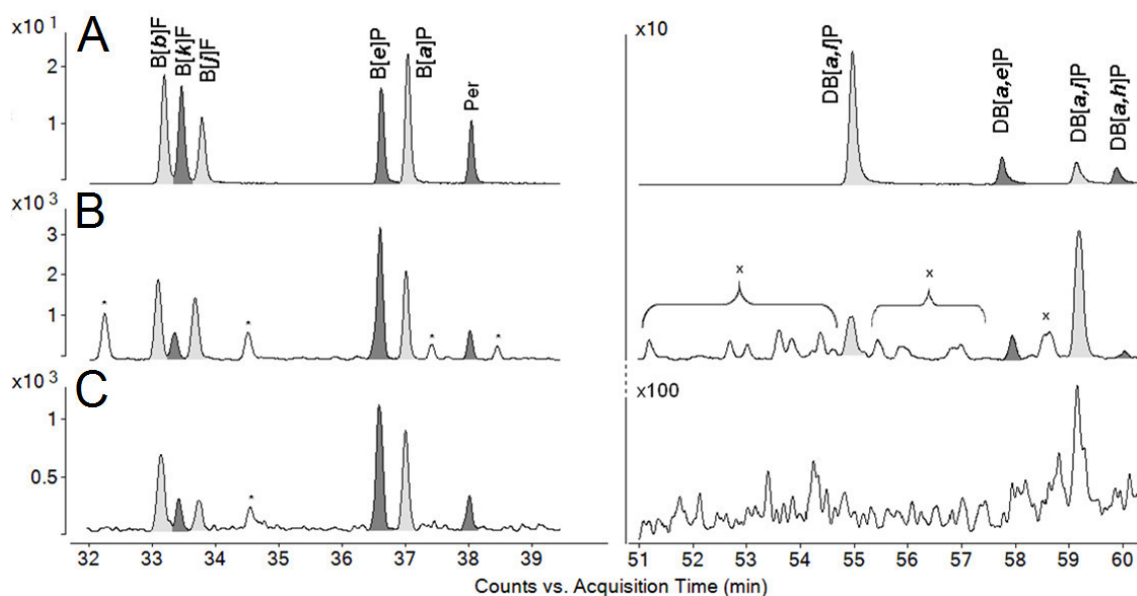


**FIGURE 6.** Chromatographic evaluation of skin model systems for penetrating PAHs (GC-EI-MS/MS in multiple reaction monitoring (MRM) mode). Chromatograms of the extracted molecular masses 252 (left) and 302 (right). PAH standards (A). Migration of PAHs from sample #2 into 20% ethanolic simulant during 24 h (B). Penetration of PAHs from sample #2 into porcine epidermis during 24 h (C). \*Unidentified PAHs with molecular mass of 252. <sup>x</sup>Unidentified PAHs with molecular mass of 302. Abbreviations: B[b]F, benzo[b]fluoranthene; B[k]F, benzo[k]fluoranthene; B[j]F, benzo[j]fluoranthene; B[e]P, benzo[e]pyrene; B[a]P, benzo[a]pyrene; Per, perylene; dibenzopyrene isomers: DB[a,l]P, DB[a,e]P, DB[a,i]P, and DB[a,h]P.

Since three dibenzopyrene isomers (i.e., DB[*a,l*]P, DB[*a,i*]P and DB[*a,h*]P) are rated with 10-fold higher carcinogenicity in comparison to B[*a*]P (cf. above), the dermal burden of these compounds is of particular toxicological interest. Based on the results obtained with 20% ethanol and the model compound B[*a*]P, migration tests and evaluation of the dermal load of four dibenzopyrene isomers (the three mentioned above plus DB[*a,e*]P) have also been performed under the same conditions. Due to the lower contents of these PAH congeners in the materials compared to B[*a*]P, additional requirements in the development of the analytical method had to be addressed (cf. above). Using 20% ethanol at 37°C for 24 h it could be demonstrated that both pentacyclic and hexacyclic PAHs were released by sample #2 (**Figure 6B**). Conversely, the hexacyclic PAHs could not be quantified when using porcine skin in the Franz cell chamber assay (**Figure 6C**). **Figure 2** depicts the dermal load of B[*a*]P divided into single compartments as evaluated for human skin upon incubation with sample #2. The results obtained for B[*a*]P and for the sum of dibenzopyrenes after 24 h of incubation of sample #2 with 20% ethanolic simulant are also shown for comparison purposes. The individual TEF values were taken into account when evaluating the dibenzopyrene load in **Figure 2** (right bar). In consideration of the level of migration of B[*a*]P and the four dibenzopyrene isomers from hammer sample #2 into 20% ethanol, the overall skin load on highly toxic dibenzopyrenes equals about 20% of the corresponding B[*a*]P load (**Figure 2**). Based on these results and their higher toxicity, we propose that the penetration of hexacyclic PAHs certainly requires attention and further investigation in order to reliably assess the risks associated with PAH-containing products that come into contact with human skin.

## CONCLUSIONS

The solubility of polymers including their additives has an influence on the properties of the material and the migration of its constituents. Material's surface and the degrees of maceration and porosity can all be affected upon contact with solvents. A commonly used solvent in the prediction of dermal exposure is the aqueous sweat simulant. Yet, the data presented here clearly indicate that an aqueous simulant is not suitable for migration testing of lipophilic substances. Since this simulant led to a 100-fold underestimation of the extent of migration in the case of lipophilic compounds such as B[*a*]P, we established an alternative ethanol-based approach. Best results for the prediction of the dermal load with B[*a*]P were obtained with 20% ethanol at 37°C. The amounts obtained were in excellent agreement with the migration levels measured in real human skin *ex vivo* for four polymers of different composition. It is therefore proposed that this system could serve as model for

the testing of consumer products and the assessment of the dermal exposure against lipophilic ingredients of the respective materials. Using migration studies, only the matrix derived barrier for PAHs can be taken into account. The comparison to Franz cell studies is based on the aim to generate a model that needs no skin or artificial skin. It admittedly cannot mirror the combined skin penetration and migration of the respective PAH, but it serves as a good model to get an impression on the overall amounts that might become bioavailable during skin contacts. In terms of B[a]P migration testing 20% ethanol at 37°C turned out to be an even better predictive model than other commonly used skin models applicable in the Franz cell chamber (EpiDerm, Strat-M or porcine skin) (Figure 3). Using this model we could further show that the fraction of highly carcinogenic dibenzopyrenes can contribute to the health risks mediated via skin contacts of PAH-containing plastics and elastomers.

Along with the visual evaluation of cryosections of human skin following contacts with PAH-containing commodities, we established a system that enables to assess dermal exposure in detail. An advantage of using real skin specimens results from the possibility to analyze different depths of penetration and to monitor the dermal biokinetics of the compounds investigated (cf. Figures 2 and 4).

#### **ACKNOWLEDGMENTS**

The authors would like to thank Barbara Gerding and Karsten Schön for excellent technical assistance and Dr. Christian Witzel for providing human skin from plastic surgery.

#### **FUNDING**

This study was financially supported by internal funding of the German Federal Institute for Risk Assessment (BfR), grants No. 1322-343, 1322-514 and 72-003.

#### **REFERENCES**

- 1 **Andrady A. L., and M. A. Neal:** Applications and societal benefits of plastics. *Philos T Roy Soc B.* 2009;364(1526):1977-1984.
- 2 **Tsai P.-J., H.-Y. Shieh, L.-T. Hsieh, and W.-J. Lee:** The fate of PAHs in the carbon black manufacturing process. *Atmos Environ.* 2001;35(20):3495-501.
- 3 **Biedermann M., and K. Grob:** Comprehensive two-dimensional GC after HPLC pre-separation for the characterization of aromatic hydrocarbons of mineral oil origin in contaminated sunflower oil. *J Sep Sci.* 2009;32(21):3726-37.

- 4 **Granella, M., C. Ballarin, B. Nardini, M. Marchioro, and E. Clonfero:** Mutagenicity and contents of polycyclic aromatic hydrocarbons in new high-viscosity naphthenic oils and used and recycled mineral oils. *Mutat Res.* 1995;343(2-3):145-50.
- 5 **Galea, K.S., A. Davis, D. Todd, L. MacCalman, C. McGonagle, and J.W. Cherrie:** Dermal exposure from transfer of lubricants and fuels by consumers. *J Expo Sci Environ Epidemiol.* 2014;24(6):665-72.
- 6 **Luch, A.:** Polycyclic aromatic hydrocarbon-induced carcinogenesis - an introduction. *The carcinogenic effects of polycyclic aromatic hydrocarbons:* Imperial College Press, distributed by World Scientific Publishing Co.; 2005;1-18.
- 7 **Whitehead, T., C. Metayer, R.B. Gunier, M.H. Ward, M.G. Nishioka, P. Buffler, et al.:** Determinants of polycyclic aromatic hydrocarbon levels in house dust. *J Expo Sci Environ Epidemiol.* 2011;21(2):123-32.
- 8 **Regulation (EC) No 1272/2008** of the European Parliament and of the Council of 16 December 2008 on classification, labelling and packaging of substances and mixtures, amending and repealing Directives 67/548/EEC and 1999/45/EC, and amending Regulation (EC) No 1907/2006.
- 9 **Brinkmann, J., K. Stolpmann, S. Trappe, T. Otter, D. Genkinger, U. Bock, et al.:** Metabolically competent human skin models: activation and genotoxicity of benzo[*a*]pyrene. *Toxicol Sci.* 2013;131(2):351-9.
- 10 **Paschke, M., C. Hutzler, J. Brinkmann, F. Henkler, and A. Luch:** Polycyclic aromatic hydrocarbons in newspaper inks: migration, metabolism, and genotoxicity in human skin. *Polycycl Aromat Comp.* 2014;35(1):32-40.
- 11 **IARC:** Polycyclic aromatic compounds - monographs on the evaluation of the carcinogenic risk of chemicals to humans, 35 (1985).
- 12 **Cal-EPA:** Air toxics hot spots program risk assessment guidelines, part II technical support document for describing available cancer potency factors. 2005.
- 13 **US-EPA:** Technical factsheet on: polycyclic aromatic hydrocarbons (PAHs). 2002.
- 14 **Collins J.F., J.P. Brown, G.V. Alexeeff, and A.G. Salmon:** Potency equivalency factors for some polycyclic aromatic hydrocarbons and polycyclic aromatic hydrocarbon derivatives. *Regul Toxicol Pharm.* 1998;28(1):45-54.
- 15 **European standard:** DIN EN 71-10:2005 Safety of toys - Part 10: Organic chemical compounds - Sample preparation and extraction.

- 16 **Franz, T.J.:** Percutaneous absorption on the relevance of *in vitro* data. *J Invest Dermatol.* 1975;64(3):190-5.
- 17 **Ng, S.-F., J. Rouse, F. Sanderson, V. Meidan, and G. Eccleston:** Validation of a static Franz diffusion cell system for *in vitro* permeation studies. *AAPS PharmSciTech.* 2010;11(3):1432-41.
- 18 **European standard:** DIN EN ISO 105-E04:2013-08 Textiles - Tests for colour fastness - Part E04: Colour fastness to perspiration.
- 19 **ZLS (Zentralstelle der Länder für Sicherheitstechnik):** Testing and validation of polycyclic aromatic hydrocarbons (PAH) in the course of GS-mark certification, ZEK 01.4-08 2011. Available at: [http://www.zls-muenchen.de/de/left/aktuell/pdf/zek\\_01\\_4\\_08\\_pak\\_verbindlich\\_engl\\_30112011.pdf](http://www.zls-muenchen.de/de/left/aktuell/pdf/zek_01_4_08_pak_verbindlich_engl_30112011.pdf), effective 02/2014.
- 20 **Hutzler, C., A. Luch, and J.G. Filser:** Analysis of carcinogenic polycyclic aromatic hydrocarbons in complex environmental mixtures by LC-APPI-MS/MS. *Anal Chim Acta.* 2011;702(2):218-24.
- 21 **Tsuge, S., H. Ohtani, and C. Watanabe:** *Pyrolysis-GC/MS data book of synthetic polymers - pyrograms, thermograms and MS of pyrolyzates.* Oxford: Elsevier. 2010.
- 22 **Mukhopadhyay, S., P.P. De, and S.K. De:** A self-vulcanizable and miscible blend system based on hypalon and carboxylated nitrile rubber. *J Appl Polym Sci.* 1991;43(2):347-55.
- 23 **Hamm, S., T. Frey, R. Weinand, G. Moninot, and N. Petiniot:** Investigations on the extraction and migration behavior of polycyclic aromatic hydrocarbons (PAHS) from cured rubber formulations containing carbon black as reinforcing agent. *Rubber Chem Technol.* 2009; 82(2): 214-228.
- 24 **Van de Sandt, J.J.M., M. Dellarco, J.J. Van Hemmen:** From dermal exposure to internal dose. *J Expo Sci Environ Epidemiol.* 2007;17(S1):S38-S47.
- 25 **Spalt, E.W., J.C. Kissel, J.H. Shirai, A.L. Bunge:** Dermal absorption of environmental contaminants from soil and sediment: a critical review. *J Expo Sci Environ Epidemiol.* 2008;19(2):119-48.
- 26 **Wester, R.C., H.I. Maibach, D.A.W. Bucks, L. Sedik, J. Melendres, C. Liao, et al.:** Percutaneous absorption of [<sup>14</sup>C]DDT and [<sup>14</sup>C]benzo[*a*]pyrene from soil. *Toxicol Sci.* 1990;15(3):510-6.

- 27 **Chu, I., D. Dick, R. Bronaugh, and L. Tryphonas:** Skin reservoir formation and bioavailability of dermally administered chemicals in hairless guinea pigs. *Food Chem Toxicol.* 1996;34(3):267-76.
- 28 **Council Directive 82/711/EEC** of 18 October 1982 laying down the basic rules necessary for testing migration of the constituents of plastic materials and articles intended to come into contact with foodstuffs, (1982).
- 29 **Simoneau, C., and P. Hannaert:** Stability testing of selected plastics additives for food contact in EU aqueous, fatty and alternative simulants. *Food Addit Contam.* 1999;16(5):197-206.
- 30 **The European Commission:** Commission regulation (EU) No 10/2011 of 14 January 2011 on plastic materials and articles intended to come into contact with food. 2011.

### **6.3 Chemical stabilization of polymers: Implications for dermal exposure to additives**

Nastasia Bartsch, Mathilde Girard, Lidia Schneider, Valerie van de Weijger, Amelie Wilde, Oliver Kappenstein, Bärbel Vieth, Christoph Hutzler, Andreas Luch, *Journal of Environmental Science and Health, Part A*.

Published online: 15 Jan 2018

DOI: 10.1080/10934529.2017.1412192

Link: <https://doi.org/10.1080/10934529.2017.1412192>

Involvement of the author within this publication: Project planning: 70%, project execution: 50%, data analysis: 70%, writing of the manuscript: 90%



## ABSTRACT

Technical benefits of additives in polymers stand in marked contrast to their associated health risks. Here, a multi-analyte method based on gas chromatography coupled to tandem mass spectrometry (GC-MS/MS) was developed to quantify polymer additives in complex matrices such as low-density polyethylene (LDPE) and isolated human skin layers after dermal exposure *ex vivo*. That way both, technical aspects and dermal exposure were investigated. The effects of polymer addition on the material were studied using the example of LDPE. To this end, a tailor-made polymer was applied in aging studies that had been furnished with two different mixtures of phenol- and diarylamine-based antioxidants, plasticizers and processing aids. Upon accelerated thermo-oxidative aging of the material, the formation of LDPE degradation products was monitored with attenuated total reflectance—Fourier transformed infrared (ATR–FTIR) spectroscopy. Compared to pure LDPE, a protective effect of added antioxidants could be observed on the integrity of the polymer. Further, thermo-oxidative degradation of the additives and its kinetics were investigated using LDPE or squalane as matrix. The half-lives of additives in both matrices revealed significant differences between the tested additives as well as between LDPE and squalane. For instance, 2-*tert*-butyl-6-[(3-*tert*-butyl-2-hydroxy-5-methylphenyl)methyl]-4-methylphenol (Antioxidant 2246) showed a half-life 12 times lower when incorporated in LDPE as compared to squalane. As a model for dermal exposure of consumers, human skin was brought into contact with the tailor-made LDPE containing additives *ex vivo* in static Franz diffusion cells. The skin was then analyzed for additives and decomposition products. This study proved ten polymer additives of diverse physicochemical properties and functionalities to migrate out of the polymer and eventually overcome the intact human skin barrier during contact. Moreover, their individual distribution within distinct skin layers was demonstrated. This is exemplified by the penetration of the procarcinogenic antioxidant *N*-phenylnaphthalen-2-amine (Neozon D) into the viable epidermis and the permeation through the skin of the neurotoxic plasticizer *N*-butylbenzenesulfonamide (NBBS). In addition, the analyses of additive degradation products in the isolated skin layers revealed the presence of 2-*tert*-butyl-4-methylphenol in all layers after contact to a polymer with substances of origin like Antioxidant 2246. Thus, attention needs to be paid to absorption of polymer additives together with their degradation products when it comes to dermal exposure assessment.

**KEYWORDS:** Polymer aging; Additives; LDPE; Squalane; GC-MS/MS; ATR–FTIR; Dermal exposure; Franz diffusion cell; Percutaneous absorption

## 1. INTRODUCTION

To look into the diverse fields of polymer additives and their degradation products, diverse analytical methods are required <sup>[1,2]</sup>. It has already been shown for food contact materials that additivation of polymers leads to the formation of certain reaction products and impurities. These usually differ completely in their physicochemical properties from the originally applied parent compounds and even lack toxicological evaluation <sup>[3]</sup>. Due to their origin in the food contact materials area, follow-up products from additives are referred to as non-intentionally added substances (NIAS). Additives of low molecular weight as well as degradation products from larger molecules usually migrate out of the polymer matrix faster than higher molecular components <sup>[4]</sup>. Therefore, low-molecular chemical species have a higher probability of coming into direct contact with consumers who are using products made of polymers. With regard to biological surfaces, e.g. the skin barrier, smaller molecules are likely to be of particular toxicological relevance. This is because smaller molecules more easily overcome biological barriers as compared to larger ones of similar polarity <sup>[5]</sup>. Therefore, a multi-analyte analysis was performed based on gas chromatographic separation coupled to tandem mass spectrometry for 26 different additives in the molecular weight range of <550 Da and potential degradation products. These substances are either of particular toxicological concern or are widely used in the polymer industry in general. The neurotoxic plasticizer *N*-butylbenzenesulfonamide (NBBS) was found to be one of the top 30 micro-organic contaminants in the aquatic environment in England and Wales <sup>[6]</sup>. Also, a rapid distribution of NBBS in tissues was determined by Kumar et al. in rat after iv administration <sup>[7]</sup>. Due to its ubiquitous occurrence and application in polymers that are potentially intended for skin contacts, the multi-analyte method was applied to NBBS and nine more additives (**Figure 1**) in skin penetration studies to emphasize the transdermal path to internal body burden. The additives have been chosen to cover diverse functionalities within polymers and a broad range of lipophilicity. The technical aspects of polymer stabilization and depletion of additives were investigated in the light of polymer and additive aging processes. In order to evaluate the processes' individual kinetics, two different aging scenarios using either a squalane or a low-density polyethylene (LDPE) matrix were evaluated. Advantageously, the squalane model after Beißmann et al. <sup>[8]</sup> can easily be standardized and additives investigated separately. In contrast, the polymer mimicking fluid squalane is an artificial matrix. Therefore, classic aging studies on LDPE matrix were performed in this study in

addition. Attenuated total reflectance—Fourier transformed infrared (ATR–FTIR) spectroscopy is a well-known technique in the field of material science. Studies on thermo-oxidized LDPE have shown that, typical ketone- and aldehyde- groups are formed as a consequence of material degradation <sup>[9]</sup>. Here, the characteristic bands for LDPE degradation products and additives were monitored in ATR–FTIR spectroscopy long-term studies. That way, a protective effect of the tested set of antioxidants on the polymer integrity against oxidation and thermal degradation was revealed. Moreover, the results of IR analyses were transferred to complex biological matrices. Typically assigned IR bands of additives were not only traced in the material itself but also in human skin after dermal contact to the investigated material *ex vivo* by applying IR-microscopy. The dermal penetration pathway of the secondary aromatic amine *N*-phenyl-2-naphthylamine was visualized for the first time thereby.

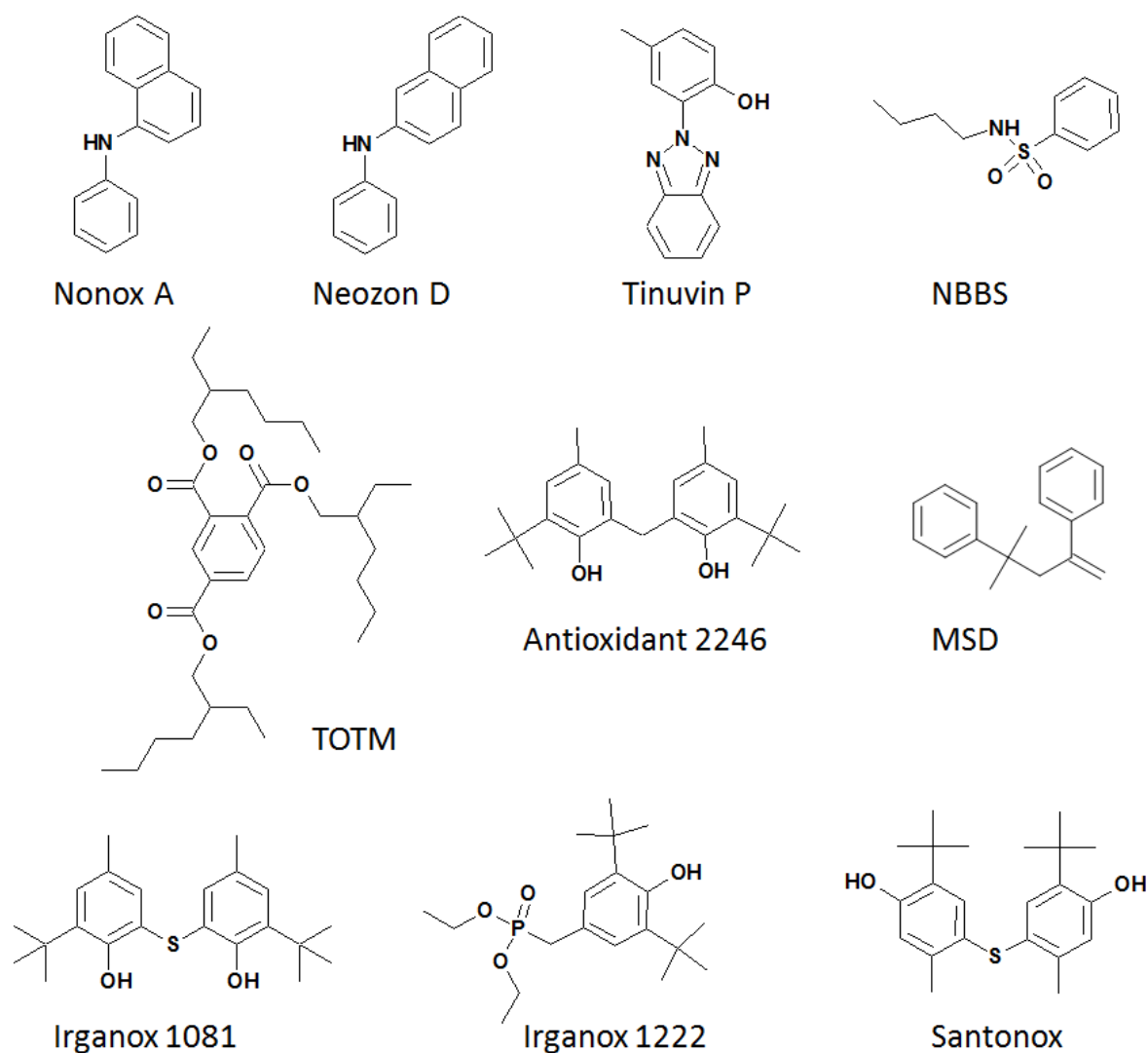


FIGURE 1: Chemical structures of additives included in the degradation studies performed. Table 2 contains a more detailed description. Nonox A: *N*-phenylnaphthalen-1-amine, Neozon D: *N*-phenylnaphthalen-2-amine, Tinuvin P: 2-(benzotriazol-2-yl)-4-methylphenol, NBBS: *N*-butylbenzenesulfonamide, TOTM: tris(2-ethylhexyl) benzene-1,2,4-tricarboxylate, Antioxidant 2246: 2-*tert*-butyl-6-[(3-*tert*-butyl-2-hydroxy-5-methylphenyl)methyl]-4-methylphenol,  $\alpha$ -MSD: 2,4-diphenyl-4-methyl-1-pentene, Irganox 1081: 2-*tert*-butyl-6-(3-*tert*-butyl-2-hydroxy-5-methylphenyl)sulfanyl-4-methylphenol, Irganox 1222: 2,6-di-*tert*-butyl-4-(di-ethoxyphosphorylmethyl)phenol, Santonox: 2-*tert*-butyl-4-(5-*tert*-butyl-4-hydroxy-2-methylphenyl)sulfanyl-5-methylphenol.

## 2. EXPERIMENTAL

### 2.1. Materials and Chemicals

2-*tert*-Butyl-4-(5-*tert*-butyl-4-hydroxy-2-methylphenyl)sulfanyl-5-methylphenol (Santonox), 2,6-di-*tert*-butyl-4-(diethoxyphosphorylmethyl)phenol (Irganox 1222) and 2-*tert*-butyl-6-[(3-*tert*-butyl-2-hydroxy-5-methylphenyl)methyl]-4-methylphenol (Antioxidant 2246) were purchased from abcr GmbH (Karlsruhe, Germany). Squalane was purchased from Sigma-Aldrich (St. Louis, MO, USA), as well as all the remaining additives included in the multi-analyte method. Standard substances with a purity of  $\geq 97\%$  were utilized to prepare a mixture in acetonitrile with concentrations of 10  $\mu\text{g/ml}$  each.

The following labeled substances were used as internal standards: *p*-cresol- $\text{d}_8$  (CIL: Cambridge Isotope Laboratories, Inc. Tewksbury, MA, USA), acetophenone- $\text{d}_8$  (Sigma-Aldrich), benzophenone- $\text{d}_{10}$  (Sigma-Aldrich), 2-aminonaphthalene- $\text{d}_7$  (CIL), *p*-terphenyl- $\text{d}_{14}$  (CIL), di-(2-ethylhexyl)-phthalate- $\text{d}_4$  (CIL), 2-isopropyl- $\text{d}_7$ -thioxanten-9-one (Sigma-Aldrich) and di-*n*-nonylphthalate-3,4,5,6- $\text{d}_4$  (Dr. Ehrenstorfer GmbH, Augsburg, Germany). A stock solution of internal standards with a concentration of 10  $\mu\text{g/ml}$  each in acetonitrile was prepared. Solvents for GC analyses and for sample preparation (toluene, acetone, acetonitrile, ethyl acetate, methanol, ethanol and hexane) were purchased from Sigma-Aldrich (St. Louis, MO, USA) or Merck KGaA (Darmstadt, Germany).

Tailor-made polymer material was purchased from Clariant (Gersthofen, Germany), aiming to provide an accurately defined polymer-based model for accelerated aging studies and skin penetration studies of additives. LDPE powder (SABIC<sup>®</sup> 1922Z900) was used as matrix for 10 selected additives, subdivided into two applied recipes (LDPE 1 and LDPE 2, cf. **Table 1**). The raw LDPE material was used with the following specifications: a melt volume index (MVI) of 22 g/10 min, melting temperature (10°C/min) of 107°C, a heat deflection temperature (HDT) of 83°C and a density of 919 kg/m<sup>3</sup> [10]. To increase the homogeneity of the final material, compounding took place by preparing a master batch of LDPE pellets containing the respective additives. Pellets of the master batches together with pure LDPE were extruded followed by injection molding to specimens with a size of 60 x 60 x 1 mm and a scheduled final concentration of each additive of 10 g/kg. The process was conducted with a rotation speed of 300 rpm and the following temperature

zones (T<sub>1</sub>-T<sub>10(Die)</sub>): T<sub>1</sub>: 170°C, T<sub>2</sub>: 180°C, T<sub>3</sub>: 180°C, T<sub>4</sub>: 185°C, T<sub>5</sub>: 185°C, T<sub>6</sub>: 190°C, T<sub>7</sub>: 190°C, T<sub>8</sub>: 200°C, T<sub>9</sub>: 200°C, T<sub>10(Die)</sub>: 200°C.

## 2.2. GC-MS/MS – A Multi-Method to Quantify Polymer Additives and Degradation Products

A method for the determination of 21 additives and 5 potential degradation products was developed using GC-MS/MS. Based on GC-MS/MS screening of consumer products and data from the literature<sup>[11, 12]</sup>, commonly used additives were identified and a multi-analyte method using the most sensitive and selective multiple reaction monitoring (MRM) mode was established. Details on analytes and transitions used for quantification, logP<sub>O/W</sub> values and qualifiers are summarized in **Table 2**. A GC-MS/MS system consisting of a GC 7890A and a tandem mass detection system MS7000A in electron impact ionization mode (70 eV) (all Agilent, Santa Clara, CA, USA) was used for analysis of additives and their degradation products. For chromatographic separation, an Rxi-17SilMS GC column (30 m x 0.25 mm i.d., 0.25 µm df; Restek, Bad Homburg, Germany) equipped with a pre-column (5 m x 0.25 mm i.d.; Phenomenex, Aschaffenburg, Germany) and helium as carrier gas (purity ≥ 99.999%, Linde, Pullach, Germany) was used. The following GC temperature program was applied: 70°C for 1.5 min, structured ramp: 25°C/min to 250°C with a hold time of 7 min, 3°C/min to 280°C for 1 min, 25°C/min to 300°C for 9 min.

The instrument was utilized with an autosampler MPS 2XL (MultiPurpose Sampler; Gerstel, Mülheim, Ruhr, Germany). A cooled injection system (PTV-type CIS; Gerstel) was used with an initial injection temperature of 45°C, followed by a ramp of 12°C/s to 280°C with a hold time of 20 min and a second ramp of 12°C/s towards 340°C. The injection volume applied was 1 µl.

GC-MS/MS data were acquired using the Enhanced MassHunter B.06.00 software (Agilent) and Maestro 1.4. software (Gerstel) with a Dell workstation. MassHunter workstation software (Qualitative Analysis version B.06.00 and Quantitative Analysis version B.05.00, Agilent) was applied to the GC-MS/MS data of additives and degradation products. For all analytes, linear regression calibrations in concentrations of 15 to 500 ng/ml were performed. Selected qualifier and quantifier ions were extracted and automatically integrated accompanied by manual control. Two tailed Student's t-tests with

$\alpha=0.05$  as well as calculation of exponential degradation curves were performed using Microsoft Excel 2010.

### 2.3. Investigations of Additives Incorporated in the LDPE Matrix

To characterize the effect of additivation on LDPE, aging studies of the respective additives incorporated into the polymer matrix were performed *in situ*. To this end, an LDPE-based model polymer was designed with additive blends according to the GC-MS/MS multi-method and ordered from Clariant (Gersthofen, Germany). In parallel, the pure polymer without additivation was treated as negative control. The detailed recipes applied to LDPE, together with the GC-MS/MS results of additive quantification in the final material, are shown in **Table 1**.

Table 1. Composition of tailor-made polymers. The recovery of analytes in the final material is shown for two LDPE compositions.

ID	Additivation	Scheduled/ determined amount [g/kg]	ID	Additivation	Scheduled/ determined amount [g/kg]
LDPE	$\alpha$ -MSD	10/ $6.5 \pm 0.9$	LDPE	Tinuvin P	10/ $3.5 \pm 0.6$
1	NBBS	10/ $4.6 \pm 0.8$	2	Nonox A	10/ $3.2 \pm 0.5$
	Irganox 1222	10/ $1.6 \pm 0.2$		Neozon D	10/ $2.1 \pm 0.7$
	Irganox 1081	10/ $0.6 \pm 0.04$		Antioxidant 2246	10/ $3.1 \pm 0.1$
	Santonox	10/ $4.1 \pm 0.05$		TOTM	10/ $4.2 \pm 0.2$

The LDPE samples were stored at 4°C, wrapped in aluminum foil and with the absence of air upon analyses. Specimens of the respective polymer were cut to a size of maximum 1-2 mm edge length as optimized in the extraction procedure. Subsequently, the cut material was merged to randomize the sampling. For the experimental set-up,  $12.8 \pm 0.9$  mg were placed into dark 20 ml headspace vials and sealed with an aluminum/polytetrafluoroethylene (PTFE) cap. Specimens of the pure polymer as well as an empty vial were used as blank. A time period of 25 days was covered, evaluating time points at 0.5 h, 3 d, 7 d, 14 d, 18 d and 25 d. Experiments were conducted at 70°C and at 130°C (oven type 720 FED; Binder, Tuttlingen, Germany). At least three independent set-ups for each time point and temperature were evaluated together with two additive-free

LDPE blanks. To ensure complete extraction of the additives, the extraction conditions were optimized. Both cryo-milled (Pulverisette 0; FRITSCH GmbH, Idar-Oberstein, Germany) polymer samples and cut material were subjected to the optimization of extraction procedure. To this end, ultrasonic extraction with different solvents and varying duration was evaluated individually for each additive. Acetonitrile, toluene, methanol and ethyl acetate were the solvents tested, applying extraction times of 0.5 h, 1 h and 2 h. Since extraction of cut polymer in toluene for 1 h was revealed to be the best option and sufficient for all compounds, incubated samples were cooled to room temperature after incubation, submerged in 10 ml toluene and subsequently treated for 1 h in the ultrasonic bath. As positive control, 250  $\mu$ l of the standard substance mixture (10  $\mu$ g/ml in acetonitrile) was filled with toluene to a final volume of 10 ml, covering all analytes present in the polymers with final concentrations of 250 ng/ml each. The internal standard mixture (10  $\mu$ g/ml in acetonitrile) was then added to aliquots of the extracts, yielding a final concentration of labeled substances of 100 ng/ml each. Finally, the samples were analyzed by GC-MS/MS. Recoveries of positive controls ranged from  $76 \pm 8\%$  for Santonox to  $95 \pm 7\%$  for the  $\alpha$ -methylstyrene dimer (2-methyl-4-phenylpent-4-en-2-yl) ( $\alpha$ -MSD) (cf. supplementary information Table S1). The actual amounts of additives present in the final material compared to the scheduled amount remained lower than 65% for all additives, however (**Table 1**). This loss was found to be associated with the manufacturing process of the polymer. Rotation speed along with temperatures of up to 200°C was applied to the material and evidentially caused depletion of analytes.



Table 2. Classification of analytes and MRM parameters for additives, degradation products and internal standards. The individual limits of detection (LOD) have been calculated using the signal-to-noise method with respective quantifier transition <sup>[27]</sup>. Octanol-water partition coefficients LogP<sub>O/W</sub> refer to the assigned sources <sup>[28-34]</sup>. CAS: Chemical abstracts service.

No.	IUPAC name	Trivial name	CAS-number	Function	Log P <sub>O/W</sub>	LOD [ng/ml]	Precursor Ion	Product Ion <sub>Quanti</sub>	Product Ion <sub>Quali</sub>	Rf [min]
1	Benzaldehyde	BA	100-52-7	Antimicrobial	1.5 <sup>[28]</sup>	0.5	106	77	51	4.76
2	4-Methylphenol	<i>p</i> -Cresol	106-44-5	Degradation product	1.9 <sup>[28]</sup>	19.1	108	77	51	5.30
3	2,4-Dimethylphenol	2,4-Xylenol	105-67-9	Degradation product	2.3 <sup>[28]</sup>	15.0	122	107	91	5.75
4	2,4,6-Trimethylphenol	Mesitol	527-60-6	Degradation product	2.7 <sup>[29]</sup>	0.4	136	121	91	6.11
5	2-Ethyl-4-methylphenol	2-Ethyl- <i>p</i> -cresol	3855-26-3	Degradation product	3.0 <sup>[30]</sup>	0.6	136	121	91	6.19
6	Isothiocyanatocyclohexane	-	1122-82-3	Process aid	3.0 <sup>[32]</sup>	0.3	141	55	112; 83	6.42
7	2- <i>tert</i> -Butyl-4-methylphenol	2- <i>t</i> -Butyl- <i>p</i> -cresol	2409-55-4	Degradation product	3.6 <sup>[32]</sup>	5.7	164	149	121	6.82
8	2-Methyl-1,2-thiazol-3-one	MI	2682-20-4	Antimicrobial	0.1 <sup>[30]</sup>	4.1	115	87	91; 59	6.95
9	2,6-Di- <i>tert</i> -butyl-4-ethylphenol	Antioxidant BHEB	4130-42-1	Antioxidant	5.7 <sup>[32]</sup>	0.2	219	159	131	7.68
10	2- <i>tert</i> -Butyl-4-methoxyphenol	BHA	25013-16-5	Antioxidant	3.3 <sup>[30]</sup>	0.8	180	165	137	7.79
11	<i>N</i> -benzyl-1-phenylmethanamine	DBA	103-49-1	Vulcanization, stabilization	2.7 <sup>[30]</sup>	6.0	197	106	92	9.25
12	(2-Methyl-4-phenylpent-4-en-2-yl)benzene	$\alpha$ -MSD	6362-80-7	Crosslinking agent	6.2 <sup>[30]</sup>	0.2	119	91	65	9.30
13	<i>N</i> -benzyl-1-phenylmethanimine	N-BIBA	780-25-6	Vulcanization, stabilization	3.2 <sup>[32]</sup>	6.7	195	116	91	9.46
14	<i>N</i> -Butylbenzenesulfonamide	NBBS	3622-84-2	Plasticizer	2.0 <sup>[30]</sup>	0.1	170	77	141; 51	9.87
15	2-(Benzotriazol-2-yl)-4-methylphenol	Tinuvin P	2440-22-4	UV Stabilizer	4.2 <sup>[30]</sup>	3.0	225	93	168	11.84
16	2,6-Di- <i>tert</i> -butyl-4-(diethoxyphosphorylmethyl)phenol	Irganox 1222	976-56-7	Antioxidant	4.7 <sup>[32]</sup>	1.9	356	341	285	12.00
17	1- <i>N</i> -phenyl-4- <i>N</i> -propan-2-ylbenzene-1,4-diamine	Vulkanox 4010	101-72-4	Antioxidant, antiozonant	3.3 <sup>[30]</sup>	1.7	211	168	118	12.38
18	2,4-Di- <i>tert</i> -butyl-6-[1-(3,5-di- <i>tert</i> -butyl-2-hydroxyphenyl)ethyl]phenol	Irganox 129	35958-30-6	Antioxidant	10.1 <sup>[32]</sup>	1.3	233	173	191	13.37
19	<i>N</i> -Phenyl-naphthalen-1-amine	Nonox A	90-30-2	Antioxidant	4.2 <sup>[28]</sup>	1.0	219	217	115	13.57
20	<i>N</i> -Phenyl-naphthalen-2-amine	Neozon D	135-88-6	Antioxidant	4.4 <sup>[33]</sup>	3.4	219	217	115	15.10
21	2- <i>tert</i> -Butyl-6-[(3- <i>tert</i> -butyl-2-hydroxy-5-methylphenyl)methyl]-4-methylphenol	Antioxidant 2246	119-47-1	Antioxidant	6.3 <sup>[34]</sup>	1.7	177	119	91	15.25

## Chemical stabilization of polymers: Implications for dermal exposure to additives

22	2- <i>tert</i> -Butyl-6-(3- <i>tert</i> -butyl-2-hydroxy-5-methylphenyl)sulfanyl-4-methylphenol	Irganox 1081	90-66-4	Antioxidant	7.0 <sup>[30]</sup>	58.0	358	164	149	15.52
23	2- <i>tert</i> -Butyl-6-[(3- <i>tert</i> -butyl-5-ethyl-2-hydroxyphenyl)methyl]-4-ethylphenol	Cyanox 425	88-24-4	Antioxidant	8.1 <sup>[32]</sup>	3.7	191	135	163	16.34
24	2- <i>tert</i> -Butyl-4-(5- <i>tert</i> -butyl-4-hydroxy-2-methylphenyl)sulfanyl-5-methylphenol	Santonox	96-69-5	Vulcanization, stabilization	7.4 <sup>[32]</sup>	5.7	358	343	179	24.43
25	1-N,4-N-diphenylbenzene-1,4-diamine	DPPD	74-31-7	Antioxidant, process aid	5.0 <sup>[32]</sup>	1.7	260	183	167	25.87
26	Tris(2-ethylhexyl) benzene-1,2,4-tricarboxylate	TOTM	3319-31-1	Plasticizer	8.8 <sup>[30]</sup>	4.5	305	193	165	31.63
<b>Internal standards (Istd)</b>										
1	4-Methylphenol-d <sub>8</sub>	<i>p</i> -Cresol-d <sub>8</sub>	190780-66-6		1.9 <sup>[30]</sup>		115	85	96	5.32
2	1-Phenylethanone-d <sub>8</sub>	-	19547-00-3		1.6 <sup>[30]</sup>		110	54	82	5.46
3	Naphthalen-2-amine-d <sub>7</sub>	2-AN-d <sub>7</sub>	93951-94-1		5.0 <sup>[30]</sup>		150	121	93	8.85
4	Diphenylmethanone-d <sub>10</sub>	BP-d <sub>10</sub>	22583-75-1		2.9 <sup>[30]</sup>		110	82	54	8.96
5	1,4-Diphenylbenzene-d <sub>14</sub>	<i>p</i> -Terphenyl-d <sub>14</sub>	1718-51-0		5.6 <sup>[32]</sup>		244	122	108	13.52
6	<i>Bis</i> (2-ethylhexyl)benzene-1,2-dicarboxylate-d <sub>4</sub>	DEHP-d <sub>4</sub>	93951-87-2		6.4 <sup>[31]</sup>		153	97	125	15.78
7	1-Propan-2-ylthioxanthen-9-one-d <sub>7</sub>	ITX-d <sub>7</sub>	1173019-24-3		4.5 <sup>[32]</sup>		243	153	225	17.22
8	Dinonyl benzene-1,2-dicarboxylate - 3,4,5,6-d <sub>4</sub>	DnNP-d <sub>4</sub>	1202865-43-7		8.8 <sup>[30]</sup>		153	69	97	24.13

#### 2.4. Permeation of Additives and Decomposition Products Through Human Skin

Abdominal human skin specimens from plastic surgery were brought into direct contact with discs of LDPE1 or LDPE 2 and pure LDPE as negative control. The samples were punched out of the sheets of polymer with a diameter of 1.3 cm amounting to a contact surface of 1.33 cm<sup>2</sup>. In static Franz diffusion cells, the 500 µm-thick skin tissues were incubated with the polymer for 24 h under conditions according to the OECD guideline <sup>[13]</sup> and as described previously <sup>[5]</sup>. The donor chambers were thoroughly covered with parafilm (American National Can, Greenwich, CT). Physiologic saline was used as receptor medium. In addition, quality control was performed assuring the integrity of the skin in the Franz cells as requested by the OECD guideline 428 <sup>[13]</sup>. For this purpose, measurements of the transepidermal water loss (TEWL) were conducted utilizing the AquaFlux device AF200 (Biox systems Ltd, London, UK). The TEWL is considered as the flux of water diffusing from the viable epidermis through the *stratum corneum* (*s.c.*, that is, the horny layer) towards the outer atmosphere *in vivo*. In case of the Franz cell set-up, it is the water diffusing from the receptor chamber through the skin specimen to the donor chamber. An increased TEWL is therefore indicative of damaged skin. Utilizing polytetrafluoroethylene (PTFE) donor cells with a coupling system for the AquaFlux device (both Biox systems Ltd) <sup>[14]</sup>, the individual TEWL was determined per mounted skin sample. A skin sample would have been excluded from further investigations if the respective TEWL value exceeded the tolerable deviation of 30% compared to the mean TEWL of the investigated skin type previously determined in validation studies. For the present study, skin of three individual donors was used, no specimen needed to be discarded due to lack of integrity and the mean TEWL value was  $6.9 \pm 1.6$  g/(m<sup>2</sup>h) at an endpoint of 0.075 standard deviation of the TEWL curve and a cap factor of 2.8. Additionally, the quality of the utilized skin model system was confirmed comparing the *ex vivo* with *in vivo* TEWL measurements. This values were in excellent accordance with *in vivo* data for human TEWL of the volar forearm ( $10.9 \pm 3.5$  g/(m<sup>2</sup>h)) and with data described in literature for TEWL of various sites of the hand <sup>[15]</sup>. The TEWL of twenty volunteers was determined in triplicates at an endpoint of 0.075 standard deviation of the TEWL curve and a cap factor of 1.0 using the AquaFlux device with a cap for *in vivo* measurement. TEWL curves with sweat gland activity events were excluded for further calculation of the mean value (technical replicates n = 52).

The four compartments of the Franz cell set-up (saline wash solution of donor chamber, isolated *s.c.* layers on tape strips, remaining epidermal layers and receptor medium) were treated according to the hereinafter described protocol in order to quantify the respective amounts of additives and degradation products present after incubation with the LDPE material. The procedure was optimized to meet extraction requirements of all investigated substances simultaneously. Toluene showed to be the most efficient solvent for a combined extraction. In a first validation study, compartment fluids were provided with additives of a final concentration of 300 ng/ml using 30  $\mu$ l of the additive mixture in acetonitrile (10  $\mu$ g/ml each substance). The recovery was determined without an incubation period to cover the analytical quality of the method and potential matrix effects solely (supplementary information Table S3). A second validation study was conducted to include biological variance with human and porcine skin in order to optimize the incubation parameters and extraction techniques. For this purpose the skin samples were mounted in the Franz cells as described above and incubated for 24 h with 100  $\mu$ l of the additive mixture in acetonitrile on top (10  $\mu$ g/ml each substance, total amount 1  $\mu$ g per substance and skin sample). The recovery was calculated as the sum of the amounts of the respective substance present in all four compartments. The distribution of analytes within the skin layers was also investigated using this set-up (supplementary information Figure S1). Interestingly, a higher accumulation of all additives in the human *s.c.* was noticeable compared to the *s.c.* of porcine skin of the flank. In the latter, the largest portion of additives was present in the deeper epidermis. This is in line with the increased TEWL of porcine skin ( $18.2 \pm 2.9$  g/(m<sup>2</sup>h)). It points to a weaker barrier function as against the data in this validation study for human skin *ex vivo* with a TEWL similar to the *in vivo* situation ( $10.1 \pm 1.3$  g/(m<sup>2</sup>h)). Thus, further investigations of additives were performed with human skin. Consequently, liquid-liquid extractions were conducted for the aqueous compartments, namely wash solution and receptor medium. Both liquids were quantitatively transferred into test tubes with ground glass joints and the exact volume documented. Ten ml toluene were added to each sample and mixed thoroughly. After accelerated phase separation using a centrifuge (Heraeus Multifuge 1S-R, Thermo Fisher Scientific, Waltham, MA USA) at 4°C and 4000 rpm for 10 min, the upper toluene layer was removed and directly analyzed for components. To investigate the outermost layers of the *s.c.*, five tape strips were applied onto the skin surface uniformly using forceps and removed consecutively. The strips containing isolated outermost *s.c.* layers were collected in a dark 20 ml headspace vial, suspended in 10 ml toluene and sealed with a screw cap with PTFE septum. The remaining

epidermal tissue was separately placed in a vial and also submerged in 10 ml toluene. Both compartments were subject to ultrasonic assisted extraction at room temperature for 30 min. To remove glue and skin matrix, the toluene extracts underwent liquid-liquid extraction in the same way as the wash solution and receptor medium by adding 10 ml of saline to the toluene extracts. The separated toluene phase was used for further analysis. Thirty  $\mu$ l of internal standard stock solution (10  $\mu$ g/ml acetonitrile) were added to all incremental samples prior to the individual extraction protocol. All resulting toluene extracts were concentrated to a volume of 100 - 1000  $\mu$ l under gentle nitrogen stream at 40°C in order to overcome the respective limit of detection (LOD, cf. Table 2) utilizing a concentration workstation (Turbovap, Biotage, Uppsala, Sweden) and finally analyzed using the GC-MS/MS-MRM method.

## 2.5 Analysis of Accelerated Aging of Additives in Squalane

To mimic accelerated aging, the squalane model introduced by Beißmann and colleagues was applied to three polymer additives<sup>[8]</sup>. Ten mg of the following additives were placed separately into a 2 ml vial together with 1.0 ml squalane matrix each and mixed thoroughly using a Vortex test tube mixer (neoLab, Heidelberg, Germany): 2-*tert*-butyl-6-(3-*tert*-butyl-2-hydroxy-5-methylphenyl)sulfanyl-4-methylphenol (Irganox 1081), Antioxidant 2246, *N*-phenylnaphthalen-1-amine (Nonox A). These additives were selected to investigate analytes which are structurally related (Irganox 1081 and Antioxidant 2246) together with an additive that structurally differs (Nonox A) (cf. Figure 1). The vials were sealed using a layer of aluminum foil followed by a cap with a PTFE septum and placed into an oven (type 720 FED; Binder, Tuttlingen, Germany) at 130°C. The aluminum foil had been heated to 390°C for 24 h prior to usage to avoid contamination.

Aging studies were performed covering a time span of 18 days and comprising 5 time points (0.5 h, 3 d, 7 d, 14 d and 18 d). To determine the kinetics of degradation, independent triplicates were evaluated for each time point. Pure squalane without additives was used as negative control and prepared for each time point in duplicate. After the respective incubation period, the samples were cooled to room temperature and then stored at -20°C upon extraction to ensure simultaneous clean-up of all samples and analytical evaluation referring to one sequence only.

For extraction purposes, the squalane mixture was spiked with 500  $\mu\text{l}$  of an internal standard solution (2,2'-methylene-bis(4-ethyl-6-*tert*-butylphenol (Cyanox 425), 20 mg/ml in acetonitrile) and quantitatively transferred into test tubes with ground glass joints, applying five rinsing steps to the vial with 1 ml acetonitrile each. Subsequently, two liquid-liquid extraction steps using a total of 9 ml acetonitrile each were conducted. After phase separation, the acetonitrile phases were combined and filled up to a volume of 50 ml. Aliquots of the resulting solution were analyzed by means of GC-MS/MS.

The extraction method was optimized prior to the aging experiments. The recoveries of additives were determined as follows:  $53 \pm 1\%$  (Nonox A),  $61 \pm 3\%$  (Irganox 1081), and  $69 \pm 2\%$  (Antioxidant 2246). Since these numbers were reproducible, samples were cleaned up by applying two liquid-liquid extraction steps as described above. To compensate for the loss of analytes during extraction and to improve quantification, matrix calibration was performed. Five different amounts of individual additives (each in the range of 4 mg to 12 mg) were freshly dissolved in 1 ml squalane and treated simultaneously to the aging samples. The recoveries found after 0.5 h were as follows:  $93 \pm 6\%$  (Antioxidant 2246),  $108 \pm 17\%$  (Irganox 1081), and  $104 \pm 7\%$  (Nonox A) (cf. supplementary information Table S2).

## 2.6. ATR-FTIR

### 2.6.1. Investigations in view of material integrity

To characterize the aged LDPE, ATR-FTIR spectra were collected using a Nicolet™ 6700 spectrometer (Thermo Electron Corporation, Madison, WI, USA). Specimens of the pure material and of LDPE with additivation were prepared as described above (see 2.3.) and placed into an oven (type 720 FED; Binder) at 130°C. After cooling down to room temperature, spectra of the material were collected comprising the wave number range of 600 – 4000  $\text{cm}^{-1}$  at four time points (0, 3, 14, 15 days).

FTIR data were evaluated with Omnic 8.3 software (Thermo Fisher Scientific). Atmospheric suppression was performed on each spectrum and an average spectrum obtained by three particular spectra per specimen.

### 2.6.2. Investigations in view of transepidermal absorption of additives

In order to visualize the penetration pathway through the skin, FTIR- microscopy was conducted (Nicolet™ 6700, Atlas; Thermo Electron Corporation). The results were outlined using the example of naphthylamines due to their toxicological relevance and prominent IR bands in the LDPE matrix. Human skin was cut to size and specimens of full thickness skin with a surface area of 1 cm<sup>2</sup> were embedded in 6-well plates into physiological saline solution, the *s.c.* tending upwards. The skin was either incubated with a stock solution of Neozon D in acetonitrile at a final concentration of 1 µg/cm<sup>2</sup> or brought into direct contact with LDPE 2 for 24 h. Prior to cryo sections of 8 µm using a cryotome (Thermo Fisher Scientific, HM 550 OP), the skin was fixed in Tissue-Tek® O.C.T.™ Compound (Sakura, Staufen, Germany). IR spectra were collected applying FTIR-mapping with a number of sample scans and background scans of 32, a resolution of 4.000 and a mapping step size of 12 µm.

## 3. RESULTS AND DISCUSSION

Additives included in this study were selected due to their widespread use in consumer products and with respect to their toxicological relevance in exposure assessment. In certain cases, degradation products of the additives could be expected which are potentially harmful to human health (e.g. phenol derivatives of antioxidants such as Antioxidant 2246). In all remaining cases, the parent compound itself was of special interest due to its large application range in commodities. The usage of tris(2-ethylhexyl)benzene-1,2,4-tricarboxylate (TOTM), for example, has increased over the last number of years as a substitute for the reprotoxic plasticizer di-(2-ethylhexyl)-phthalate (DEHP) [16]. Also, the presence of the antioxidant Neozon D in polymeric consumer products is of concern since it is metabolized to one of the most potent bladder carcinogens 2-naphthylamine *in vivo* [17]. Considering that, the capacity of substances to overcome the intact human skin barrier was investigated using the most realistic *ex vivo* scenario with excised human skin in contact with polymeric test materials. The LDPE test material was manufactured using 10 selected additives. All of them penetrated human skin *ex vivo*. The total amounts and distribution within the epidermal layers varied as a function of lipophilicity and molecular weight of substances.

This tailor-made polymer also underwent accelerated aging and subsequent GC-MS/MS and IR evaluation to focus on the technical perspective of polymer additivation. Furthermore, macroscopic alterations of the integrity of the polymer such as yellowing and brittling were documented. Oxidation in non-stabilized LDPE generally occurs through the formation of radicals, and propagation of the reaction predominates over termination reactions<sup>[18]</sup>. Due to their ability to form mesomerically stabilized phenoxy radicals, sterically hindered phenols are commonly used as stabilizers to slow down this process<sup>[19]</sup>. A protective effect of antioxidative equipment on the material integrity was noticeable accordingly.

### 3.1. ATR-FTIR Studies of LDPE Integrity

The IR studies of the model polymer LDPE revealed significant effects of additivation. Figure 2 shows the individual spectra of LDPE materials (**Figure 2A-C**) as an overlay of three different time points during aging. The spectrum of the model polymer is in accordance with LDPE spectra described in the literature<sup>[20]</sup>. Characteristic —CH<sub>2</sub> derived bands of the LDPE spectrum were assigned as follows: 2916 (asymmetric stretching), 2848 (symmetric stretching) and 1467 cm<sup>-1</sup> (scissoring)<sup>[20, 21]</sup>. Additionally, spectra of two pure additives that are present in LDPE 2 were compared and prominent bands assigned to the tailor-made polymer (**Figure 2D-E**). While LDPE 1 showed only minor changes in its spectrum upon additivation compared to pure LDPE (**Figure 2B**), the additives in LDPE 2 caused several analyte-characteristic bands (**Figure 2C**). Most of the bands that form the characteristic pattern of LDPE 2 were derived from *N*-phenylnaphthalen-2-amine (Neozon D) and Nonox A: 3392 & 3052 (both —N-H stretching), 1303 (—C-N stretching) and 735 cm<sup>-1</sup> (—C-H<sub>aryl</sub> out of plane vibration)<sup>[22]</sup>. All of these vibrations decreased in their extent or even disappeared completely with increased aging time. For example, the bands at 3393 and 3052 cm<sup>-1</sup>, which are clearly present in the day 0 spectrum of LDPE 2 (black spectrum) disappeared after 14 days at 130°C (blue spectrum). This points to some kind of modification of the analytes in the material over time.

Degradation of pure LDPE was correlated with the emergence of signals at 1732 and 1716 cm<sup>-1</sup> (**Figure 2A**)<sup>[9]</sup>, which coincided with brittling and yellowing of the material after 14 days (Figure S2A). The bars in Figure S2 refer to the heights of three characteristic bands for pure LDPE as well as for both spiked materials LDPE 1 and LDPE 2.



The  $\text{—CH}_2$  derived solid bars found at 2916, 2848 and 1467  $\text{cm}^{-1}$  remained stable in the LDPE samples upon additivation (Figure S2B, C). However, a decrease of all characteristic bands was noticeable in pure LDPE over time, while the oxidation-specific  $\text{—C=O}$  stretching bands at 1732 (aldehyde) and 1716  $\text{cm}^{-1}$  (ketone, dashed bars) <sup>[22]</sup> increased (Figure S2A). This observation provides evidence of oxidative decomposition of pure LDPE during aging.

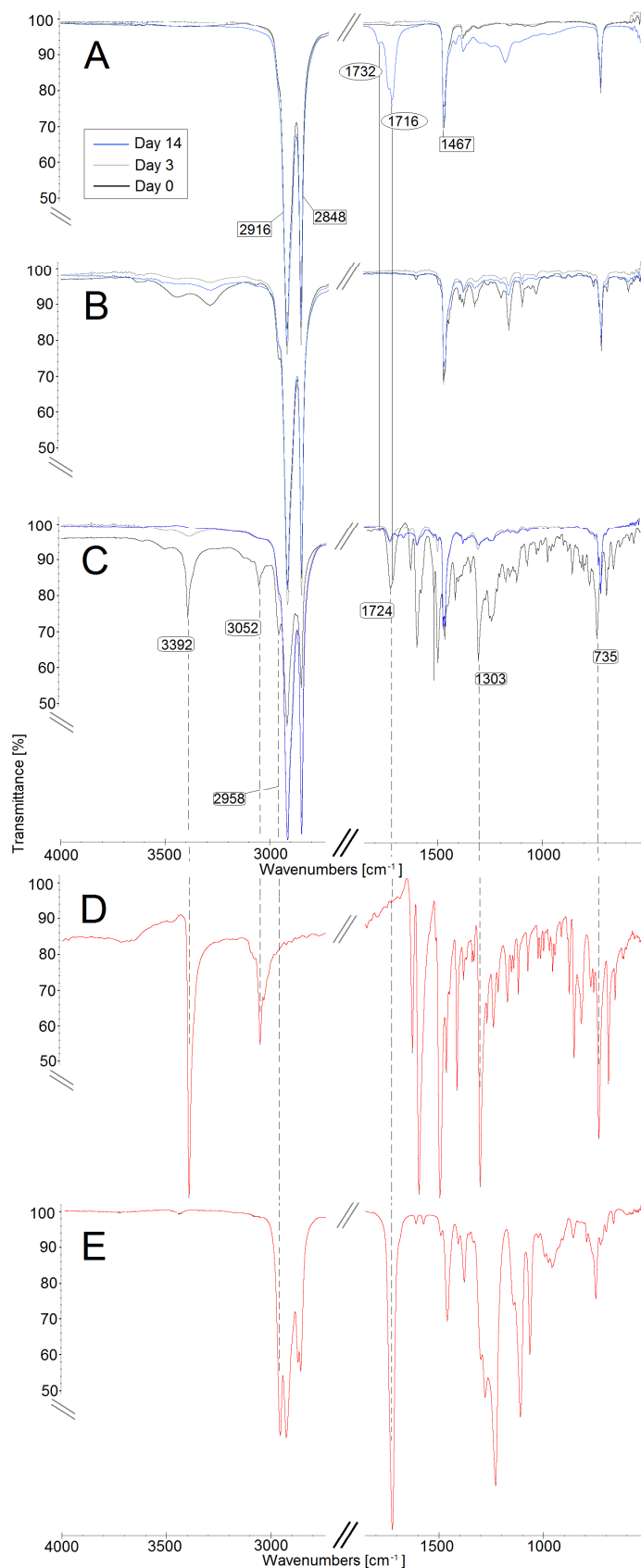


FIGURE 2: ATR-FTIR spectra over time after aging at 130°C of A: pure LDPE; B: LDPE 1, C: LDPE 2 with individual additivation (cf. Table 1), D: Neozon D. E: TOTM. The graph shows representative spectra of the tested material during aging studies at three time points. LDPE-specific bands at 2916, 2848 and 1467 cm<sup>-1</sup> are highlighted as well as the LDPE degradation bands at 1732 and 1716 cm<sup>-1</sup>. The latter are highlighted in all LDPE spectra (solid lines). Quantitative evaluation of these bands is depicted in Figure 3. Spectra of pure substances are compared to the spiked material, and additive specific bands are highlighted (dashed lines).

Conversely, protection of the LDPE model due to antioxidative additivation was observable via IR evaluation of both additive recipes, LDPE 1 and LDPE 2 (**Table 1**), even at 130°C. Here LDPE lacked typical oxidation-related bands when antioxidants were present. As a consequence, LDPE-specific bands at 2916, 2848 and 1467  $\text{cm}^{-1}$  remained stable and brittleness was absent (Figure S2B-C). However, there may be an overlay of the prominent TOTM-derived band at 1724  $\text{cm}^{-1}$  (ketone,  $\text{—C=O}$  stretching) in LDPE 2 (**Figure 2C**) with a potential LDPE degradation band at 1716  $\text{cm}^{-1}$ . Therefore, changes of the well-separated aldehyde degradation band at 1732  $\text{cm}^{-1}$  were taken into account in the spectrum of LDPE 2 for evaluation purposes. Since only a slight increase in band intensity over time was noticeable, the polymer protection effect of additives in LDPE 2 was proven. Apart from the TOTM band at 1724  $\text{cm}^{-1}$ , an additional signal at 2958  $\text{cm}^{-1}$  (methyl,  $\text{—C-H}$  stretching) was present in LDPE 2 that was related to the spectrum of the pure plasticizer (**Figure 2E**).

Obviously, the integrity of LDPE was preserved when antioxidants like Neozon D were present in the material. Together with the quantification results of particular additives in this aging scenario (cf. **Figure 3**), these findings provide evidence that LDPE can maintain its oxidation state at the material surface at the expense of stabilizer depletion<sup>[18]</sup>.

### 3.2. Aging of Additives in the LDPE Matrix

Two different tailor-made LDPE specimens were tested at temperatures of 70°C and 130°C in terms of degradation behavior of the analytes in question. At six time points (0, 3, 7, 14, 18 and 25 days) both LDPE samples which contained a mixture of five additives each, along with pure LDPE as blank control, were extracted in toluene as described in section 2.3. Utilizing the GC-MS/MS multi-method (**Table 2**), additive contents of LDPE without aging were determined (**Table 1**) as well as the amounts of additives remaining after the respective incubation period. **Figure 3** illustrates the resulting kinetics for the depletion of 10 different additives. In general, faster depletion was reported for additives from the group of antioxidants (Irganox 1081, Antioxidant, Santonox, Neozon D or Nonox A). In contrast, processing aids like  $\alpha$ -MSD or plasticizers such as TOTM remained comparatively stable over time. Chromatograms of LDPE extracts at day 0 and the corresponding reference additives are shown in **Figure 4**.

The content of additives in the original polymer without applying aging processes was also determined. According to the optimized recipe, 10 g of each additive were added per kg raw polymer. There are two main parameters that affected the amounts of additives present in the final product: as well as potential loss due to technical processing such as compounding and injection molding, all analytes were exposed to high temperatures during the manufacture of the LDPE samples facing extrusion temperatures of 170-200°C (cf. 2.1). This particular processing step might have caused degradation of the analytes in the first place. The extent of these effects became noticeable as the determined content of additives in the final material was less than the scheduled 10 g/kg per additive in all cases (**Table 1**). The determined contents varied from  $0.6 \pm 0.04$  g/kg for Irganox 1081 to  $6.5 \pm 0.9$  g/kg for  $\alpha$ -MSD. These findings are consistent with the aging studies applied hereinafter: the additives present in both kinds of recipes revealed no significant time-dependent decrease at 70°C (**Figure 3**). However, important differences in the degradation processes of the analytes at 130°C were noticeable depending on their chemical structure and functionality. For example, TOTM showed no significant time-dependent degradation at this temperature. While the plasticizer NBBS and the processing aid  $\alpha$ -MSD decreased only slightly over the period of 25 days, Antioxidant 2246 degraded most rapidly. Compared to other antioxidants in this study, Antioxidant 2246 revealed the shortest half-life of 0.6 days at 130°C in LDPE (cf. **Table 3**). As expected based on their isomeric relationship, the diarylamines Nonox A and Neozon D showed a similar depletion behavior, quite different from that of Antioxidant 2246. Nonox A had a half-life of 5.1 days under these conditions. Furthermore, Irganox 1081 appeared to be a more stable phenol derivative than Antioxidant 2246 with a half-life of 5.3 days.

### 3.3. Aging of additives in the squalane matrix

The polymer mimicking the triterpene-derived hydrocarbon squalane is known to act as a suitable matrix to form a liquid model system for polyolefins <sup>[8]</sup>. Degradation kinetics of the three additives Irganox 1081, Antioxidant 2246, and Nonox A were conducted in squalane matrix under similar conditions as used in the LDPE experiments. Each additive was separately incubated at 130°C in squalane. After extraction as described in section 2.5 was performed, the remaining amounts of analytes in the extract were quantified using the GC-MS/MS multi-method (**Figure 5**). Data on the stabilities of analytes, as revealed from LDPE analyses, were confirmed using this set-up. Again, Antioxidant 2246 underwent fast

degradation while Nonox A and Irganox 1081 showed a half-life three times higher (cf. **Table 3**). The recovery in squalane is significantly lower for Antioxidant 2246 compared to the structurally related Irganox 1081 from day 3 onwards (**Figure 5**). Irganox 1081 differs from Antioxidant 2246 only in a sulphur bridge (cf. **Figure 1**). Consequently, this structural difference is responsible for the significant differences determined in stability. Evaluation of individual breakdown products of additives in distinct aging scenarios is subject to further investigation.

Table 3. Kinetics studies of additives in two different model matrices. Overview of half-lives at 130°C with corresponding equation.

<b>Matrix</b>	<b>Additive</b>	<b>Half-life 130°C [days]</b>	<b>Equation</b>	<b>R<sup>2</sup></b>
Squalane	Irganox 1081	23.9	$y = 109.93e^{-0,033x}$	0.981
	Antioxidant 2246	7.5	$y = 108.81e^{-0,103x}$	0.984
	Nonox A	20.9	$y = 105.93e^{-0,036x}$	0.900
LDPE	Irganox 1081	5.3	$y = 719.51e^{-0,18x}$	0.918
	Antioxidant 2246	0.6	$y = 1972.5e^{-0,374x}$	0,867
	Nonox A	5.1	$y = 4000.9e^{-0,178x}$	0.971

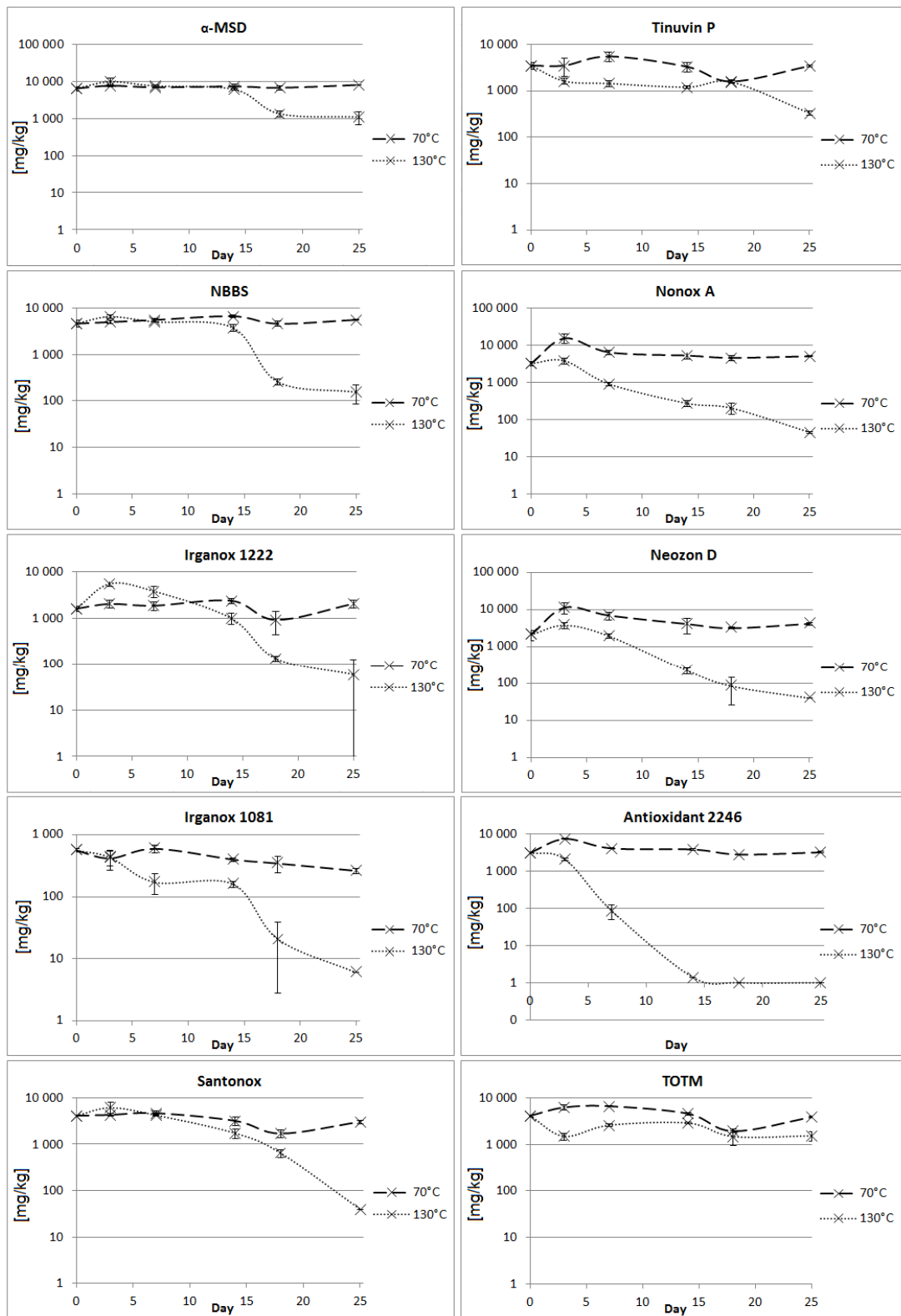


FIGURE 3: Quantification of additives at different time points of aging in LDPE. Depletion of additives in LDPE 1 (left) and LDPE 2 (right) at different temperatures. Error bars show standard deviation of the mean in three independent experiments.

It can thus be assumed from the results that the additives probably underwent similar degradation pathways in both kinds of aging matrices but with varying half-lives. In all cases, calculated values were higher when compared to the results obtained with LDPE. This is partially related to the fact that the surface between the additive-containing matrix and ambient air is larger in the set-up using LDPE as compared to squalane.

#### 3.4. Relevance of Polymer Additivation and Decomposition for Dermal Exposure

The tested LDPE samples entailed additives in the range of 0.1 - 0.7 % as it can be expected from polymers used in consumer products. The quantification of additives present in isolated skin layers of skin that has been in contact with this polymer revealed their individual potential to migrate out of the material, overcome the skin barrier and enter the viable epidermis. The chromatograms in **Figure 4** demonstrate the quality of the developed GC-MS/MS-MRM method to selectively determine additives in polymeric, biological and aqueous matrices. Further, the presence in the extracts of Franz cell compartments among additives is remarkably opposed. Exemplarily, the peak for the antioxidant Santonox was clearly present in the extract of the *s.c.* (**Figure 4**, no. 24, B-1), decreased in the extract of the epidermis (B-2) and is absent in the receptor fluid (B-3). This tendency appeared to be the other way around for NBBS (**Figure 4**, no. 14, B-1 - B-3).

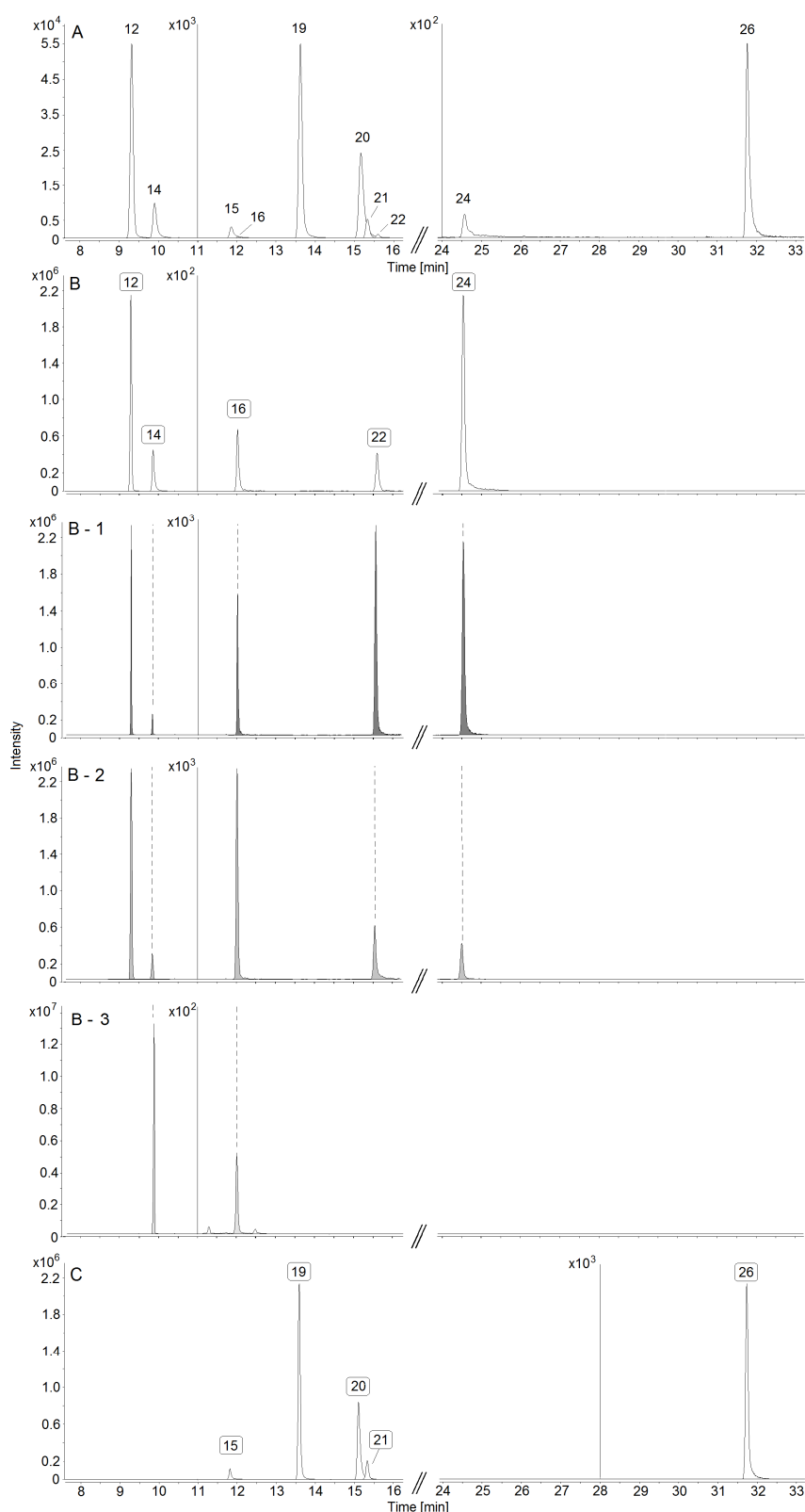


FIGURE 4:  
 Extracted ion chromatograms (EIC) of the LDPE 1 (B) and LDPE 2 (C) extracts at day 0 together with a standard solution of additives (A) at a concentration of 250 ng/ml in acetonitrile. Additives in human skin are depicted as a consequence of contact to LDPE 1 in Franz cell assay after 24 h: EIC of extracts of compartments after clean up procedure: B-1 *s.c.*; B-2 remaining epidermis; B-3 receptor solution. Precursor ions of the respective additives were extracted and signals labelled according to Table 2.



All of the ten tested additives penetrated the skin to a variable extent. Inferences about bioavailability of additives after dermal contacts can be drawn from this most realistic set-up. Only NBBS ( $\log P_{O/W}$  2.0) was mainly present in the receptor solution after incubation and to a lesser extent in the epidermal layers (**Figure 6**). This finding is indicative for skin permeation and high bioavailability of this neurotoxic plasticizer.

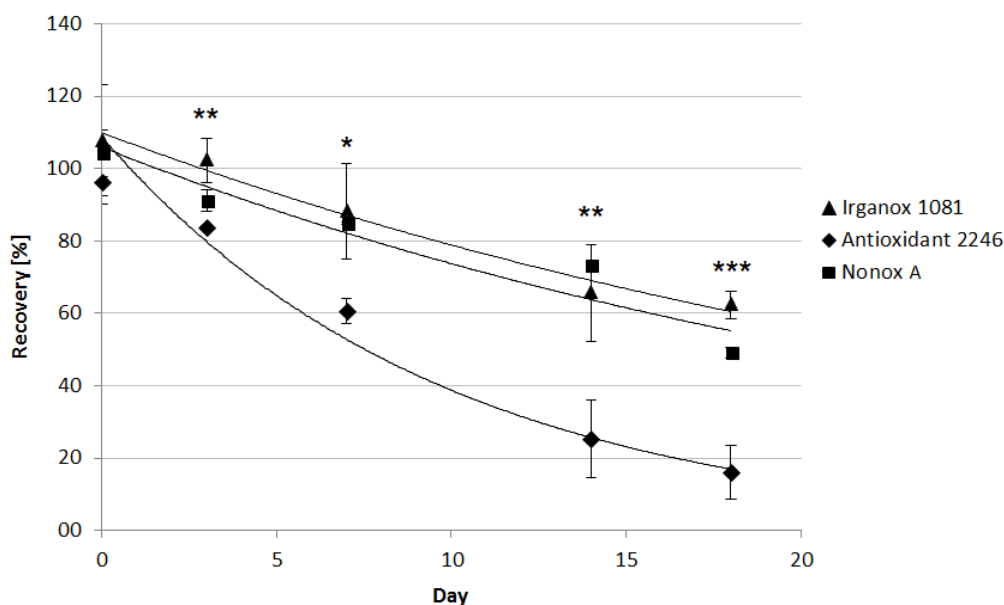


FIGURE 5: Degradation kinetics at 130°C of 3 antioxidants in squalane, representative of different chemical classes. Error bars show standard deviation of the mean of three independent experiments. The corresponding equation can be found in Table 3. Asterisks indicate significant differences concerning recovery of Antioxidant 2246 compared to Irganox 1081 (\*\*\*  $p < 0.001$ ; \*\*  $p < 0.01$ ; \*  $p < 0.05$ ).

The other additives with higher  $\log P_{O/W}$  values penetrated the skin and are distributed in the viable epidermal layers and the *s.c.* according to the lipophilicity of substances (cf. Table 2). The higher the  $\log P_{O/W}$  value of the additive, the smaller was the portion that entered the viable layers of the skin. The same is true for size related evaluation. While the additive with the lowest molecular weight (NBBS: 213.1 Da) was present in the receptor fluid to more than 80 % referring to the total amount of determined substance, the distribution appears to be inverted for the higher molecular weight components tested (e.g. Irganox 1081/ Santonox: 358.2 Da, TOTM: 546.4 Da) (**Figure 6**). A rapid absorption of the neurotoxic plasticizer NBBS through the skin is of concern since it was shown in previous studies in rats that 98% of iv administered NBBS is removed from plasma during the first minute<sup>[7]</sup>.

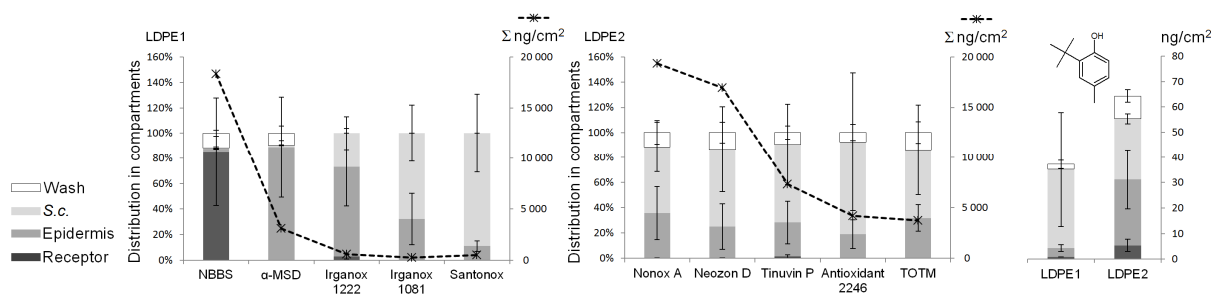


FIGURE 6: Distribution of additives and the degradation product 2-*t*-butyl-*p*-cresol (right) in human skin after Franz diffusion cell assay with a contact area of 1.33 cm<sup>2</sup>. The skin was incubated for 24 h at 33.5°C in direct contact with either LDPE 1 (left) or LDPE 2 (middle). LDPE 1 entails Irganox 1081 as precursor additive while LDPE 2 entails Antioxidant 2246 as potential source for 2-*t*-butyl-*p*-cresol formation. Columns represent the percentage distribution of the respective additive within the skin layers and the wash solution. The dashed graphs depict the total amount of each additive present in all compartments of the Franz cell (wash, *stratum corneum*: *s.c.*, epidermis and receptor solution) after incubation. Bars show the standard deviation of the mean with n=3.

This is indicative for a rapid transport to other tissues including the brain. The *s.c.* forms the natural barrier against xenobiotics and consists mainly of dead keratinocytes and lipids. Expectedly, enhanced accumulation in this outermost layer of skin was noticeable with increased size and lipophilicity of additives. This accumulation is far from being negligible. Marek and coworkers emphasized the reservoir function of the *s.c.* at the example of Neozon D in porcine skin *ex vivo* [17]. In accordance with the present study, they proved Neozon D to penetrate the skin and gradually enter the deeper skin layers. In a Franz cell set-up optimized for evaluation of the exposure of workers in the printing industry, the percutaneous absorption of Neozon D was determined. After application of a comparatively high level of Neozon D (1.9 mg/cm<sup>2</sup> solved in 96 % dichloromethane, 4 % turpentine oil) and 48 h incubation in dynamic Franz diffusion cells, a total penetrated amount of 105.7 µg/cm<sup>2</sup> was determined by Marek and colleagues [17], meaning 5.5 % of applied substance entered the skin. Depending on the concentration applied, the solvent and the test system used, they recovered up to 16.1 % of the substance in the porcine skin after 48 h. Further, it has been shown recently that the matrix of topically applied aromatic amines leads to significant differences concerning the degree of skin penetration [23]. Dennerlein and coworkers determined a significantly higher skin penetration when Neozon D was applied solved in hexane compared to the application of a lubricant containing Neozon D. Evidentially, penetration rates are not transferable among exposure scenarios.

In the present study, the focus was on dermal contacts to polymers equipped with additives including the procarcinogenic antioxidant Neozon D. Thus, the application was conducted incorporated in LDPE acting as model polymer. The material entailed 2.1 g Neozon D per kg LDPE (cf. Table 1). With a mean weight of  $120.8 \pm 1.5$  mg per disc, the specimens served a total amount of 253.7  $\mu\text{g}$  Neozon D per skin sample ( $190.8 \mu\text{g}/\text{cm}^2$ ). The total penetrated amount determined after 24 h was  $14.7 \mu\text{g}/\text{cm}^2$  (**Figure 6**, recovery without wash solution), amounting to 7.7 % of the originally applied additive.

Here it was approved that not only fluids but also polymers can be an additional source of human exposure to additives. Additionally, FTIR-microscopy confirmed both, accumulation of Neozon D in the upper epidermal layers when being applied solved in acetonitrile or after contact with LDPE 2. **Figure 7A** depicts the distribution of Neozon D as false color heat map in a section of human skin that was incubated with  $1 \mu\text{g}/\text{cm}^2$  of the substance in acetonitrile. An equal distribution within the *s.c.* is noticeable with additionally hotspots in the deeper epidermis. These are mainly present in regions with folds of skin or hair follicles. Here it could be shown, that these transdermal routes prominently contribute to dermal absorption of Neozon D when topically applied in solution. Also, the intensity of the arylamine specific band at  $3052 \text{ cm}^{-1}$  was traced in the skin that was in contact with LDPE 2 or pure LDPE (**Figure 7B**). It revealed accumulation of the analyte in the *s.c.* after 24 h depicted as red areas with highest intensity (red spectrum). While the band was absent in the spectrum of the *s.c.* of skin that was in contact with pure LDPE (blue spectrum).

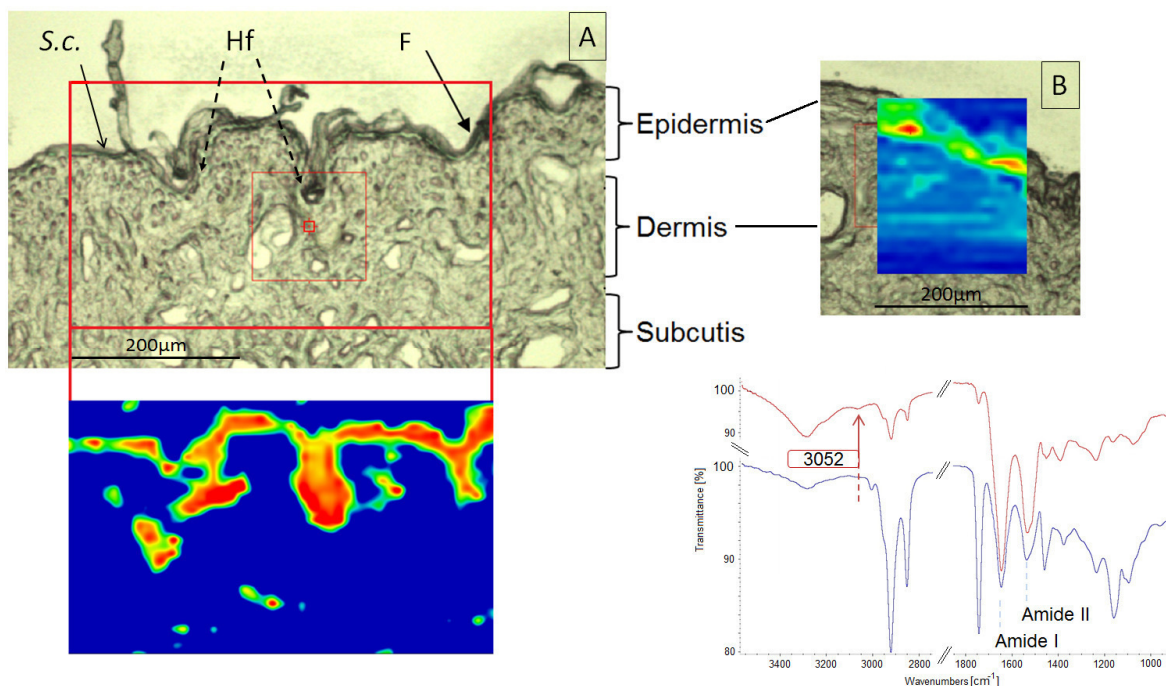


FIGURE 7: FTIR mapping in microscopy of human skin sections after 24 h incubation with Neozon D in acetonitrile ( $1 \mu\text{g}/\text{cm}^2$ ) (A) or after 24 h contact with LDPE 2 entailing the arylamines Neozon D and Nonox A (B). Distribution of Neozon D depicted as false color heat map with atmospheric suppression. A: variance scaling at Neozon D specific bands  $3392/1626 \text{ cm}^{-1}$ . Differences in spectra of *s.c.* comparing skin in contact with pure LDPE (blue, bottom spectrum) and with LDPE 2 (red, top spectrum) are highlighted using an overlay and visualized as heat map distribution of arylamine specific band at  $3052 \text{ cm}^{-1}$  (B). *S.c.*: *stratum corneum*; Hf: hair follicle; F: fold.

Most phenol-based additives included in this study are derivatives of *p*-cresol (cf. **Figure 1**). This potential degradation product was therefore included in the MRM multi-method, along with four structurally related degradation products, and evaluated further (**Table 2**). Cresol is harmful to health after absorption through skin or swallowing<sup>[24]</sup> and thus of toxicological relevance. Since phenol derivatives are known degradation products of several antioxidants<sup>[25]</sup>, the occurrence of cresol and its derivatives after skin contact with LDPE 1 and LDPE 2 was monitored in human epidermis. Of all derivatives investigated, only 2-*t*-butyl-*p*-cresol was present in the skin layers after incubation with the polymers. Its distribution within human epidermis and other compartments of the Franz cell is shown in **Figure 6**.

Being embedded in LDPE in the form of antioxidant precursors, 2-*t*-butyl-*p*-cresol penetrated the skin at up to  $55 \text{ ng}/\text{cm}^2$  after a contact time of 24 h (**Figure 6**, sum of *s.c.*,

epidermis, receptor fluid LDPE 2). While the major part remained in the outermost five layers of the *s.c.* (strip 1-5) and in the rest of the epidermal tissue, only small amounts of the degradation product permeated the whole skin and entered the receptor medium. Noticeably, higher amounts of 2-*t*-butyl-*p*-cresol were released into the skin from LDPE 2 when the Antioxidant 2246 acted as precursor substance compared to Irganox 1081 in LDPE 1. These findings are consistent with the aging tests discussed in the present work, since Antioxidant 2246 showed the weakest stability of all additives investigated.

#### 4. CONCLUSIONS

This study presents a GC-MS/MS method to equally quantify a broad range of polymer additives in complex polymeric and biological matrices. Furthermore, an LDPE- and a squalane-based aging scenario for additives were investigated and compared with respect to the half-lives of additives. For three selected additives, degradation kinetics revealed significant differences concerning half-life, not only between the additives but also with respect to the individual aging scenarios applied. In general, the depletion of all additives is faster in LDPE than in squalane. Nonox A and Irganox 1081 are approximately four times more stable when incorporated in squalane as compared to LDPE. Furthermore, Antioxidant 2246 showed a half-life 12 times higher in squalane as compared to the LDPE matrix. However, the impact of diffusion processes on the depletion process of additives needs to be further characterized in emission or additional degradation studies. To assess the quality of aging scenarios in a model system, the effect of physical loss is negligible as the diverse polymers of everyday products are also subject to diffusion and migration processes to varying extents. Since LDPE studies mirror real matrix and surface conditions more realistically, any results based on the usage of squalane as model for the prediction of additive stability have to be viewed with caution. Further investigations of real consumer product samples which are broadly furnished with additives and consist of versatile matrices are required to decide whether either of the models might be suitable for assessing the stability of additives under real conditions. Nevertheless, additive breakdown products are of particular concern when it comes to dermal exposure of consumers. The resulting breakdown product 2-*t*-butyl-*p*-cresol showed degradation of precursor additives in the investigated polymer matrices during skin contact.

Breakdown products of phenol-based antioxidants have already been suggested for further evaluation due to their toxicological relevance <sup>[26]</sup>. With the depletion process of phenol-based antioxidants in LDPE, a potential source of exposure of consumers to cresol derivatives has been characterized here. In light of the current *ex vivo* Franz cell results for 2-*t*-butyl-*p*-cresol, the dermal exposure of consumers to cresol derivatives through the use of commodities made of polymers with antioxidative addition needs to be taken into consideration in future assessments. Moreover, it has been proven that substances of concern migrate from LDPE to the skin surface and overcome the natural skin barrier *ex vivo* according to their size and lipophilicity. Therefore, the usage of additives in polymers because of their technical benefits should be carefully considered whenever the product is designated for skin contacts.

#### ACKNOWLEDGEMENTS

The authors would like to thank Karsten Schön for his excellent technical assistance as well as Dr. Alexander Lichtblau and Dr. Sebastian Hörold for advising on polymer design (Clariant, Germany) and Dr. Christian Witzel for providing human skin from plastic surgery (Charité, Germany). This study was supported financially by internal funding of the German Federal Institute for Risk Assessment (BfR) [grant numbers 1322-343, 1322-514 and 72-003].

#### 5. APPENDIX

#### REFERENCES

- [1] Bart, J.C.J. Polymer additive analysis at the limits. *Polym Degrad Stabil* **2003**, 82(2),197-205.
- [2] Klampfl, C.W. Mass spectrometry as a useful tool for the analysis of stabilizers in polymer materials. *Trends Analyt Chem* **2013**, 50:53-64.
- [3] Castillo, R.; Biedermann, M.; Riquet, A.-M.; Grob, K. Comprehensive on-line HPLC-GC for screening potential migrants from polypropylene into food: The effect of pulsed light decontamination as an example. *Polym Degrad Stabil*. **2013**, 98(9), 1679-87.
- [4] Limm, W.; Hollifield, HC. Modelling of additive diffusion in polyolefins. *Food Addit Contam.* **1996**, 13(8), 949-67.

- [5] Bartsch, N.; Heidler, J.; Vieth, B.; Hutzler, C.; Luch, A. Skin permeation of polycyclic aromatic hydrocarbons: A solvent-based *in vitro* approach to assess dermal exposures against benzo[*a*]pyrene and dibenzopyrenes. *J Occup Environ Hyg.* **2016**, 13(12), 969-979.
- [6] Manamsa, K.; Crane, E.; Stuart, M.; Talbot, J.; Lapworth, D.; Hart, A. A national-scale assessment of micro-organic contaminants in groundwater of England and Wales. *Sci Total Environ.* **2016**, 568(Supplement C), 712-26.
- [7] Kumar, G.; Smith, QR.; Hokari, M.; Parepally, J.; Duncan, MW. Brain Uptake, Pharmacokinetics, and Tissue Distribution in the Rat of Neurotoxic N-Butylbenzenesulfonamide. *Toxicol Sci.* **2007**, 97(2), 253-64.
- [8] Beißmann, S.; Reisinger, M.; Grabmayer, K.; Wallner, G.; Nitsche, D.; Buchberger, W. Analytical evaluation of the performance of stabilization systems for polyolefinic materials. Part I: Interactions between hindered amine light stabilizers and phenolic antioxidants. *Polym Degrad Stabil* **2014**, 110(0), 498-508.
- [9] Westphal, C.; Perrot, C.; Karlsson, S. Py-GC/MS as a means to predict degree of degradation by giving microstructural changes modelled on LDPE and PLA. *Polym Degrad Stabil.* **2001**, 73(2), 281-7.
- [10] Baur, E.; Thiel, C. Material data center datasheet for SABIC® LDPE Powder 1922Z90. Obtained from: <http://www.materialdatacenter.com/ms/>, (accessed May 2017).
- [11] Himmelsbach, M.; Buchberger, W.; E. Reingruber Determination of polymer additives by liquid chromatography coupled with mass spectrometry. A comparison of atmospheric pressure photoionization (APPI), atmospheric pressure chemical ionization (APCI), and electrospray ionization (ESI). *Polym Degrad Stabil* **2009**, 94(8), 1213-9.
- [12] Bouma, K.; Schakel DJ. Migration of phthalates from PVC toys into saliva simulant by dynamic extraction. *Food Addit Contam* **2002**, 19(6), 602-10.
- [13] OECD guideline for the testing of chemicals. Test No. 428: Skin Absorption: *In vitro* method: OECD Publishing, Paris, **2004**.
- [14] Imhof, B.; Xiao, P.; Angelova-Fischer, I. TEWL, closed-chamber methods: AquaFlux and VapoMeter. In: Berardesca, E.; Maibach, H.I.; Wilhelm, K.-P. editors. *Non invasive diagnostic techniques in clinical dermatology*. Springer Berlin Heidelberg: Berlin, Heidelberg, 2014; 345-52.
- [15] Ramsing, DW.; Agner, T. Effect of glove occlusion on human skin. *Contact Derm.* **1996**, 34(1), 1-5.

- [16] Biedermann-Brem, S.; Biedermann, M.; Pfenninger, S.; Bauer, M.; Altkofer, W.; Rieger, K.; et al. Plasticizers in PVC toys and childcare products: What succeeds the phthalates? Market survey 2007. *Chromatographia* **2008**, 68(3), 227-34.
- [17] Marek, EM.; Koslitz, S.; Weiss, T.; Fartasch, M.; Schlüter, G.; Käfferlein, HU.; et al. Quantification of *N*-phenyl-2-naphthylamine by gas chromatography and isotope-dilution mass spectrometry and its percutaneous absorption *ex vivo* under workplace conditions. *Arch Toxicol* **2017**, <https://doi.org/10.1007/s00204-017-2046-2>.
- [18] Richaud, E. Comparison of stabilization by vitamin E and 2,6-di-*tert*-butylphenols during polyethylene radio-thermal-oxidation. *Radiat Phys Chem* **2014**, 103, 158-66.
- [19] Pospíšil, J. Chemical and photochemical behaviour of phenolic antioxidants in polymer stabilization: A state of the art report, part II. *Polym Degrad Stabil* **1993**, 39(1), 103-15.
- [20] Bentley, P.A.; Hendra P.J. Polarised FT Raman studies of an ultra-high modulus polyethylene rod. *Spectrochim Acta A: Molecular and Biomolecular Spectroscopy* **1995**, 51(12), 2125-31.
- [21] Zhang, D.; Shen, Y.R.; Somorjai, G.A. Studies of surface structures and compositions of polyethylene and polypropylene by IR+visible sum frequency vibrational spectroscopy. *Chem Phys Lett* **1997**, 281(4-6), 394-400.
- [22] Coates, J. Interpretation of infrared spectra, a practical approach. *Encyclopedia of Analytical Chemistry*: John Wiley & Sons, Ltd; 2006.
- [23] Dennerlein, K.; Göen, T.; Zobel, M.; Boos, AM.; Drexler, H.; Kilo, S. Dermal penetration and resorption of beta-naphthylamine and *N*-phenyl-beta-naphthylamine from lubricants in an *ex vivo* human skin model. *Chemosphere* **2017**, 185(Supplement C), 934-41.
- [24] Andersen, A. Final report on the safety assessment of sodium *p*-chloro-*m*-cresol, *p*-chloro-*m*-cresol, chlorothymol, mixed cresols, *m*-cresol, *o*-cresol, *p*-cresol, isopropyl cresols, thymol, *o*-cymen-5-ol, and carvacrol. *Int J Toxicol* **2006**, 25(1 suppl), 29-127.
- [25] Reingruber, E.; Himmelsbach, M.; Sauer, C.; Buchberger, W. Identification of degradation products of antioxidants in polyolefins by liquid chromatography combined with atmospheric pressure photoionisation mass spectrometry. *Polym Degrad Stabil* **2010**, 95(5), 740-5.
- [26] Bertoldo, M.; Ciardelli, F. Water extraction and degradation of a sterically hindered phenolic antioxidant in polypropylene films. *Polymer* **2004**, 45(26), 8751-9.



- [27] Beuth Verlag GmbH: *Chemical analysis - Decision limit, detection limit and determination limit under repeatability conditions - Terms, methods, evaluation* (DIN 32645:2008-11). [Standard] Beuth Verlag GmbH: Berlin, 2008.
- [28] Hansch, C.; Leo, A.; Hoekman, D. *Exploring QSAR - hydrophobic, electronic, and steric constants*. American Chemical Society: Washington, DC, 1995.
- [29] Sangster, J.: Octanol-Water Partition Coefficients of Simple Organic Compounds. *J Phys Chem Ref Data* **1989**, 18(3), 1111-1230.
- [30] Sigma-Aldrich: Material Safety Data Sheet (MSDS) obtained from <http://www.sigmaaldrich.com/germany.html>, (accessed Dec 2016).
- [31] LGC Standards: Material Safety Data Sheet (MSDS) obtained from [https://www.lgcstandards.com/medias/sys\\_master/pdfs/pdfs/h76/h47/8997761482782/CIL-DLM-1368-0.1-ST-WB-MSDS-1134525-1-1-1.pdf](https://www.lgcstandards.com/medias/sys_master/pdfs/pdfs/h76/h47/8997761482782/CIL-DLM-1368-0.1-ST-WB-MSDS-1134525-1-1-1.pdf), (accessed Dec 2016).
- [32] PubChem database: <https://pubchem.ncbi.nlm.nih.gov>, (accessed Dec 2016).
- [33] Hansch, C.; Leo, A. *The log P database*. Pomona College: Claremont, CA, 1987.
- [34] Chemicals Inspection and Testing Institute: *Biodegradation and bioaccumulation data of existing chemicals based on the CSCL Japan*. Japan Chemical Industry Ecology - Toxicology and Information Center, 1992.

## **6.4 Thermal stability of polymer additives: Comparison of decomposition models including oxidative pyrolysis**

Nastasia Bartsch, Mathilde Girard, Amelie Wilde, Torsten Bruhn, Oliver Kappenstein, Bärbel Vieth, Christoph Hutzler, Andreas Luch, *Journal of Vinyl and Additive Technology*.

Due to copyright reasons, this paper is not included in the online version.

Published online: 17 Sep 2018

DOI: 10.1002/vnl.21654

Link: <https://doi.org/10.1002/vnl.21654>

Involvement of the author within this publication: Project planning: 70%, project execution: 50%, data analysis: 60%, writing of the manuscript: 85%

## 7 Discussion

Several substances of toxicological concern were identified in consumer products made of polymeric materials within this work. For this purpose several targeted multi-analyte-methods were developed to characterize the composition of different materials. In general, the cumulative exposure of consumers by oral, dermal or inhalative pathways must be considered to perform a comprehensive risk assessment. But often evaluation of dermal exposure with respect to consumer products is difficult because realistic data on migration and skin penetration or permeation are missing or the available methods are not suitable. Here, the dermal route of exposure was investigated in detail and thereby severe underestimations for contact to lipophilic components like PAHs revealed. Other polymer additives and degradation products that were not yet characterized with respect to skin contact were proven to overcome the skin barrier.

### 7.1 PAHs and mineral oil components in consumer products

PAHs are constituents of mineral oils and consequently of the mostly highly alkylated MOAH. The idea behind determining non-alkylated PAHs and MOAH in polymeric consumer products was to test if there is a certain ratio of MOAH content to PAHs content present in the material. The definition of a factor that is valid for polymeric material would be an asset to the exposure assessment. This work however demonstrated that the sum of eight EU PAHs that are classified by CLP Regulation as presumably carcinogenic for humans (carc. Cat. 1B) present in the final material does not correlate with the MOAH content (7). It further contributed to the identification of additional technical sources of mineral oil and PAHs contamination in consumer products. The correlation of the MOSH volatility maximum with multiple MOAH volatility maxima revealed several sources for PAHs entry into the polymeric final product like usage of carbon black in combination with extender oil. This aspect can be used to further minimize the content of carcinogenic PAHs and of the aromatic hydrocarbon fraction by substitution of the raw material with less harmful components.

From the current perspective, the carcinogenicity of mineral oil is associated with the MOAH and PAH contents of products. The usage of mineral oil and its composition and purity requirements are regulated and subject to monitoring for

polymeric material designated for food contact (28, 127), for cosmetic products (128), but not yet for polymeric material with foreseeable skin contact. In case of cosmetics, products must be manufactured according to the Regulation (EC) No 1223/2009 (128). According to this regulation only mineral oil fractions with a detailed description of the refining process and that are proven to be not carcinogen are allowed to be used in cosmetics. There is evidence that mineral oils vary in their carcinogenic potential with the degree of refining (129). It is therefore to be expected that usage of higher processed mineral oils in consumer products would decrease the total amount of MOAH and PAHs present in the final material and pose a reduced cancer risk with respect to dermal exposure.

### **7.2 PAHs in skin contact**

The natural human skin barrier is continuously challenged by xenobiotics. The *s.c.* is accounted the most efficient barrier structure and rate limiting for skin permeation of substances (130). Even though the *s.c.* significantly retards skin permeation of particular PAHs, it promotes reservoir formation of lipophilic compounds. This is of concern because mutagenic components like B[a]P and dibenzopyrenes can migrate out of the elastomer or rubber, enter the *s.c.* leading to an accumulation and can steadily be released into the systemic circulation as a consequence. Moreover, cutaneous bioactivation of PAHs during prolonged skin permeation may contribute to mutations that ultimately lead to skin cancer (54).

The ubiquitous occurrence of PAHs is a further aspect that necessitates a detailed assessment of dermal availability of the substances. The dermal exposure to PAHs can contribute to aggregate exposure considerably. This has been proven by FDC-assay with human skin and by using an adjusted sweat simulant. It has been clearly demonstrated, that former PAH-migration studies using aqueous sweat simulant resulted in a distinct underestimation of exposure because the lipophilicity of PAHs and the influence of SSFL were not considered. Based on these methods and findings, the BfR suggested in 2010 to restrict the maximum content of PAHs in consumer products with foreseeable skin contact as low as reasonably achievable (ALARA principle for genotoxic carcinogens) to minimize this exposure pathway (131). It was further demonstrated that only a few samples exceeded the proposed limit of 0.2 mg/kg, which is the LOQ of the analytical method.

The results of this thesis are in excellent accordance with previously reported studies on dermal exposure to cosmetics entailing mineral oils. An accumulation in the outer most layers of skin was reported for mineral oil components in porcine ear and excised human skin (132, 133). This particular distribution was also found for PAHs and MOAH in this work after contacts to standard solutions, contaminated polymeric consumer products, printing ink and vaseline (16), (chapter 4.2.1, unpublished data). A size and volatility dependent distribution within the skin layers has been demonstrated additionally within all hydrocarbon subgroups, the PAHs and also for MOSH and MOAH.

The characterization of the polymeric material was an important aspect for the investigations of skin contact in FDC-assay but also for the development of a simulant based alternative testing method. The order of magnitude of PAH release (either into skin or 20% ethanol simulant) was similar comparing four consumer products of different material and of different PAH content. There were slight differences, however, normalizing the released PAH amount to the respective PAH content. There is evidence that PAH migration can be hindered by carbon black because of its high sorption capacities (134). On the other hand, the migration can be facilitated by material aging and by the presence of additives that interfere with the material integrity. Therefore, the actual migration or penetration of leachables of polymers needs to be considered as a result of the respective physico-chemical properties of the substances and the material condition.

### **7.3 Characterization of stabilizers, plasticizers and degradation products in polymers and skin penetration**

The polymer protecting capacity of additives was demonstrated using a qualitative ATR-FTIR spectroscopy approach monitoring material degradation specific bands. The GC-MS/MS multi-method was applied in addition to quantify the concomitant depletion of additives. Differences concerning the depletion of the additives were referred to structural characteristics. Additives with minor structural differences were selected to investigate the particular impact on degradation and stabilization properties. An interesting outcome was the sulfur based higher stability of Irganox 1081 compared to the carbon bridged Antioxidant 2246. The results on half-life times in squalane impressively mirror the properties of a multifunctional stabilizer like Irganox 1081 resulting in prolonged stability compared to the

structural similar antioxidant with radical chain terminating properties only. The high stability can be ascribed to the electron donating capacity of the sulfur atom (135).

Depth profiles of polymer additives in human skin were generated. The barrier function was emphasized by quantification of the additives in distinct skin layers after contact to an additive-containing polymer. The developed MRM multi-analyte-method based on GC-MS/MS has been applied to this end. The results demonstrate the discrimination properties of the skin tissue acting similar to a sieve. A signal of high intensity was present in the chromatograms representing the outer most skin layers for comparatively large and lipophilic compounds like Santonox or Irganox 1081. This signal decreased with increasing depth of the skin layer analyzed. It was just the other way around for smaller less lipophilic additives like NBBS.

It has been demonstrated in previously performed studies that porcine skin shows a 1.2 to 1.7 fold higher permeability *in vitro* over 24 h as compared to human skin at the example of heptane, hexadecane and xylene (133, 136). This thesis confirms these findings for a range of substance classes used as polymer additives. The permeability of all tested polymer additives ranging from  $\log P_{O/W}$  2.0 to  $\log P_{O/W}$  8.8 was higher in porcine skin compared to human skin in the FDC-assay, despite a similar overall penetration (Annex III, Figure S1).

Up to now, dermal exposure assessment focused on the skin penetration by particular additives or contaminants. But little has been known on skin penetration of degradation products. There is evidence also for degradation products of initially applied additives to enter the skin. This was shown at the example of 2-*t*-butyl-*p*-cresol being present in human skin *ex vivo* after contact to polymers containing Irganox 1081 or Antioxidant 2246 as precursor additives. These results emphasize a need for further material research including potential degradation products and an extended dermal exposure assessment to evaluate possible health risks by those degradation products.

#### **7.4 Prediction of additive degradation products**

The comparison of seven degradation models allowed evaluation with respect to most frequently formed degradation products of polymer additives. The application

of quantum-chemical calculations confirmed the experimental findings and both resulted in synergistic valuable insights into structural relations.

The 2-*t*-butyl-*p*-cresol was identified as degradation product of several additives in consumer products as expected from the preliminary FDC-assay (cf. chapter 7.3). Particularly degradation products with increased toxicity as compared to the precursor additive are of concern. This is the case for the phthalate substitute plasticizer TOTM. In this work, it has been demonstrated that DEHP and bis(2-ethylhexyl)benzene-1,3-dicarboxylate (DOIP) result from accelerated aging of TOTM. The strength of the C-C bond from benzene to the carboxylate group in position 2 appeared to be significantly stronger in the Fukui depiction for radical attack of the chemical structure, which explained formation of DOIP and DEHP with no formation of the 1,4-dicarboxylate derivative. This hypothesis means for further investigations on polymer composition, that the presence of DEHP can either be intentional or a result of degradation of a DEHP substitute.

Interestingly, it was found in previously reported studies that DOIP often accompanies DEHP in environmental surveys (137). This also maintains the assumption that both contaminants might have the same precursor substance and that their occurrence is at least partially a result of the degradation of TOTM used as plasticizer.

The progression of the radical chain mechanisms responsible for material aging is mostly independent from the initially formed radical (138). This means that thermal impact can simulate comprehensive material aging and the results on degradation products of polymer additives compiled in this work can be transferred to material aging under real conditions.

## 8 Conclusion & Outlook

Additives, contaminants and NIAS of polymers were characterized within this thesis because they are part of consumer products, may contribute to dermal exposure and thus pose a potential risk for consumers upon usage. The main focus was on products designated for skin contact because of the extensive application of polymeric materials in this field. Therefore, the interaction of polymeric material with the natural human skin barrier was investigated and the capability of several compounds to overcome this barrier assessed. It was necessary to prioritize and group the ingredients with respect to toxicological and technical relevance because of the diversity of polymer leachables. As an overall result of this work the transdermal route of exposure was emphasized for several components present in polymers. A major task was to create as realistic *ex vivo/ in vitro* conditions as possible. The extent of skin penetration and permeation respectively has been correlated with general aspects like lipophilicity and size of the components. Skin permeation has been observed mainly for smaller analytes of comparatively low lipophilicity. High lipophilic components like dibenzopyrenes, Santonox or TOTM entered the skin only partially as a consequence. A potential systemic availability was identified for these harmful substances via reservoir formation in the upper most epidermal layers. This fact should be considered especially in the composition of products for long term usage.

A detailed description of skin penetration and permeation was given for the large substance class of PAHs. Up to now, the principal method to assess migration of PAHs has been the application of aqueous sweat simulant to the polymer of interest. With B[a]P as lead compound it was proven in this work that usage of this simulant leads to severe underestimation of migration and consequently of transdermal contribution to exposure for these highly lipophilic compounds. An alternative ethanol based testing method was developed to improve the dermal exposure assessment. This newly developed method reflects the results of the FDC-assay with human skin, which serves as reference and so-called gold standard. Further, this method was refined and validated in a trial and was recently in use in a JRC project (139). Based on these results, the usage of aqueous sweat simulant for ongoing dermal exposure assessment of other lipophilic compounds should also be critically revised to avoid underestimation. Moreover, there is a



need for further realistic migration scenarios for other substance classes. In ongoing research appropriate migration methods should be developed for classes of polymer additives.

Furthermore, there is an increased awareness of toxicity of dibenzopyrenes. This work emphasized the potential risk of transdermal exposure to four dibenzopyrenes using the ethanol based alternative testing method on PAHs entailing polymers. Dibenzo[*a,h*]pyrene and dibenzo[*a,l*]pyrene have been evaluated for a harmonized classification and labelling (CLH) by the ECHA. The Committee for Risk Assessment (RAC) of the ECHA adopted the opinion recently and there will be an entry in Annex VI of the CLP Regulation (Regulation (EC) 1272/2008) classifying the substances as carcinogen category 1B and mutagen category 2 (140, 141).

The visualization of skin penetration using IR or fluorescence microscopy contributed to the comprehension of transepidermal pathways of lipophilic polymer compounds like the procarcinogens B[*a*]P and Neozon D. Both analytes entered the viable epidermis *ex vivo*. It would therefore be of interest for ongoing research if the ultimate carcinogens are formed during the skin penetration process of metabolically active skin or skin models already and also depth profiles of the metabolites should be investigated in the FDC-assay.

Intentionally added substances were characterized with respect to potential degradation products. The comparison of different aging models revealed oxidative pyrolysis combined with quantum-chemical calculations to be a powerful tool for prediction purposes. Thereby the presence of DEHP in an initially DEHP free polymer was ascribed to TOTM degradation. Considering that TOTM is used as DEHP substitute to use less harmful additives, this fact needs to be subject to further risk assessment of plasticizers. The data compiled in this work can be used for prioritization of analytes for risk assessment in the future.

Research on mineral oil components showed that the overall amount of PAHs is not representative for the amount of MOAH present in polymeric material. Dermal exposure to MOAH entailing polymers, however, might pose a risk that needs to be further characterized. It was demonstrated within this thesis that the MOAH fraction enters the upper most epidermal layers in artificial model set-ups.

In the future, the FDC-assay should be adapted to the quantification of mineral oil fractions in tissue after exposure to real consumer products.

## 9 References

- 1 Regulation (EC) No 1272/2008 of the European Parliament and of the Council of 16 December 2008 on classification, labelling and packaging of substances and mixtures, amending and repealing Directives 67/548/EEC and 1999/45/EC, and amending Regulation (EC) No 1907/2006 (2008).
- 2 Regulation (EC) No 1907/2006 of the European Parliament and of the Council of 18 December 2006 concerning the Registration, Evaluation, Authorisation and Restriction of Chemicals (REACH), establishing a European Chemicals Agency, amending Directive 1999/45/EC and repealing Council Regulation (EEC) No 793/93 and Commission Regulation (EC) No 1488/94 as well as Council Directive 76/769/EEC and Commission Directives 91/155/EEC, 93/67/EEC, 93/105/EC and 2000/21/EC, (2006).
- 3 Commission Regulation (EU) No 1272/2013 of 6 December 2013 amending Annex XVII to Regulation (EC) No 1907/2006 of the European Parliament and of the Council on the Registration, Evaluation, Authorisation and Restriction of Chemicals (REACH) as regards polycyclic aromatic hydrocarbons, 1272/2013 (2013).
- 4 Bolzinger M-A, Briançon S, Pelletier J, Chevalier Y. Penetration of drugs through skin, a complex rate-controlling membrane. *Current Opinion in Colloid & Interface Science*. 2012;17(3):156-65.
- 5 OECD Guidance notes on dermal absorption, Draft (2010).
- 6 OECD. Test No. 427: Skin Absorption: In Vivo Method: OECD Publishing.
- 7 Bartsch N, Hutzler C, Vieth B, Luch A. Target Analysis of Polycyclic Aromatic Hydrocarbons (PAHs) in Consumer Products and Total Content of Polycyclic Aromatic Compounds (PACs). *Polycyclic Aromatic Compounds*. 2016:1-10.
- 8 Taevernier L, Veryser L, Roche N, Peremans K, Burvenich C, Delesalle C, et al. Human skin permeation of emerging mycotoxins (beauvericin and enniatins). *J Expos Sci Environ Epidemiol*. 2016(26):277–287.
- 9 Zhang Y, Tao S. Global atmospheric emission inventory of polycyclic aromatic hydrocarbons (PAHs) for 2004. *Atmospheric Environment*. 2009;43(4):812-9.
- 10 BVL. Federal Office of Consumer Protection and Food Safety: Handbuch Monitoring 2017. 2017.

- 11 Geiss O, Bianchi I, Senaldi C, Lucena A, Tirendi S, Barrero-Moreno J. Skin surface film liquid as new migration medium for the determination of PAHs released from rubber containing consumer goods. *Polycyclic Aromatic Compounds*. 2018;1-10.
- 12 Safety of toys - Part 9: Organic chemical compounds – Requirements, DIN EN 71-9:2007-09 (2007).
- 13 Textiles - Tests for colour fastness - Part E04: Colour fastness to perspiration (ISO 105-E04:2013), DIN EN ISO 105-E04:2013-08 (2013).
- 14 Malík J, Kröhnke C. Polymer stabilization: present status and possible future trends. *Comptes Rendus Chimie*. 2006;9(11–12):1330-7.
- 15 Bartsch N, Girard M, Schneider L, Van de Weijgert V, Wilde A, Kappenstein O, et al. Chemical stabilization of polymers: Implications for dermal exposure to additives. *Journal of Environmental Science and Health, Part A*. 2018;53(5):405-20.
- 16 Bartsch N, Heidler J, Vieth B, Hutzler C, Luch A. Skin permeation of polycyclic aromatic hydrocarbons: A solvent-based in vitro approach to assess dermal exposures against benzo[a]pyrene and dibenzopyrenes. *Journal of Occupational and Environmental Hygiene*. 2016;13(12):969-79.
- 17 OECD. OECD guideline for the testing of chemicals. Test No. 428: Skin Absorption: In Vitro Method. Paris: OECD Publishing; 2004.
- 18 Lademann J, Jacobi U, Surber C, Weigmann HJ, Fluhr JW. The tape stripping procedure – evaluation of some critical parameters. *European Journal of Pharmaceutics and Biopharmaceutics*. 2009;72(2):317-23.
- 19 Schäfer-Korting M, Bock U, Diembeck W, Düsing H-J, Gamer A, Haltner-Ukomadu E, et al. The use of reconstructed human epidermis for skin absorption testing: Results of the validation study. *Altern Lab Anim*. 2008;36(2):161-87.
- 20 Uchida T, Kadhum WR, Kanai S, Todo H, Oshizaka T, Sugibayashi K. Prediction of skin permeation by chemical compounds using the artificial membrane, Strat-M™. *European Journal of Pharmaceutical Sciences*. 2015;67:113-8.
- 21 Azzi C, Zhang J, Purdon CH, Chapman JM, Nitcheva D, Hebert JR, et al. Permeation and reservoir formation of 4-(methylnitrosamino)-1-(3-pyridyl)-1-butanone (NNK) and benzo[a]pyrene (B[a]P) across porcine esophageal

## References

---

- tissue in the presence of ethanol and menthol. *Carcinogenesis*. 2006;27(1):137-45.
- 22 Biox Systems Ltd. AquaFlux Brochure 2013 [Available from: [https://www.biox.biz/Downloads/Brochures/Biox\\_AquaFlux-AF200\\_Brochure\\_07a.pdf](https://www.biox.biz/Downloads/Brochures/Biox_AquaFlux-AF200_Brochure_07a.pdf)].
- 23 Reference test method for release of nickel from all post assemblies which are inserted into pierced parts of the human body and articles intended to come into direct and prolonged contact with the skin, DIN EN 1811 (2015).
- 24 Safety of toys - Part 10: Organic chemical compounds - Sample preparation and extraction, DIN EN 71-10 (2006).
- 25 Gnanamani A, Bhaskar M, Ganga R, Sekaran G, Sadulla S. Chemical and enzymatic interactions of Direct Black 38 and Direct Brown 1 on release of carcinogenic amines. *Chemosphere*. 2004;56(9):833-41.
- 26 Stefaniak AB, Harvey CJ. Dissolution of materials in artificial skin surface film liquids. *Toxicology in Vitro*. 2006;20(8):1265-83.
- 27 Harvey CJ, LeBouf RF, Stefaniak AB. Formulation and stability of a novel artificial human sweat under conditions of storage and use. *Toxicology in Vitro*. 2010;24(6):1790-6.
- 28 Commission Regulation (EU) No 10/2011 of 14 January 2011 on plastic materials and articles intended to come into contact with food, L12 (2011).
- 29 O'Neill ET, Tuohy JJ, Franz R. Comparison of milk and ethanol/water mixtures with respect to monostyrene migration from a polystyrene packaging material. *International Dairy Journal*. 1994;4(3):271-83.
- 30 Drummen G. Fluorescent Probes and Fluorescence (Microscopy) Techniques — Illuminating biological and biomedical research. *Molecules*. 2012;17(12):14067.
- 31 Bains G, Patel AB, Narayanaswami V. Pyrene: A probe to study protein conformation and conformational changes. *Molecules*. 2011;16(9):7909.
- 32 Richter H, Howard JB. Formation of polycyclic aromatic hydrocarbons and their growth to soot—a review of chemical reaction pathways. *Progress in Energy and Combustion Science*. 2000;26(4–6):565-608.
- 33 Hecht SS. Lung carcinogenesis by tobacco smoke. *International Journal of Cancer*. 2012;131(12):2724-32.

## References

---

- 34 Dyremark A, Westerholm R, Övervik E, Gustavsson J-Å. Polycyclic aromatic hydrocarbon (PAH) emissions from charcoal grilling. *Atmospheric Environment*. 1995;29(13):1553-8.
- 35 Kuljukka T, Vaaranrinta R, Veidebaum T, Sorsa M, Peltonen K. Exposure to PAH compounds among cokery workers in the oil shale industry. *Environmental Health Perspectives*. 1996;104(Suppl 3):539-41.
- 36 Polycyclic Aromatic Hydrocarbons in Food - EFSA Scientific Opinion of the Panel on Contaminants in the Food Chain. *EFSA Journal*. 2008;6(8):724.
- 37 Spahr ME, Rathon R. Carbon black as a polymer filler. In: Palsule S, editor. *Encyclopedia of Polymers and Composites*. Berlin, Heidelberg: Springer Berlin Heidelberg; 2014. p. 1-24.
- 38 Davidson T. Conductive and Magnetic Fillers. *Functional Fillers for Plastics*. Weinheim: Wiley-VCH Verlag GmbH & Co. KGaA; 2010. p. 351-72.
- 39 Association ICB. Carbon black user's guide. 2016.
- 40 McCunney RJ, Muranko HJ, Long CM, Hamade AK, Valberg PA, Morfeld P. Carbon Black. *Patty's Toxicology*: John Wiley & Sons, Inc.; 2001.
- 41 Wu X, Yue B, Su Y, Wang Q, Huang Q, Wang Q, et al. Pollution characteristics of polycyclic aromatic hydrocarbons in common used mineral oils and their transformation during oil regeneration. *Journal of Environmental Sciences*. 2017;56:247-53.
- 42 Kim K-H, Jahan SA, Kabir E, Brown RJC. A review of airborne polycyclic aromatic hydrocarbons (PAHs) and their human health effects. *Environment International*. 2013;60:71-80.
- 43 García-Suástegui WA, Huerta-Chagoya A, Carrasco-Colín KL, Pratt MM, John K, Petrosyan P, et al. Seasonal variations in the levels of PAH-DNA adducts in young adults living in Mexico City. *Mutagenesis*. 2011;26(3):385-91.
- 44 Federal Institute for Occupational Safety and Health: Annex XV restriction report; Proposal for a restriction Benzo[a]pyrene, Benzo[e]pyrene, Benzo[a]anthracene, Dibenzo[a,h]anthracene, Benzo[b]fluoranthene, Benzo[j]fluoranthene, Benzo[k]fluoranthene, Chrysene, (2010).
- 45 Andersson JT, Achten C. Time to Say Goodbye to the 16 EPA PAHs? Toward an up-to-date use of PACs for environmental purposes. *Polycyclic Aromatic Compounds*. 2015;35(2-4):330-54.

## References

---

- 46 Nisbet ICT, LaGoy PK. Toxic equivalency factors (TEFs) for polycyclic aromatic hydrocarbons (PAHs). *Regulatory Toxicology and Pharmacology*. 1992;16(3):290-300.
- 47 Hecht SS, Loy M, Maronpot RR, Hoffmann D. A study of chemical carcinogenesis: Comparative carcinogenicity of 5-methylchrysene, benzo(a)pyrene, and modified chrysenes. *Cancer Letters*. 1:147-53.
- 48 Kapitulnik J, Levin W, Conney AH, Yagi H, Jerina DM. Benzo[a]pyrene 7,8-dihydrodiol is more carcinogenic than benzo[a]pyrene in newborn mice. *Nature*. 1977;266:378.
- 49 Phillips DH. Fifty years of benzo(a)pyrene. *Nature*. 1983;303:468.
- 50 Kalkhof S, Dautel F, Loguercio S, Baumann S, Trump S, Jungnickel H, et al. Pathway and time-resolved benzo[a]pyrene toxicity on Hepa1c1c7 cells at toxic and subtoxic exposure. *Journal of Proteome Research*. 2015;14(1):164-82.
- 51 Hecht SS, Carmella SG, Villalta PW, Hochalter JB. Analysis of phenanthrene and benzo[a]pyrene tetraol enantiomers in human urine: Relevance to the bay region diol epoxide hypothesis of benzo[a]pyrene carcinogenesis and to biomarker studies. *Chemical Research in Toxicology*. 2010;23(5):900-8.
- 52 Phillips DH, Grover PL. Polycyclic hydrocarbon activation: Bay regions and beyond. *Drug Metabolism Reviews*. 1994;26(1-2):443-67.
- 53 Ralston SL, Seidel A, Luch A, Platt KL, Baird WM. Stereoselective activation of dibenzo[a,h]pyrene to (—)-anti(11R, 12S, 13S, 14R)- and (+)-syn(11S, 12R, 13S, 14R)- 11, 12-diol-13, 14-epoxides which bind extensively to deoxyadenosine residues of DNA in the human mammary carcinoma cell line MCF-7. *Carcinogenesis*. 1995;16(12):2899-907.
- 54 Brinkmann J, Stolpmann K, Trappe S, Otter T, Genkinger D, Bock U, et al. Metabolically competent human skin models: Activation and genotoxicity of benzo[a]pyrene. *Toxicological Sciences*. 2013;131(2):351-9.
- 55 Baird WM, Hooven LA, Mahadevan B. Carcinogenic polycyclic aromatic hydrocarbon-DNA adducts and mechanism of action. *Environmental and Molecular Mutagenesis*. 2005;45(2-3):106-14.
- 56 Marston CP, Pereira C, Ferguson J, Fischer K, Hedstrom O, Dashwood W-M, et al. Effect of a complex environmental mixture from coal tar containing polycyclic aromatic hydrocarbons (PAH) on the tumor initiation, PAH-DNA

- binding and metabolic activation of carcinogenic PAH in mouse epidermis. *Carcinogenesis*. 2001;22(7):1077-86.
- 57 Upham BL, Weis LM, Trosko JE. Modulated gap junctional intercellular communication as a biomarker of PAH epigenetic toxicity: structure-function relationship. *Environmental Health Perspectives*. 1998;106(Suppl 4):975-81.
- 58 Rummel AM, Trosko JE, Wilson MR, Upham BL. Polycyclic aromatic hydrocarbons with bay-like regions inhibited gap junctional intercellular communication and stimulated MAPK activity. *Toxicological Sciences*. 1999;49(2):232-40.
- 59 Weis LM, Rummel AM, Masten SJ, Trosko JE, Upham BL. Bay or baylike regions of polycyclic aromatic hydrocarbons were potent inhibitors of gap junctional intercellular communication. *Environmental Health Perspectives*. 1998;106(1):17-22.
- 60 Baird SJS, Bailey EA, Vorhees DJ. Evaluating human risk from exposure to alkylated PAHs in an aquatic system. *Human and Ecological Risk Assessment: An International Journal*. 2007;13(2):322-38.
- 61 Trosko JE, Ruch RJ. Cell-cell communication in carcinogenesis. *Frontiers in bioscience: a journal and virtual library*. 1998;3:d208-36.
- 62 Kawaguchi S, Nakamura T, Yamamoto A, Honda G, Sasaki YF. Is the comet assay a sensitive procedure for detecting genotoxicity? *Journal of Nucleic Acids*. 2010;2010.
- 63 Collins AR. The comet assay for DNA damage and repair. *Molecular Biotechnology*. 2004;26(3):249.
- 64 Reus AA, Reisinger K, Downs TR, Carr GJ, Zeller A, Corvi R, et al. Comet assay in reconstructed 3D human epidermal skin models—investigation of intra- and inter-laboratory reproducibility with coded chemicals. *Mutagenesis*. 2013;28(6):709-20.
- 65 Speight JG. *The Chemistry and Technology of Petroleum, Fifth Edition*. Boca Raton: CRC Press; 2014.
- 66 Fiselier K, Grundböck F, Schön K, Kappenstein O, Pfaff K, Hutzler C, et al. Development of a manual method for the determination of mineral oil in foods and paperboard. *Journal of Chromatography A*. 2013;1271(1):192-200.
- 67 Weber S, Schrag K, Mildau G, Kuballa T, Walch SG, Lachenmeier DW. Analytical methods for the determination of mineral oil saturated



- hydrocarbons (MOSH) and mineral oil aromatic hydrocarbons (MOAH)—A short review. *Analytical Chemistry Insights*. 2018;13:1-16.
- 68 EFSA Scientific opinion on mineral oil hydrocarbons in food. *EFSA Journal*. 2012;10(6):2704.
- 69 Cravedi JP, Grob K, Nygaard UC, Alexander J. Bioaccumulation and toxicity of mineral oil hydrocarbons in rats - specificity of different subclasses of a broad mixture relevant for human dietary exposures. *EFSA Supporting Publications*. 2017;14(2):1090E.
- 70 Andreassen M, Hjertholm H, Cravedi J-P, Grob K, Alexander J, Nygaard UC. Effect of dietary pristane and other saturated mineral oils (MOSH) on autoimmune arthritis in rats. *Toxicology Reports*. 2017;4:104-12.
- 71 Barp L, Kornauth C, Wuerger T, Rudas M, Biedermann M, Reiner A, et al. Mineral oil in human tissues, Part I: Concentrations and molecular mass distributions. *Food Chem Toxicol*. 2014;72:312-21.
- 72 S. Kezic JK, I. Jakasa, P. Boogaard, G. Minsavage. Review of dermal effects and uptake of petroleum hydrocarbons. *Concawe*. 2010;5:160.
- 73 Chasey KL, McKee RH. Evaluation of the dermal carcinogenicity of lubricant base oils by the mouse skin painting bioassay and other proposed methods. *Journal of Applied Toxicology*. 1993;13(1):57-65.
- 74 Tarnow P, Hutzler C, Grabiger S, Schön K, Tralau T, Luch A. Estrogenic activity of mineral oil aromatic hydrocarbons used in printing inks. *PLOS ONE*. 2016;11(1):e0147239.
- 75 Noti A, Grob K, Biedermann M, Deiss U, Brüscheweiler BJ. Exposure of babies to C15–C45 mineral paraffins from human milk and breast salves. *Regulatory Toxicology and Pharmacology*. 2003;38(3):317-25.
- 76 Biedermann M, Ingenhoff J-E, Zurfluh M, Richter L, Simat T, Harling A, et al. Migration of mineral oil, photoinitiators and plasticisers from recycled paperboard into dry foods: a study under controlled conditions. *Food Additives & Contaminants: Part A*. 2013;30(5):885-98.
- 77 Biedermann M, Uematsu Y, Grob K. Mineral oil contents in paper and board recycled to paperboard for food packaging. *Packaging Technology and Science*. 2011;24(2):61-73.
- 78 Laine C, Pitkänen M, Ohra-aho T, Gestranus M, Ketoja JA. Novel test approach for evaluating and modelling barrier properties of food contact

- materials against mineral oil contaminants. *Packaging Technology and Science*. 2016;29(11):571-83.
- 79 Concin N, Hofstetter G, Plattner B, Tomovski C, Fiselier K, Gerritzen K, et al. Evidence for cosmetics as a source of mineral oil contamination in women. *Journal of Women's Health*. 2011;20(11):1713-9.
- 80 Mohapatra S, Nando GB. Cardanol: a green substitute for aromatic oil as a plasticizer in natural rubber. *RSC Advances*. 2014;4(30):15406-18.
- 81 Shell. Shell Deutschland Oil GmbH: Safety data sheet Gravex 913. 2005.
- 82 Zweifel H. *Stabilization of Polymeric Materials*: Springer Berlin Heidelberg; 2012.
- 83 Tocháček J. Effect of secondary structure on physical behaviour and performance of hindered phenolic antioxidants in polypropylene. *Polymer Degradation and Stability*. 2004;86(2):385-9.
- 84 Manga P, Sheyn D, Yang F, Sarangarajan R, Boissy RE. A role for tyrosinase-related protein 1 in 4-*tert*-butylphenol-induced toxicity in melanocytes. *The American Journal of Pathology*. 2006;169(5):1652-62.
- 85 Tsuchiya T, Fukuhara K, Hata H, Ikarashi Y, Miyata N, Katoh F, et al. Studies on the tumor-promoting activity of additives in biomaterials: Inhibition of metabolic cooperation by phenolic antioxidants involved in rubber materials. *Journal of Biomedical Materials Research*. 1995;29(1):121-6.
- 86 German Federal Institute for Risk Assessment (BfR): Recommendation on food contact material XXI. Commodities based on natural and synthetic rubber, (2016).
- 87 U.S. Environmental Protection Agency. Screening-level hazard characterization: Bridged alkyl phenol category 2010 [Available from: <http://citeseerx.ist.psu.edu/viewdoc/download;jsessionid=83DA66CA044B7F1A3A933B1358FA4270?doi=10.1.1.175.5908&rep=rep1&type=pdf>].
- 88 Environment Agency Austria. Justification for the selection of a candidate CoRAP substance. European Chemicals Agency; 2013.
- 89 ECHA. European Chemicals Agency Factsheet Substance Evaluation. ECHA-11-FS-03-EN, 2012.
- 90 Reid SJ. Mechanism of antioxidant action in the stabilization of hydrocarbon systems. *Journal of Applied Polymer Science*. 1959;2(6):345-50.

## References

---

- 91 Weiss T, Bolt HM, Schlüter G, Koslitz S, Taeger D, Welge P, et al. Metabolic dephenylation of the rubber antioxidant *N*-phenyl-2-naphthylamine to carcinogenic 2-naphthylamine in rats. *Archives of Toxicology*. 2013;87(7):1265-72.
- 92 Sorahan T, Hamilton L, Jackson JR. A further cohort study of workers employed at a factory manufacturing chemicals for the rubber industry, with special reference to the chemicals 2-mercaptobenzothiazole (MBT), aniline, phenyl- $\beta$ -naphthylamine and *o*-toluidine. *Occupational and Environmental Medicine*. 2000;57(2):106-15.
- 93 IARC. Chemical Agents and Related Occupations - 2-Naphthylamine. IARC Monographs on the Evaluation of Carcinogenic Risks to Humans. 2012;100F.
- 94 Cartwright RA. Historical and modern epidemiological studies on populations exposed to *N*-substituted aryl compounds. *Environmental Health Perspectives*. 1983;49:13-9.
- 95 Altenburger R, Brack W, Greco WR, Grote M, Jung K, Ovari A, et al. On the mode of action of *N*-phenyl-2-naphthylamine in plants. *Environmental Science & Technology*. 2006;40(19):6163-9.
- 96 Federal Institute for Occupational Safety and Health. Decision on substance evaluation pursuant to article 46(1) of Regulation (EC) No 1907/ 2006 for *N*-1-naphthylamine. 2012.
- 97 Heudorf U, Mersch-Sundermann V, Angerer J. Phthalates: Toxicology and exposure. *International Journal of Hygiene and Environmental Health*. 2007;210(5):623-34.
- 98 Liou PJ, Hauser R, Gennings C, Koch HM, Mirkes PE, Schwetz BA, et al. Assessment of phthalates/phthalate alternatives in children's toys and childcare articles: Review of the report including conclusions and recommendation of the Chronic Hazard Advisory Panel of the Consumer Product Safety Commission. *Journal Of Exposure Science And Environmental Epidemiology*. 2015;25:343.
- 99 Gray JLE, Ostby J, Furr J, Price M, Veeramachaneni DNR, Parks L. Perinatal exposure to the phthalates DEHP, BBP, and DINP, but not DEP, DMP, or DOTP, alters sexual differentiation of the male rat. *Toxicological Sciences*. 2000;58(2):350-65.

- 100 Kambia K, Dine T, Gressier B, Dupin-Spriet T, Luyckx M, Brunet C. Evaluation of the direct toxicity of trioctyltrimellitate (TOTM), di(2-ethylhexyl) phthalate (DEHP) and their hydrolysis products on isolated rat hepatocytes. *International Journal of Artificial Organs*. 2004;27(11):971-8.
- 101 David RM, Lockhart LK, Ruble KM. Lack of sensitization for trimellitate, phthalate, terephthalate and isobutyrate plasticizers in a human repeated insult patch test. *Food and Chemical Toxicology*. 2003;41(4):589-93.
- 102 ter Veld MGR, Schouten B, Lousse J, van Es DS, van der Saag PT, Rietjens IMCM, et al. Estrogenic Potency of Food-Packaging-Associated Plasticizers and Antioxidants as detected in ER $\alpha$  and ER $\beta$  reporter gene cell lines. *Journal of Agricultural and Food Chemistry*. 2006;54(12):4407-16.
- 103 Lai H, Wang Z, Wu P, Chaudhary BI, Sengupta SS, Cogen JM, et al. Structure and diffusion behavior of trioctyl trimellitate (TOTM) in PVC film studied by ATR-IR spectroscopy. *Industrial & Engineering Chemistry Research*. 2012;51(27):9365-75.
- 104 Shieh YT, Liu CM. Influences of contents and molecular weights of LDPE on DOP plasticization of PVC. *Journal of Applied Polymer Science*. 2002;83(12):2548-55.
- 105 Vidéki B, Klébert S, Pukánszky B. External and internal plasticization of cellulose acetate with caprolactone: Structure and properties. *Journal of Polymer Science Part B: Polymer Physics*. 2007;45(8):873-83.
- 106 Rider CV, Janardhan KS, Rao D, Morrison JP, McPherson CA, Harry GJ. Evaluation of N-butylbenzenesulfonamide (NBBS) neurotoxicity in Sprague-Dawley male rats following 27-day oral exposure. *NeuroToxicology*. 2012;33(6):1528-35.
- 107 Strong MJ, Garruto RM, Wolff AV, Chou SM, Fox SD, Yanagihara R. N-Butyl benzenesulfonamide: a neurotoxic plasticizer inducing a spastic myelopathy in rabbits. *Acta Neuropathologica*. 1991;81(3):235-41.
- 108 Duffield P, Bourne D, Tan K, Garruto RM, Duncan MW. Analysis of the neurotoxic plasticizer n-butylbenzenesulfonamide by gas chromatography combined with accurate mass selected ion monitoring. *Journal of Analytical Toxicology*. 1994;18(7):361-8.

- 109 Jernberg J, Pellinen J, Rantalainen A-L. Qualitative nontarget analysis of landfill leachate using gas chromatography time-of-flight mass spectrometry. *Talanta*. 2013;103:384-91.
- 110 Shang D, Kim M, Haberl M. Rapid and sensitive method for the determination of polycyclic aromatic hydrocarbons in soils using pseudo multiple reaction monitoring gas chromatography/tandem mass spectrometry. *Journal of Chromatography A*. 2014;1334:118-25.
- 111 Idowu I, Francisco O, Thomas Philippe J, Johnson W, Marvin C, Stetefeld J, et al. Validation of a simultaneous method for determining polycyclic aromatic compounds and alkylated isomers in biota. *Rapid Communications in Mass Spectrometry*. 2018;32(3):277-87.
- 112 Mohler RE, O'Reilly KT, Zemo DA, Tiwary AK, Magaw RI, Synowiec KA. Non-targeted analysis of petroleum metabolites in groundwater using GC×GC–TOFMS. *Environmental Science & Technology*. 2013;47(18):10471-6.
- 113 Radović JR, Aeppli C, Nelson RK, Jimenez N, Reddy CM, Bayona JM, et al. Assessment of photochemical processes in marine oil spill fingerprinting. *Marine Pollution Bulletin*. 2014;79(1):268-77.
- 114 Hyötyläinen T, Riekkola M-L. On-line coupled liquid chromatography–gas chromatography. *Journal of Chromatography A*. 2003;1000(1):357-84.
- 115 Lachenmeier DW, Mildau G, Rullmann A, Marx G, Walch SG, Hartwig A, et al. Evaluation of mineral oil saturated hydrocarbons (MOSH) and mineral oil aromatic hydrocarbons (MOAH) in pure mineral hydrocarbon-based cosmetics and cosmetic raw materials using (1)H NMR spectroscopy. *F1000Research*. 2017;6:682.
- 116 Hiltz JA. Pyrolysis gas chromatography/mass spectrometry identification of poly(butadiene-acrylonitrile) rubbers. *Journal of Analytical and Applied Pyrolysis*. 2000;55(2):135-50.
- 117 Manfredi M, Barberis E, Marengo E. Prediction and classification of the degradation state of plastic materials used in modern and contemporary art. *Applied Physics A*. 2016;123(1):35.
- 118 Spring M, Ricci C, Peggie DA, Kazarian SG. ATR-FTIR imaging for the analysis of organic materials in paint cross sections: case studies on paint

- samples from the National Gallery, London. *Analytical and bioanalytical chemistry*. 2008;392(1):37-45.
- 119 Bassan P, Sachdeva A, Kohler A, Hughes C, Henderson A, Boyle J, et al. FTIR microscopy of biological cells and tissue: data analysis using resonant Mie scattering (RMieS) EMSC algorithm. *Analyst*. 2012;137(6):1370-7.
- 120 Lamoureux EM, Brownawell BJ. Chemical and biological availability of sediment-sorbed hydrophobic organic contaminants. *Environmental Toxicology and Chemistry*. 1999;18(8):1733-41.
- 121 Chenoweth K, Cheung S, van Duin ACT, Goddard WA, Kober EM. Simulations on the thermal decomposition of a poly(dimethylsiloxane) polymer using the ReaxFF Reactive Force Field. *Journal of the American Chemical Society*. 2005;127(19):7192-202.
- 122 Zeynalov EB, Allen NS. Simultaneous determination of the content and activity of sterically hindered phenolic and amine stabilizers by means of an oxidative model reaction. *Polymer Degradation and Stability*. 2004;85(2):847-53.
- 123 Gensler R, Plummer CJG, Kausch HH, Kramer E, Pauquet JR, Zweifel H. Thermo-oxidative degradation of isotactic polypropylene at high temperatures: phenolic antioxidants versus HAS. *Polymer Degradation and Stability*. 2000;67(2):195-208.
- 124 Pospíšil J, Habicher WD, Pilař J, Nešpůrek S, Kuthan J, Piringer GO, et al. Discoloration of polymers by phenolic antioxidants. *Polymer Degradation and Stability*. 2002;77(3):531-8.
- 125 Parra DF, do Rosário Matos J. Some synergistic effects of antioxidants in natural rubber. *Journal of Thermal Analysis and Calorimetry*. 2002;67(2):287-94.
- 126 Gerlock JL, Tang W, Dearth MA, Korniski TJ. Reaction of benzotriazole ultraviolet light absorbers with free radicals. *Polymer Degradation and Stability*. 1995;48(1):121-30.
- 127 Commission Recommendation (EU) 2017/84 on the monitoring of mineral oil hydrocarbons in food and in materials and articles intended to come into contact with food, (2017).
- 128 Regulation (EC) No 1223/2009 of the European Parliament and of the Council of 30 November 2009 on cosmetic products, (2009).

- 129 IARC. Mineral oils, untreated or mildly treated. IARC monographs on the evaluation of carcinogenic risks to humans. 2012;100:179-96.
- 130 Jepps OG, Dancik Y, Anissimov YG, Roberts MS. Modeling the human skin barrier--towards a better understanding of dermal absorption. *Advanced drug delivery reviews*. 2013;65(2):152-68.
- 131 Opinion No. 032/2010, Carcinogenic polycyclic aromatic hydrocarbons (PAHs) in consumer products to be regulated by the EU - risk assessment by BfR in the context of a restriction proposal under REACH, (2010).
- 132 Petry T, Bury D, Fautz R, Hauser M, Huber B, Markowetz A, et al. Review of data on the dermal penetration of mineral oils and waxes used in cosmetic applications. *Toxicology letters*. 2017;280:70-8.
- 133 Singh S, Zhao K, Singh J. In vitro permeability and binding of hydrocarbons in pig ear and human abdominal skin. *Drug and Chemical Toxicology*. 2002;25(1):83-92.
- 134 Ghosh U. The role of black carbon in influencing availability of PAHs in sediments. *Human and Ecological Risk Assessment: An International Journal*. 2007;13(2):276-85.
- 135 Nishiyama T, Yamaguchi T, Fukui T, Tomii K. Chain-breaking fused heterocyclic antioxidants: antioxidant activities of phenothiazines compared to related compounds. *Polymer Degradation and Stability*. 1999;64(1):33-8.
- 136 Godin B, Touitou E. Transdermal skin delivery: Predictions for humans from in vivo, ex vivo and animal models. *Advanced drug delivery reviews*. 2007;59(11):1152-61.
- 137 Rani M, Shim WJ, Han GM, Jang M, Al-Odaini NA, Song YK, et al. Qualitative analysis of additives in plastic marine debris and its new products. *Archives of Environmental Contamination and Toxicology*. 2015;69(3):352-66.
- 138 Carlsson DJ, Jensen JPT, Wiles DM. Antioxidant mechanisms of hindered amine light stabilizers. *Die Makromolekulare Chemie*. 2003;8(8):79-88.
- 139 Barrero-Moreno, J. et al., Migration of Polycyclic Aromatic Hydrocarbons (PAHs) from plastic and rubber articles, EUR 29282 EN, Publications Office of the European Union, Luxembourg, doi:10.2760/41492, JRC111476.
- 140 Committee for Risk Assessment (RAC) Opinion proposing harmonised classification and labelling at EU level of benzo[*rsf*]pentaphene, (2017).

## References

---

- 141 Committee for Risk Assessment (RAC) Opinion proposing harmonised classification and labelling at EU level of Dibenzo[*b,def*]chrysene; Dibenzo[*a,h*]pyrene, (2017).
- 142 Bausinger J, Speit G. The impact of lymphocyte isolation on induced DNA damage in human blood samples measured by the comet assay. *Mutagenesis*. 2016;31(5):567-72.



## 10 List of publications

### 10.1 Articles

- 1 Bartsch, N., Girard, M., Wilde, A., Bruhn, T., Kappenstein, O., Vieth, B., Hutzler, C. and A. Luch: Thermal stability of polymer additives: Comparison of decomposition models including oxidative pyrolysis. *J Vinyl Addit Techn.*
- 2 Bartsch, N., Girard, M., Schneider, L., van de Weijger, V., Wilde, A., Kappenstein, O., Vieth, B., Hutzler, C. and A. Luch: Chemical stabilization of polymers: Implications for dermal exposure to additives. *J Environ Sci Heal A.*
- 3 Bartsch, N., Heidler, J., Vieth, B., Hutzler, C. and A. Luch: Skin permeation of polycyclic aromatic hydrocarbons: A solvent-based in vitro approach to assess dermal exposures against benzo[a]pyrene and dibenzopyrenes. *J Occup Environ Hyg.*
- 4 Bartsch, N., Hutzler, C., Vieth, B. and A. Luch: Target analysis of polycyclic aromatic hydrocarbons (PAHs) in consumer products and total content of polycyclic aromatic compounds (PACs). *Polycycl Aromat Comp.*

### 10.2 Conferences

- 1 Talk: 6<sup>th</sup> International Network of Environmental Forensics Conference (INEF), 27 - 30 June, Örebro: "Human exposure to PAHs, mineral oil components and other hazardous constituents by skin contact to consumer products".
- 2 Poster: 82<sup>nd</sup> Annual Meeting of the German Society for Experimental and Clinical Pharmacology and Toxicology (DGPT), 29 February – 03 March 2016, Berlin. Bartsch, N., Girard, M., Schneider, C., Hutzler, C., Kappenstein, O., Vieth, B. and A. Luch: "Epidermal barrier function challenged by everyday commodities: Possible human exposure to polymer additives and their degradation products via skin contacts".
- 3 Poster - Young scientist best poster presentation: 25<sup>th</sup> International Symposium on Polynuclear Aromatic Hydrocarbons (ISPAC), 13 - 17 September 2015, Bordeaux. Bartsch, N., Hutzler, C., Vieth, B. and A. Luch: Results published in *Polycycl Aromat Comp.*

- 4 Poster: 4<sup>th</sup> Galenus Workshop: drug delivery to human skin, 25 - 27 February 2015, Saarbrücken. Mielke, N., Hutzler, C., Kappenstein, O., Vieth, B. and A. Luch: "Human skin challenged by additives and contaminants migrating from consumer products: Can we trust its barrier function?"
- 5 Poster: 81<sup>st</sup> Annual Meeting of the DGPT, 10 - 12 March 2015, Kiel. Mielke, N., Hutzler, C., Kappenstein, O., Vieth, B. and A. Luch: "Consumer products made of polymers: An unfailing source for dermal uptake of potentially harmful substances."
- 6 Poster: 80<sup>th</sup> Annual Meeting of the DGPT, 31 March – 03 April 2014, Hannover. Mielke, N., Hutzler, C., Kappenstein, O., Vieth, B. and A. Luch: "Efficiency of the skin barrier function: On the penetration of additives and contaminants from consumer products."
- 7 Poster: 44<sup>th</sup> annual meeting of the European Society for Dermatological Research (ESDR), 10 - 13 September 2014, Copenhagen. Mielke, N., Hutzler, C., Kappenstein, O., Vieth, B. and A. Luch: "Human skin challenged by additives and contaminants migrating from consumer products: Can we trust its barrier function?"

# Annex I

## Experimental

### a) Comet-assay protocol for determination of DNA damage in skin *ex vivo* after contact to highly PAH contaminated consumer products

Excised human skin from plastic surgery was cleaned from subcutaneous fat using a scalpel and immediately mounted in the FDC as follows:

Full thickness skin specimens of approx. 2 cm in diameter were punched out and placed onto the receptor chamber. The chamber was filled with Dulbecco's Modified Eagle Medium (DMEM), stirred and maintained at 37°C. The skin was in contact for 24 h with a handle of a hammer of 1 cm in diameter by placing the sample into the donor chamber directly onto the skin. The material of the handle has been characterized and found to be chloromethylated styrene-divinylbenzene copolymer (CM-SDB) with a B[a]P content of 266 mg/kg (16).

In order to implement positive controls, a solution of methyl methanesulfonate (MMS) was pipetted onto the skin with a concentration of 5 µg/cm<sup>2</sup>. MMS is an alkylating agent commonly applied in the comet-assay to cause alkaline-labile sites (142). Because a complex mixture of mineral oil products and carbon black has been expected to be part of the tested material, a coal tar reference material was used as positive control in addition. The analytical standard 1597a of the National Institute of Standards and Technology (NIST) provides a positive control that mirrors the chemical composition of the tested commodity material. The amount of coal tar solution used per FDC was calculated according to the final B[a]P concentration on the skin as compared to the polymer tested.

The skin was removed from the FDC and separation of epidermis and dermis achieved by placing the skin in trypsin for 3 h at 4°C in a 6-well plate. Afterwards, the epidermis was carefully removed using forceps.

Further clean up steps were performed for both skin tissues:

- Placed in mincing buffer (20mM ethylenediaminetetraacetic acid (EDTA) in Hanks' Balanced Salt Solution (HBSS) + 10% dimethyl sulfoxide (DMSO))
- Cut in fragments using scissors
- Resulting cell suspension filtered through cell strainer 70 µm

- Centrifugation of filtrate with 200 g for 5 min at 4°C
- Resuspension of cell pellet and incorporation of single cells in agarose

Comet-assays were carried out as described previously (54) conducting lysis of cells, electrophoresis and staining.

b) FDC protocol for dermal exposure assessment of liquid or paste-like mineral oil formulations

Human epidermis (thickness 500 µm) from plastic surgery was incubated in FDC with either 200 µl Gravex solution (1 mg/ml in hexane; area related concentration 114 ng/cm<sup>2</sup>) or 10 – 15 mg vaseline (5.7 – 8.5 mg/cm<sup>2</sup>) for 24 h at conditions as described previously (15, 16) and according to the OECD guideline 428. The Gravex solution was directly pipetted into the donor chamber. Vaseline was initially placed onto a teflon septum for weighing purposes, subsequently placed onto the skin with the septum tending upwards and slightly pressed onto the skin surface using forceps. The clean-up procedure of compartments after incubation was as follows:

**Wash:** The septum was removed from the skin in case of vaseline incubation and placed into a test tube with ground glass joint to determine the amount of mineral oil components that did not enter the skin. In addition, the donor chamber was rinsed three times with 1 ml sodium chloride solution each. The washing solutions were combined in test tubes and filled up to 5 ml. A liquid-liquid-extraction (LLE) was performed adding 5 ml hexane. The hexane phase was removed after phase separation using pipettes and subject to online-LC-GC-FID analyses.

**Strips:** The five outer most s.c. layers (s.c.1-5) were removed by tape stripping and treated separately. The strips were placed in headspace vials, submerged in 10 ml acetonitrile and mineral oil components extracted applying ultrasonic treatment for 30 minutes. The extract was transferred quantitatively into test tubes with ground glass joints and LLE performed using 5ml hexane in order to remove glue residues. The supernatant was removed after phase separation and used for analyses.

MOAH determination in strip compartments was conducted using an external matrix calibration because of slight interferences with the glue material ( $R^2 > 0.99$ ).

Defined amounts of vaseline or Gravex were placed onto strips accordingly and treated just like the incubated skin samples.

**Remaining epidermis:** The skin was placed into a headspace vial after tape stripping, submerged in 5 ml hexane and underwent ultrasonic treatment for 30 minutes. The extract was analyzed without further clean-up steps.

**Receptor solution:** The receptor solution was transferred into test tubes with ground glass joints, the exact volume documented and a LLE performed as for the wash compartment.

Internal standards were added to every single compartment prior to extraction and clean-up procedure (5  $\mu$ l of a standard mixture with a final scheduled concentration of 300 ng/ml; MOSH: n-undecane (C11), n-tridecane (C13), Bicyclohexyl (CyCy), cholestane; MOAH: pentylbenzene (5B), 1-methylnaphthalene (1-MN), 2-methylnaphthalene (2-MN), 1,3,5-tri-*tert*-butylbenzene (TBB)). All glass and teflon materials were cleaned prior to analyses applying rinsing steps of 1x acetone/ water (9:1) and 3x hexane.

## **Annex II**

### **SUPPLEMENTARY INFORMATION**

#### **TITLE**

Skin permeation of polycyclic aromatic hydrocarbons:  
A solvent-based *in vitro* approach to assess dermal exposures against benzo[a]pyrene and dibenzopyrenes

#### **AUTHORS**

Bartsch, N., Heidler, J., Vieth, B., Hutzler, C., Luch, A.  
German Federal Institute for Risk Assessment (BfR), Department of Chemical and Product Safety, Berlin, Germany

#### **JOURNAL**

*Journal of Occupational and Environmental Hygiene*, 2016, 13: 969-979.

Link: <https://doi.org/10.1080/15459624.2016.1200724>

#### **KEYWORDS**

dibenzopyrenes, benzo[a]pyrene, dermal exposure, skin models, Franz cell, migration

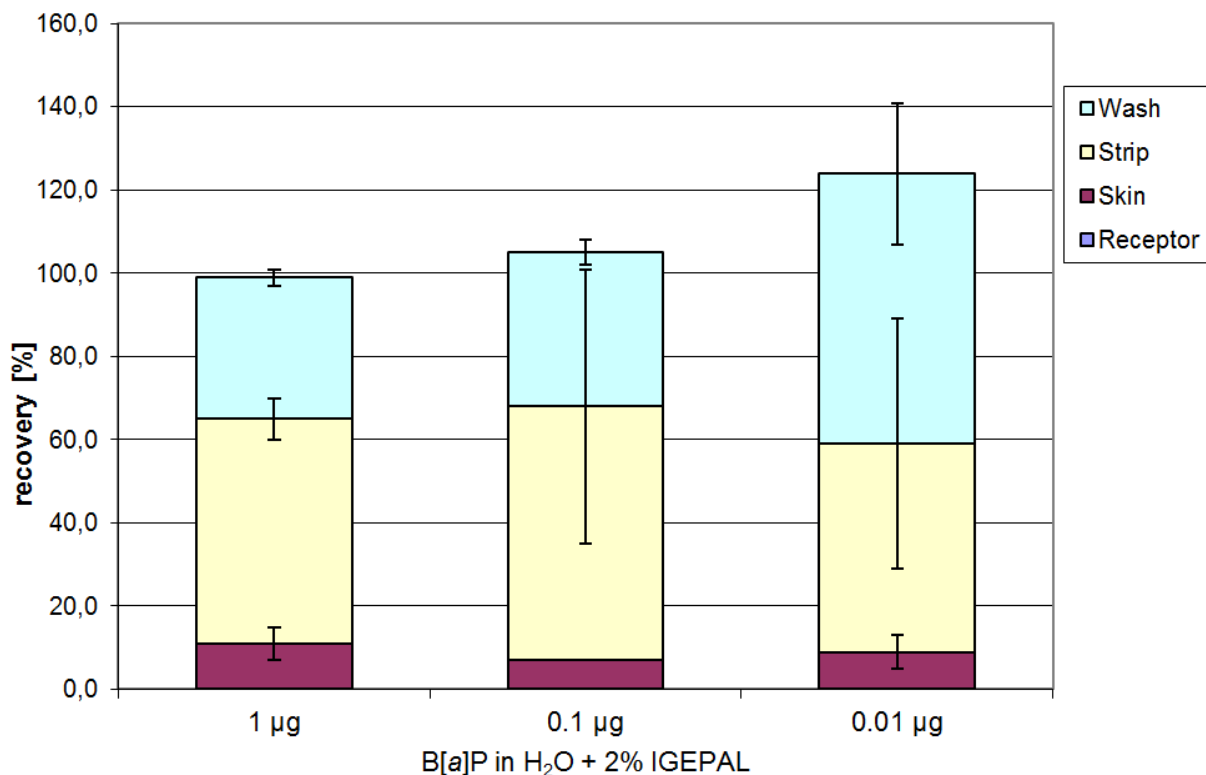


**FIGURE A.** Validation of the Franz cell assay with regard to B[a]P recovery in human skin. The volume applied was 15 µl each concentration. Experiments have been performed in triplicates and bars show the standard error of the mean for each compartment of Franz cell.

SUPPLEMENTARY INFORMATION  
*Bartsch et al. J Occup Environ Hyg*

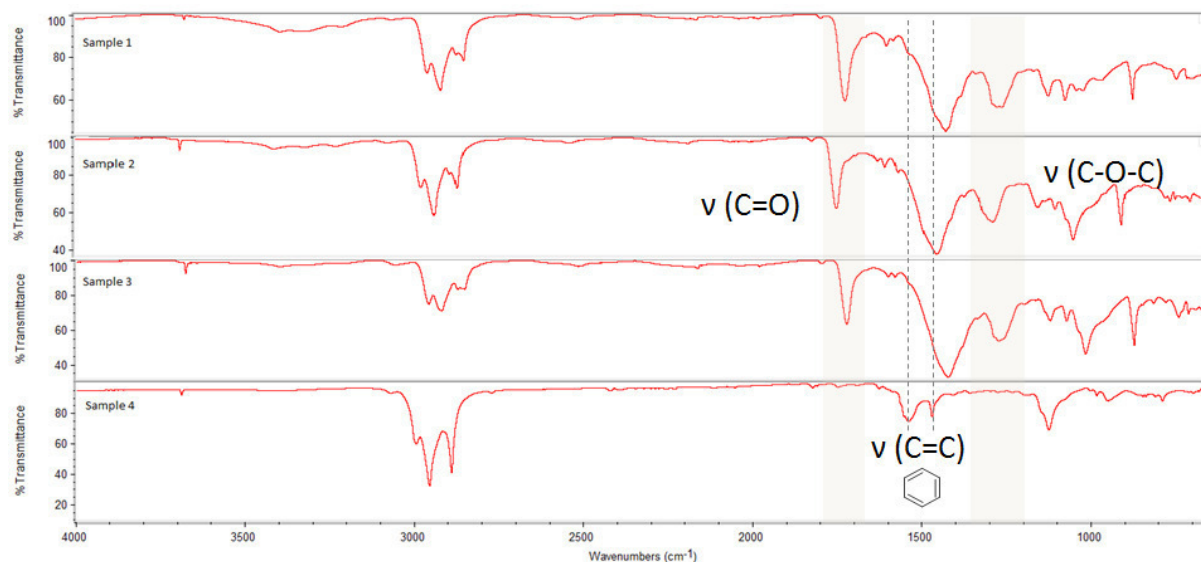


**FIGURE B.** Characterization of the polymeric material in samples #1-4 by Fourier transformed infrared (ATR-FTIR) spectra. Highlighted bands for carbonyl ( $1750\text{ cm}^{-1}$ ) and ester bond vibrations ( $1250\text{ cm}^{-1}$ ) and typical aromatic ring bands ( $1490\text{ cm}^{-1}$ ,  $1590\text{ cm}^{-1}$ ).



SUPPLEMENTARY INFORMATION  
*Bartsch et al. J Occup Environ Hyg*

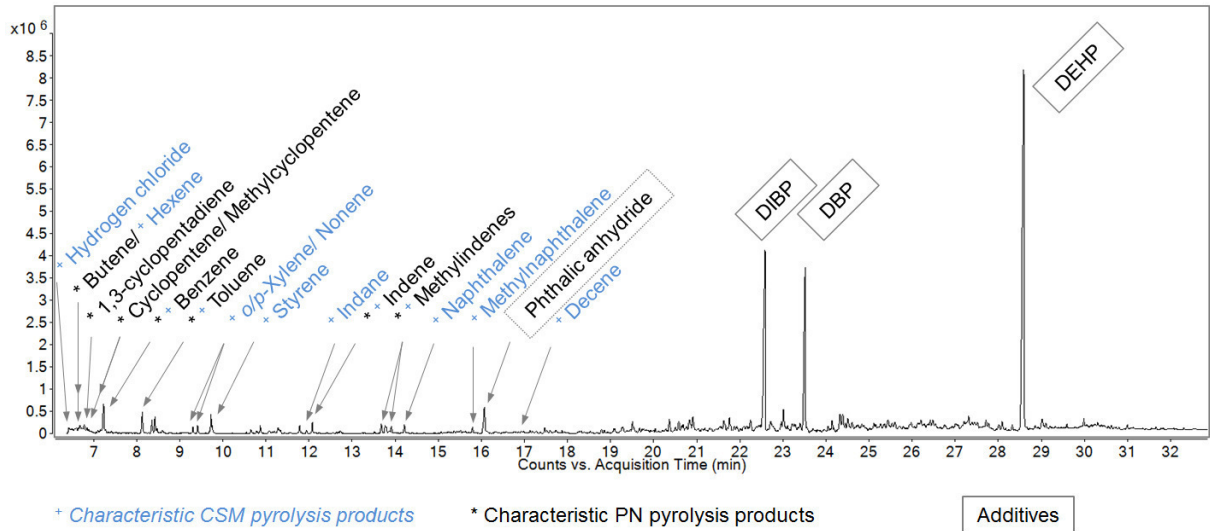


**FIGURE C 1**

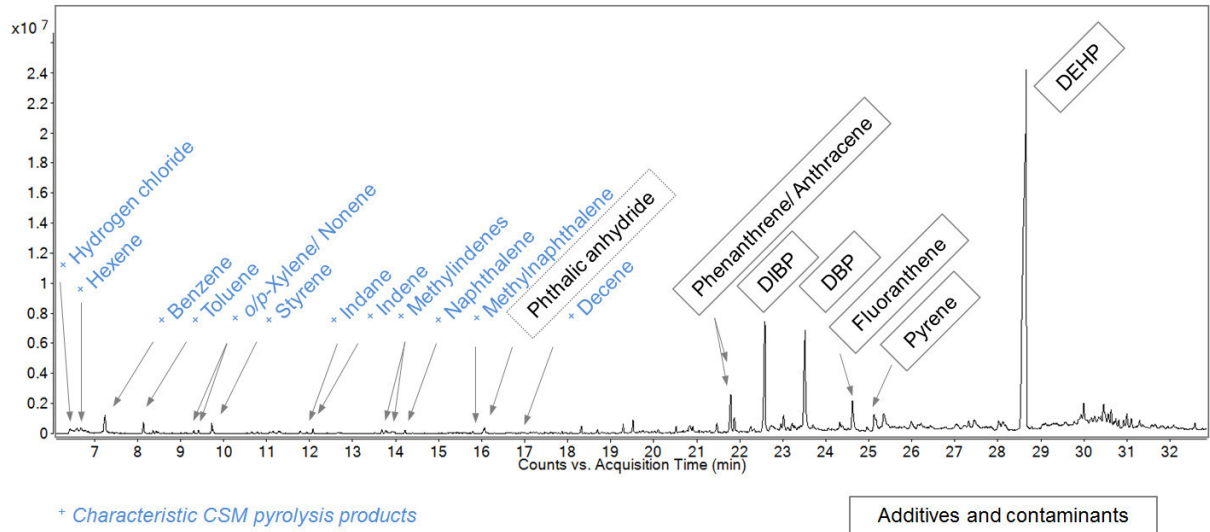


**FIGURE C 2**

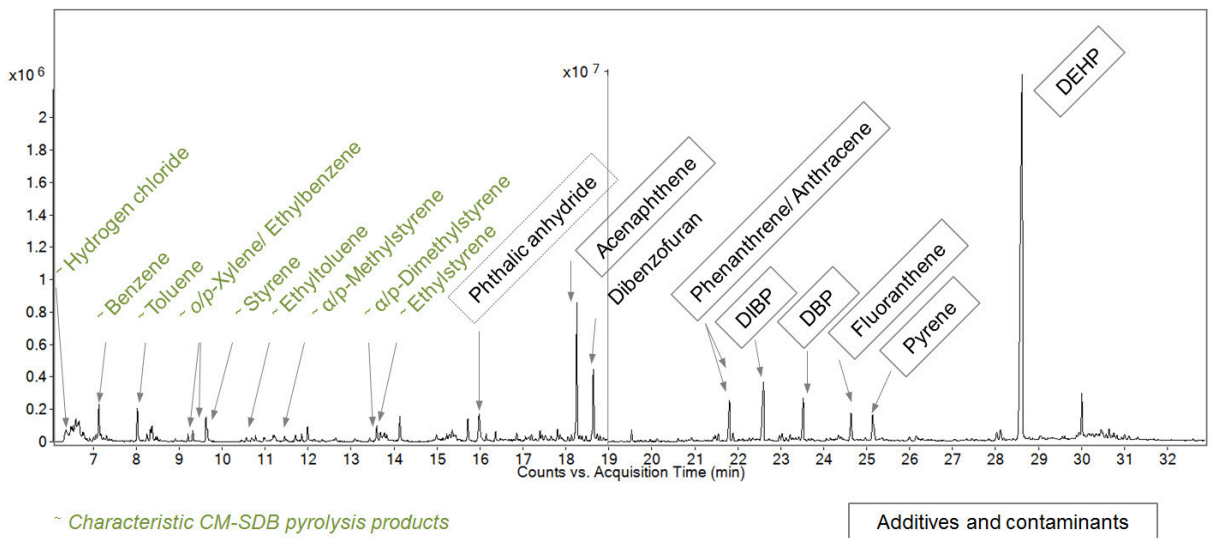


**FIGURE C 3**

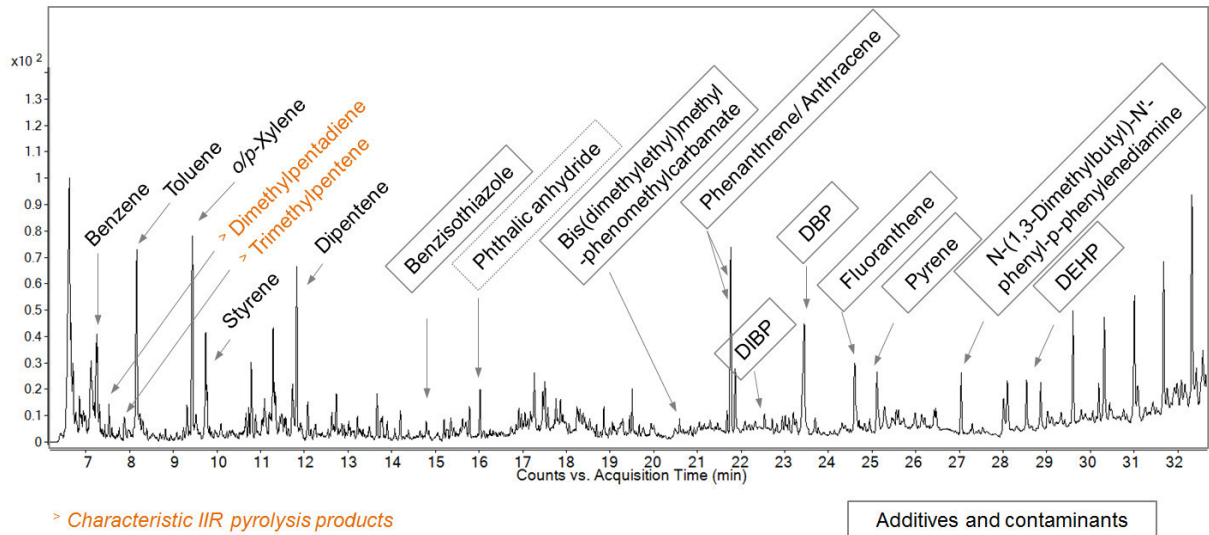


**FIGURE C 4**

**FIGURE C.** Pyrograms of samples #1-4 after the processing of the data obtained with MassHunter deconvolution in TCC mode. Characterization of polymer material using Pyr-GC-MS, characteristic pyrolysis products of each polymer are highlighted as well as additives and contaminants. Abbreviations: DIBP, diisobutyl phthalate; DBP, dibutyl phthalate; DEHP, diethylhexylphthalate (also named bis(2-ethylhexyl)phthalate).

SUPPLEMENTARY INFORMATION  
*Bartsch et al. J Occup Environ Hyg*

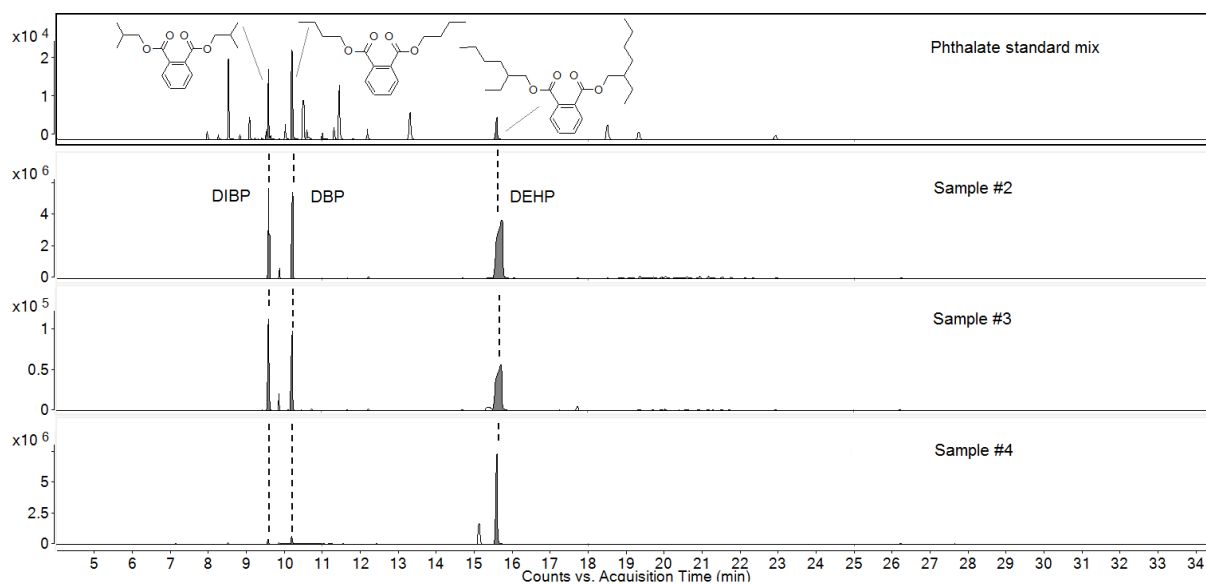


**FIGURE D.** Chromatographic evaluation of acetone extracts of sample #2-4 compared against a phthalate standard mix (GC-EI-MS/MS in MRM mode). Chromatograms show total ion chromatograms each. Three identified phthalates are highlighted: DIBP, diisobutyl phthalate; DBP, dibutyl phthalate; DEHP, diethylhexylphthalate (also named bis(2-ethylhexyl)phthalate).

SUPPLEMENTARY INFORMATION  
Bartsch et al. J Occup Environ Hyg

Table A: Summary of experimental set up with  $\Sigma n = 92$ .

Test system	Comparison of test systems - consumer product samples 1-4							
	Solvent				Skin/ skin surrogate			
	50% EtOH 37°C	20% EtOH 37°C	20% EtOH 22°C	Aq. sweat 37°C	Human skin 33°C	Epider m	Porcine skin	Strat- M
<b>Sample 1</b>								
B[a]P [ng/cm <sup>2</sup> ]	-	23.1	18.0	0.1	13.6	-	-	-
Stdev [ng/cm <sup>2</sup> ]	-	4.7	3.4	0.1	-	-	-	-
n	-	3	3	4	1	-	-	-
<b>Sample 2</b>								
B[a]P [ng/cm <sup>2</sup> ]	694.3	101.1	57.9	0.8	102.3	15.5	29.9	11.8
Stdev [ng/cm <sup>2</sup> ]	68.3	10.3	12.1	0.2	-	4.8	11.8	0.3
n	3	3	3	4	1	2	2	3
<b>Sample 3</b>								
B[a]P [ng/cm <sup>2</sup> ]	-	109.4	49.7	-	80.1	17.5	30.0	17.0
Stdev [ng/cm <sup>2</sup> ]	-	16.0	9.7	-	26.2	0.5	1.3	3.6
n	-	3	3	-	3	2	2	3
<b>Sample 4</b>								
B[a]P [ng/cm <sup>2</sup> ]	-	75.9	47.7	-	41.9	21.9	21.1	66.9
Stdev [ng/cm <sup>2</sup> ]	-	17.5	4.1	-	16.1	1.1	7.1	1.1
n	-	3	3	-	3	2	2	3
Test system	Validation of Franz cell assay - B[a]P in H <sub>2</sub> O + 2% IGEPAL							
					Human skin 33°C	Epider m	Porcine skin	
<b>1000 ng/ 1.76cm<sup>2</sup></b>								
$\Sigma$ [%] 4 compartments					99.6	141.6	83.4	
Stdev $\Sigma$ [%]					2.8	5.5	15.2	
n					3	3	3	
<b>100 ng/ 1.76cm<sup>2</sup></b>								
$\Sigma$ [%] 4 compartments					105.2	138.1	109.0	
Stdev $\Sigma$ [%]					30.9	31.4	39.6	
n					3	4	3	
<b>10 ng/ 1.76cm<sup>2</sup></b>								
$\Sigma$ [%] 4 compartments					124.6	220.7	116.3	
Stdev $\Sigma$ [%]					46.0	19.1	96.0	
n					3	3	3	

## **Annex III**

### **SUPPLEMENTARY INFORMATION**

#### **TITLE**

Chemical Stabilization of Polymers: Implications for Dermal Exposure to Additives

#### **AUTHORS**

Bartsch, N., Girard, M., Schneider, L., van de Weijgert, V., Wilde, A., Kappenstein, O., Vieth, B., Hutzler, C., Luch, A.

#### **JOURNAL**

*Journal of Environmental Science and Health, Part A*. 2018;53(5):405-20

Link: <https://doi.org/10.1080/10934529.2017.1412192>

#### **KEYWORDS**

Polymer aging; Additives; LDPE; Squalane; GC-MS/MS; ATR-FTIR; Dermal exposure; Franz diffusion cell; Percutaneous absorption

FIGURES

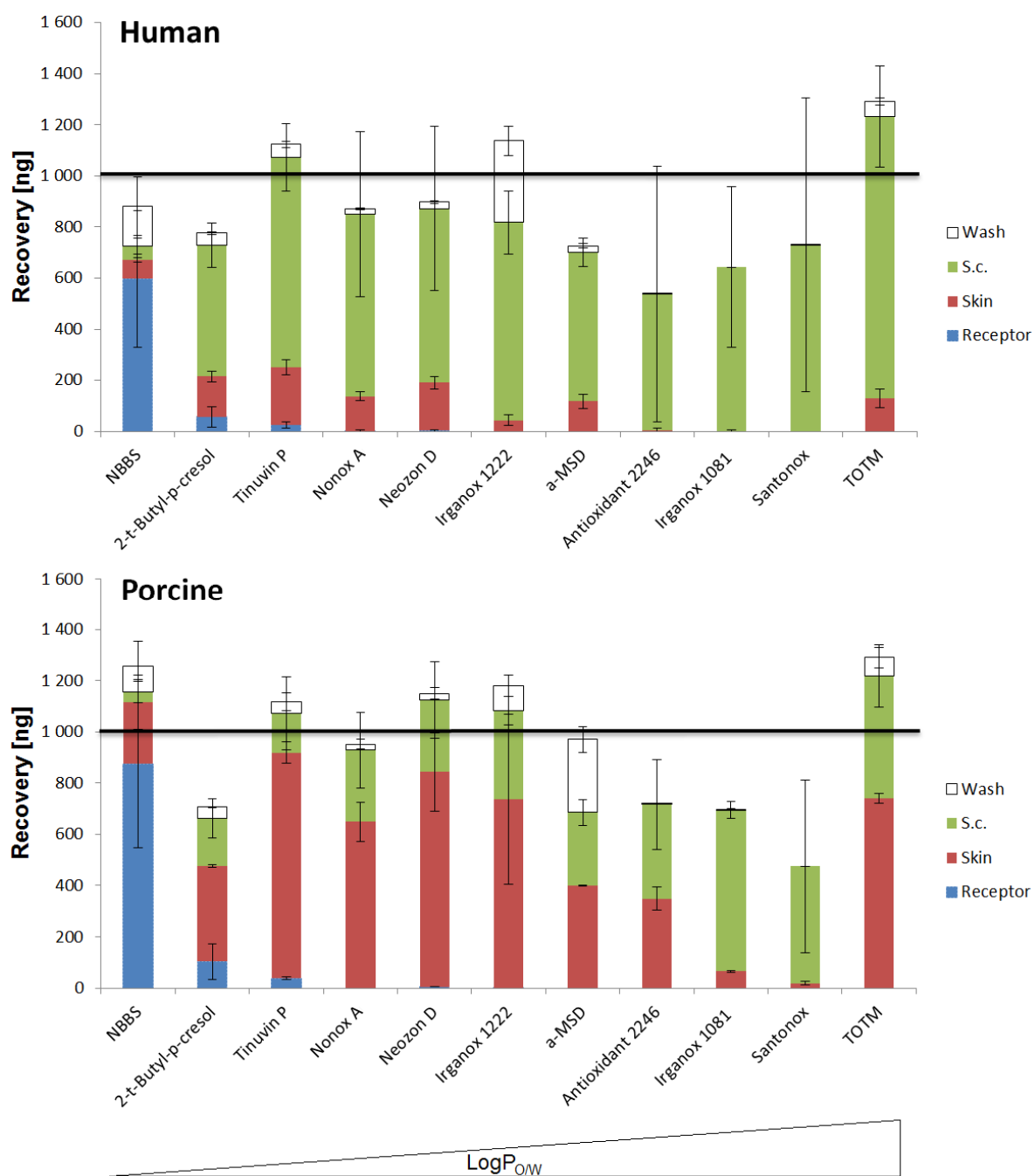


Figure S1: Recoveries of 2<sup>nd</sup> validation set-up Franz cell assay: Human and porcine epidermis (flank) was incubated in Franz cell with 1000 ng of each additive for 24 h (100  $\mu$ l of 10 $\mu$ g/ml in acetonitrile). 100  $\mu$ l acetonitrile were added as negative control. Error bars show standard deviation of the mean of three independent experiments for human skin samples. Porcine skin was analyzed in duplicates. TEWL<sub>human</sub>: 10.1  $\pm$  1.3 g/(m<sup>2</sup>h) TEWL<sub>porcine</sub>: 18.2  $\pm$  2.9 g/(m<sup>2</sup>h).

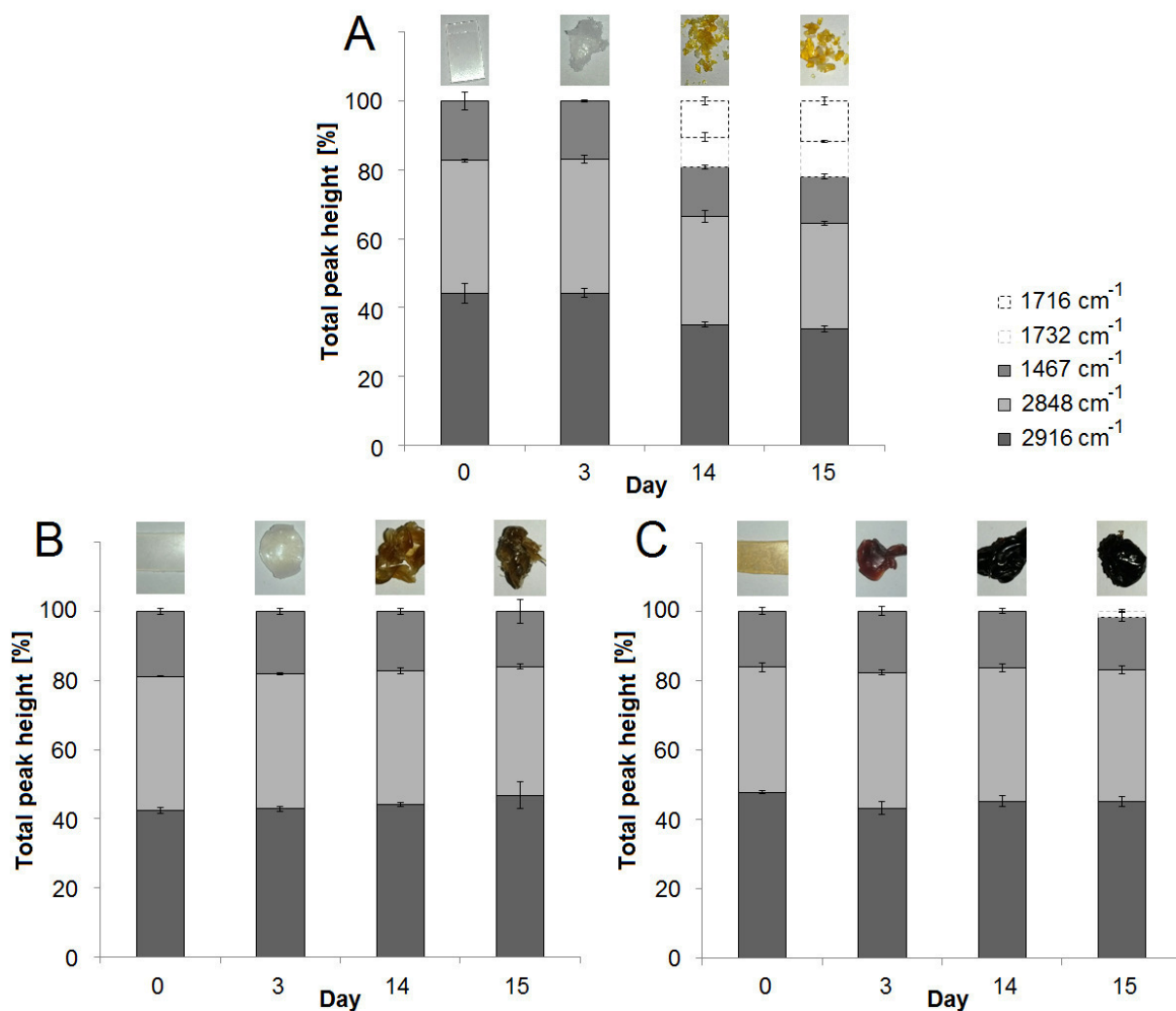


Figure S2: Percentage distribution of LDPE-specific bands at 2916, 2848 and 1467 cm<sup>-1</sup> (—CH<sub>2</sub> derived, solid bars) and degradation-specific bands at 1732 and 1716 cm<sup>-1</sup> (—C=O derived, dashed bars) over time at 130°C. **A**: pure LDPE; **B**: LDPE 1, **C**: LDPE 2 with individual additivation (cf. Table 1). Individual signal height (% transmittance) was evaluated in relation to the sum of transmittance for all participating bands. Error bars show standard deviation of the mean of three independent experiments. Figures A, B and C document macroscopic changes in material integrity at time points of 0, 3, 14 and 15 days.

SUPPLEMENTARY INFORMATION  
Bartsch et al. *J Environ Sci Heal A*

TABLES

Table S1: Recoveries (Rec.) of positive control samples from investigations of additives incorporated in LDPE together with standard deviation (STD). A mixture of 250 ng/ml of each additive in toluene was used as positive control. It was treated in parallel to LDPE samples utilizing ultrasonic assisted extraction.

Sample	Additive yield [%]									
	NBBS	$\alpha$ -MSD	Irganox 1222	Irganox 1081	Santonox	TOTM	Antioxidant 2246	Nonox A	Neozon D	Tinuvin P
<b>Rec. 1</b>	87.8	103.2	79.1	93.9	67.7	78.9	83.8	92.7	92.1	89.3
<b>Rec. 2</b>	80.2	89.3	80.0	87.6	81.7	84.0	76.6	96.2	94.5	82.1
<b>Rec. 3</b>	84.9	92.8	84.2	101.6	79.7	92.8	84.7	91.7	92.2	84.3
<b>Mean Rec.</b>	84.3	95.1	81.1	94.3	76.4	85.2	81.7	93.5	93.0	85.2
<b>STD</b>	3.9	7.2	2.7	7.0	7.6	7.0	4.4	2.4	1.4	3.7



SUPPLEMENTARY INFORMATION  
*Bartsch et al. J Environ Sci Heal A*

---

Table S2: Recoveries (Rec.) of positive control samples from investigations of additives in squalane together with standard deviation (STD). Amounts of 4-12 mg of the respective additive were dissolved in 1 ml squalane and directly underwent an extraction procedure in parallel to the aged samples.  $R^2$  of the matrix calibration is shown.

Sample	Additive yield [%]		
	Nonox A	Antioxidant 2246	Irganox 1081
Rec. 1	99.1	96.4	126.8
Rec. 2	111.7	96.3	97.1
Rec. 3	101.8	86.3	99.5
Mean Rec.	104.2	93.0	107.8
STD	6.7	5.8	16.5
$R^2$	0.998	0.991	0.990

SUPPLEMENTARY INFORMATION  
Bartsch et al. J Environ Sci Heal A

Table S3: Recoveries (Rec.) of 1<sup>st</sup> validation set-up Franz cell assay: positive control samples from investigations of LDPE in skin contact with standard deviation (STD). Substances were dissolved in acetonitrile, added to the respective compartment of Franz cell with a final concentration of 300 ng/ml and directly underwent the clean-up procedure according to the protocol described in 2.4. *S.c.*: *stratum corneum*.

	Receptor	Skin	S.c.	Wash
<b>NBBS</b>				
Rec. 1	92.2	88.0	130.0	111.1
Rec. 2	111.6	79.8	142.7	111.4
Rec. 3	111.0	88.7	139.8	107.4
Mean Rec. (%)	104.9	85.5	137.5	110.0
STD (%)	11.0	4.9	6.7	2.2
<b>2-<i>t</i>-Butyl-<i>p</i>-cresol</b>				
Rec. 1	98.5	100.4	125.2	111.7
Rec. 2	108.0	105.1	117.0	110.2
Rec. 3	114.7	107.3	122.0	105.7
Mean Rec. (%)	107.1	104.3	121.4	109.2
STD (%)	8.2	3.5	4.1	3.1
<b>Tinuvin P</b>				
Rec. 1	86.1	78.2	119.8	70.5
Rec. 2	111.8	73.6	155.2	88.9
Rec. 3	83.7	74.2	142.1	83.9
Mean Rec. (%)	93.9	75.3	139.1	81.1
STD (%)	15.6	2.5	17.9	9.5
<b>Nonox A</b>				
Rec. 1	82.5	87.0	122.7	89.0
Rec. 2	80.2	94.5	128.7	91.1
Rec. 3	82.3	99.6	125.9	96.4
Mean Rec. (%)	81.6	93.7	125.8	92.2
STD (%)	1.3	6.4	3.0	3.8
<b>Neozon D</b>				
Rec. 1	91.0	81.9	118.1	95.4
Rec. 2	85.2	89.6	122.9	106.5
Rec. 3	86.3	95.4	109.4	100.8
Mean Rec. (%)	87.5	89.0	116.8	100.9
STD (%)	3.1	6.8	6.8	5.5
<b>Irganox 1222</b>				
Rec. 1	42.9	127.6	137.0	72.5

SUPPLEMENTARY INFORMATION  
*Bartsch et al. J Environ Sci Heal A*

Rec. 2	93.7	109.8	168.3	95.9
Rec. 3	49.4	104.6	162.1	60.5
Mean Rec. (%)	62.0	114.0	155.8	76.3
STD (%)	27.6	12.1	16.6	18.0
<b>a-MSD</b>				
Rec. 1	107.4	98.3	126.1	109.6
Rec. 2	111.3	98.3	118.8	116.1
Rec. 3	104.8	103.1	122.0	106.0
Mean Rec. (%)	107.8	99.9	122.3	110.6
STD (%)	3.2	2.8	3.7	5.1
<b>Antioxidant 2246</b>				
Rec. 1	97.1	77.3	112.4	103.6
Rec. 2	96.0	92.4	115.8	100.8
Rec. 3	96.9	112.4	114.7	99.2
Mean Rec. (%)	96.7	94.0	114.3	101.2
STD (%)	0.6	17.6	1.7	2.2
<b>Irganox 1081</b>				
Rec. 1	44.8	68.5	105.4	58.8
Rec. 2	54.5	69.5	112.7	60.6
Rec. 3	58.5	75.6	108.2	62.5
Mean Rec. (%)	52.6	71.2	108.8	60.7
STD (%)	7.0	3.8	3.6	1.8
<b>Santonox</b>				
Rec. 1	58.3	147.3	163.8	85.6
Rec. 2	70.1	156.4	146.7	100.4
Rec. 3	81.0	168.4	134.7	86.0
Mean Rec. (%)	69.8	157.4	148.4	90.7
STD (%)	11.4	10.6	14.6	8.4
<b>TOTM</b>				
Rec. 1	94.2	112.7	115.7	115.3
Rec. 2	107.8	118.6	116.1	126.5
Rec. 3	98.1	106.6	117.5	118.9
Mean Rec. (%)	100.0	112.7	116.4	120.2
STD (%)	7.0	6.0	0.9	5.8

## **Annex IV**

### **SUPPLEMENTARY INFORMATION**

#### **TITLE**

Thermal stability of polymer additives:

Comparison of decomposition models including oxidative pyrolysis

#### **AUTHORS**

Bartsch, N., Girard, M., Wilde, A., Bruhn, T., Kappenstein, O., Vieth, B., Hutzler, C., Luch, A.

German Federal Institute for Risk Assessment (BfR), Department of Chemical and Product Safety, Berlin, Germany

#### **JOURNAL**

*Journal of Vinyl and Additive Technology*

Link: <https://doi.org/10.1002/vnl.21654>

#### **KEYWORDS**

antioxidants, quantum chemistry, polyamides, polyethylene (PE), degradation

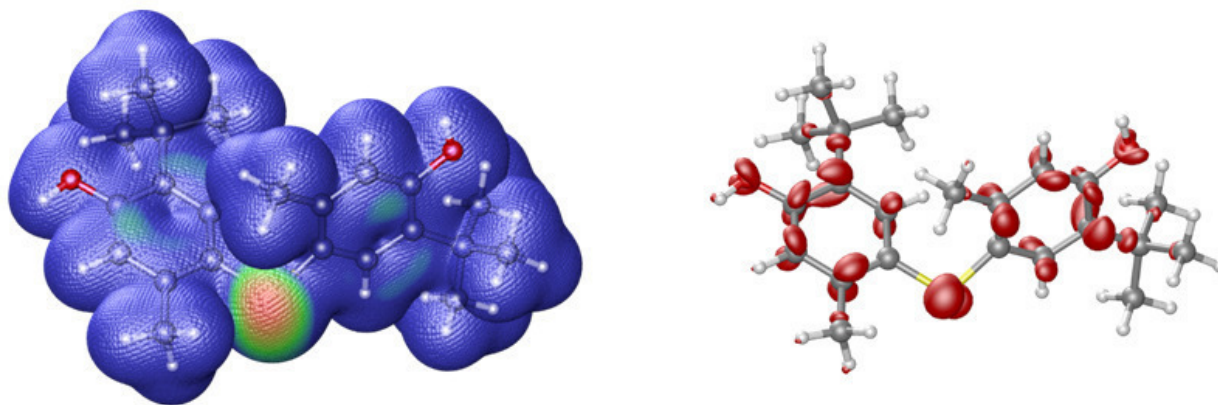


**FIGURE S1**

Quantum-chemical calculations of Santonox: ALIE surface (left) and Fukui function  $f^0$  (right).

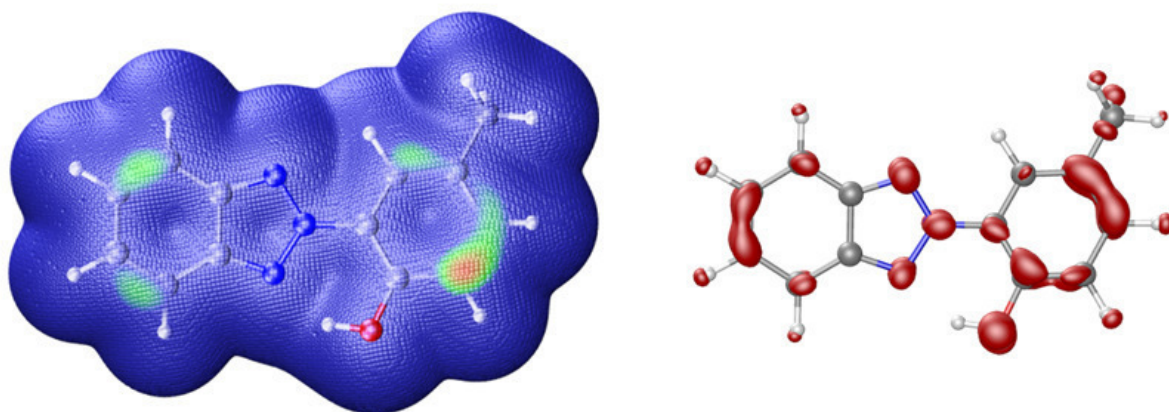


**FIGURE S2**

Quantum-chemical calculations of Tinuvin P: ALIE surface (left) and Fukui function  $f^0$  (right).

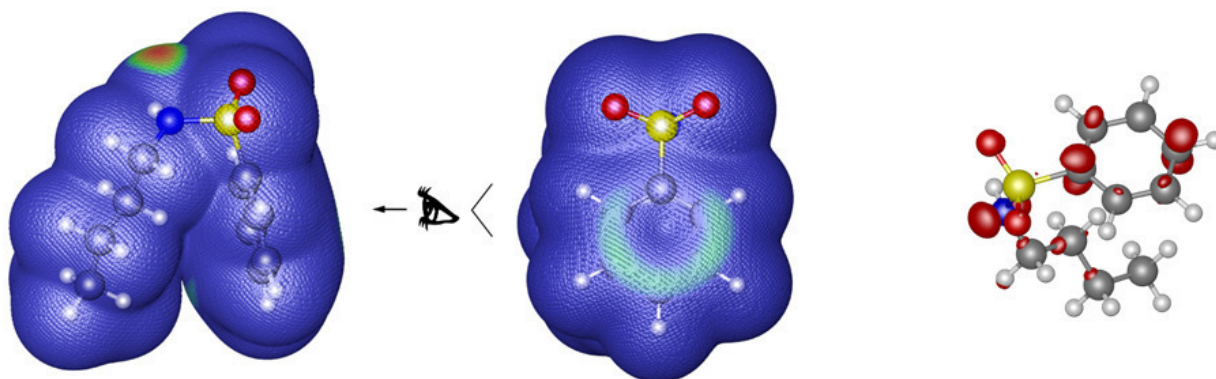


**FIGURE S3**

Quantum-chemical calculations of NBBS: ALIE surface (left) side and front view and Fukui function  $f^0$  (right).